Design, development and clinical application of a modular xenohybrid bone graft for entire vertebral segments substitutions

Ashkan Kashipazha

Supervisors
Cristina Bignardi
Giuseppe Perale
Alessandro Gasbarrini

Department
polytechnic of turin
Italy, Turin
April 2019

Title:

Design, development and clinical application of a modular xenohybrid bone graft for entire vertebral segments substitutions

Ashkan Kashipazha

Supervisors:

Giuseppe Perale
Industrie Biomediche Insubri
Alessandro Gasbarrini
Istituto Ortopedico Rizzoli
Cristina Bignardi
polytechnic of turin

Abstract

The objective of this thesis was to draw a model in Smartbone® capable of replacing a vertebral body extracted from the spine after a surgical operation of vertebrectomy. The work began by studying the cases previously operated on at the Istituto Ortopedico Rizzoli in Bologna and from these cases a database was built in which all the data useful to us was collected such as: CT images before and after the surgery of patients, age, sex, cause of the operation and the prosthesis used. from these results was studied mainly the prostheses used previously and the result obtained with them in the phase after the intervention. was seen the problems and especially how to improve the performance of these prostheses. For this reason we have started to create a new prosthesis that gives better results than the prosthesis previously used.We found two main problems with titanium and carbon prostheses which for the first is that in oncology cases a metal prosthesis makes radiotherapy less effective due to scattering phenomena and also difficult to define how much must be the length of the removed tract, while for carbon prosthesis the problama was complicated assembly, costs and need to be combined with a bone segment to facilitate osseointegration.

Smartbone® is a biodegradable scaffolds were relevant in Tissue Engineering, thanks to the possibility to provide an optimal microenvironment where new tissue could be shaped. In particular, the scaffold proposed by I.B.I, which was called Smartbone®, was constituted by bovine bone matrix reinforced by a micrometric thin poly(L-lactic-co-epsilon-caprolactone) film embedding RGD-containing collagen fragments (extracted by purified bovine gelatine).

being of bovine origin the Smartbone® has limited dimensions and for this reason in order to cover a vertebral segment it is necessary to use more segments of Smartbone® together, for which it has been opted to use a modular model similar to the modular prosthesis in carbon but with the difference that the different models are not connected together with a screw. In fact, having a biodegradable material and having the possibility of modelling the material, we have chosen to create a interlocking model until we have covered the chosen size.

now the most important question was to study the shape of the joint because it has the task of holding the different modules together and blocking the torsional movement of the modules. another problem was the insertion of the peduncular screw because the joint should not facilitate the insertion of the screw and should not come into contact with it. this because under stress and after many cycles of fatigue you could get to the failure of the model. We have opted for the trapezoidal model as it meets all the requirements listed above and whose understressing characteristics we have studied in the case of compression and bending.

After seeing the results of the test we continued with the production of the model, that is, starting from a parallelepiped of Smartbone® we went to remove with the

cutter layer by layer until arriving at a shape very similar to the vertebral body so as to be more similar to the physiological and natural model of the human vertebra.

after production, the model was implanted in two cancer patients with cancer in the lumbar and thoracic areas of the spinal column and it was seen that in both cases the day of implantation the model worked very effectively.

PREFACE

This master thesis in biomedical engineering by Mr. Ashkan Kashipazha is part of a wider multidisciplinary research project coordinated by Industrie Biomediche Insubri SA, a.k.a. IBI, a Swiss med-tech company manufacturing orthobiological medical devices.

IBI is continuously improving its product portfolio, running both internal R&D activities and clinical studies on a wide variety of different clinical indications.

Here, Ashkan was confronted, and accomplished, with the development of a new design of vertebral segments substitutes, made using IBI custom-made platform and bone graft "Smartbone® on demand™". He started from scratch to a highly satisfactory small surgical case series! In the spirit of offering an industrial perspective and given the overall complexity of the task to be addressed in a relatively short timeframe, Ashkan was teamed with a biomedical engineering master student, Vincenzo Maurelli, from the Politecnico di Milano, mostly focused on computational biomechanical aspects, and with Eleonora Pesce, a master student in biomedical sciences from University of Genoa, mostly focused on clinical epidemiology and surgical aspects.

This master thesis work is, hence, the successful result of 9 months of work by a multicompetence team, to which Ashkan provided an essential contribution. Indeed, the supervision and guidance was provided by the team from IBI, namely product engineer Ing. Carlo Grottoli, with the extremely precious cooperation of Dr. Alessandro Gasbarrini and his team from the vertebral unit of the Rizzoli Hospital in Bologna, hosting site for this master work, all being scientifically coordinated by myself.

Giuseppe Perale

Prof. Dr. Giuseppe Perale, PhD
Exececutive Vice President
Industrie Biomediche Insubri SA
Switzerland

Mezzovico-Vira, 25.03.2019

Ringraziamenti

E' proprio vero, questo è l'ultimo capitolo della mia tesi e ammetto che sto facendo più fatica a scrivere questo che tutto il resto. Questi due anni sono stati difficili e duri ma pieno di ricordi che mi porterò dentro per tutta la vita. A rendere più speciali questi anni sono state tutte le persone che mi sono state vicino e che mi hanno accompagnato in tutte le esperienze. Non mi basta scrivere una pagina per ringraziarvi per il tutto ma ci tengo a scrivere queste due righe per ringraziare tutti. In primis ringrazio i miei fantastici genitori, mio papà che con tutti i suoi sacrifici mi ha permesso di arrivare qui dove sono e mi ha sempre spinto ad andare sempre più in alto. Mia mamma con la sua unica preoccupazione di farmi mangiare più possibile mentre studiavo perché ''il cervello ha bisogno di carburante mentre si studia"e mio fratello che è sempre stato presente e il mio compagno da sempre per tutte le cose fatte assieme.

Ci tengo a ringraziare la Professoressa Bignardi che è sempre stata disponibile e Giuseppe Perale con cui sono riuscito a creare un rapporto diverso che con un professore. Ringrazio Alessandro Gasbarrini che mi ha dato tanta fiducia per rendere realizzabile il progetto. Ringrazio Carlo e Cristiana e Valerio con cui ho diviso l'ufficio e che mi hanno sopportato e supportato per questi mesi della tesi.

Ci tengo a fare un ringraziamento speciale a Lamanna che mi ha dato una grande mano durante questo periodo, Davide con cui ho iniziato questi due anni e con cui li finisco oltre tutto con la stessa media e alla fine Zozzo con cui ho diviso tutti i gruppi e tutti i momenti di studio .

Ringrazio Alessio, Fabio, Marco che sono tra le prime persone che ho conosciuto da quando sono in Italia e son persone che mi sono sempre state vicino e con cui ho condiviso tante esperienze e tanti ricordi. Ringrazio anche Lorenzo , Luca e Alessio che ho conosciuto grazie ad un campo rosso e due canestri e siamo riusciti a trasformare quella conoscenza in un legame molto forte che ci portiamo avanti da tantissimo tempo.Ringrazio Livio e Acu per tutto il tempo passato davanti all'aula 29 e per tutti i caffè presi e per tutte le urla e i suoi versi che mi rendevano speciali le giornate.

Ci tengo a Ringraziare Ivan, Fra(pupu) che sono le persone che ho conosciuto nei primi anni dell'università e che hanno sopportato tutte le mie insistenze per trascinarli a fare ciò che non li andava di fare e vi assicuro che ce ne saranno ancora di le rotture di scatole anche nei prossimi anni. Ringrazio Vittorio Gattuso , Luca Barberio anche se ci siamo visti poco, Fabio Marcuccio per tutte le cene a cui ha rinunciato per vedermi, Chiara pusillo e Andrea Compagno per tutto il vino bevuto assieme. Ci tengo a ringraziare ancora Gaia, Giorgia, Maria, Sharon, Paola, Alessio, Luca, Antonio per aver condiviso con me tutte le giornate e tutti i posti che mi hanno tenuto.

Un ultimo ringraziamento ci tengo a dedicarlo a Jacopo che sicuramente mi sta

guardando da là su e che anche se non ci sei più sarai sempre nel mio cuore

Contents

Chapter 1

Anatomical and mechanical structure of bone tissue

1.1 Anatomical structure

1.1.1 The Bone tissue

The bone tissue is a connective tissue with a dynamic function, continuously remodelled during the life of a human being. It consists of different inorganic materials that represent the 66% in weight of the whole tissue, and these are mainly [1] Hydroxyapatite (HA, $Ca5(PO_4)_3OH$), carbonate-apatite ($Ca_5(PO_4)_3CO_3$) and fluorine-apatite ($Ca5(PO_4)_3F$). The remaining percentage is divided into a 25% of organic material and 9% of water. The extracellular matrix (ECM), which represents the organic fraction of the bone, is constituted by collagen type I (90-95 %), proteoglycans (biglycan and decorine) and glycoproteins (osteonectine, alkaline phosphatase, fibronectin, osteocalcinontine), that play a key role in osteoblastic differentiation and tissue mineralization processes. Due to the mineralization of extracellular components, the bone tissue has both a significant stiffness to support deformations and flexibility to adsorb energy. These properties makes the bone tissue perfect to sustain the body, to protect internal organs and to permit the movement and locomotion. Finally, it also presents connection sites for the muscles. Finally, another important aspect of the bone tissue is the maintenance of the calcium homeostasis and the haematopoiesis. Bone assume different variety of shape and size such as ear ossicles or leg long bones. the variety is classified into three groups:

- Long bones
- Short bones
- Flat bones
- Irregular bones

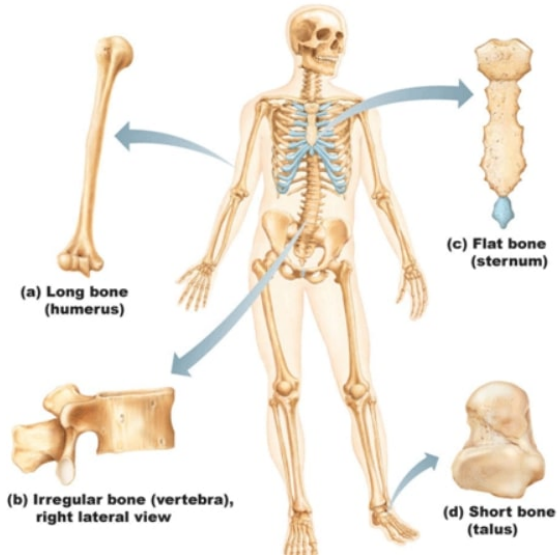

Figure 1.1: Different bone tissue

The thick cortical walls of the diaphysis become thinner and increase in diameter as they form the metaphysis, and articular cartilage covers the epiphyses where they form synovial joints. The metacarpals, metatarsals, and phalanges, like the larger limb bones, have the form of long bones. Short bones,like the tarsals, carpals, and centra of the vertebrae, have approximately the same length in all directions. Flat or tabular bones have one dimension that is much shorter than the other two, like the scapula or wing of the ilium. Examination of the cut surface of a bone shows that the tissue assumes two forms: the outer cortical or compact bone and the inner cancellous or trabecuar bone.
Cortical bone forms about 80% of the skeleton and surrounds the thin bars or plates of cancellous bone with compact lamellae. ln long bones, dense cortical bone forms the cylindrical diaphysis that surrounds a marrow cavity containing little or no trabecular bone. In the metaphyses of long bones, the cortical bone thins and trabecular bone fills the medullary cavity. Short and flat bones usually have thinner cortices than the diaphyses of long bones and contain cancellous bone. Cancellous and cortical bone modify their structure in response to persistent changes in loading, hormonal influences, and other factors. Because of their differences in density and organization, equal size blocks of cortical and cancellous bone have different mechanical properties. The two types of bone have the same composition, but cortical bone has much greater density. Because the compression strength of bone is proportional to the square of the density, cortical bone has compressive strength that may be in order of magnitude greater than that of cancellous bone. Differences in the organization and orientation of cortical and cancellous bone matrices may also make a difference in their mechanical properties.

Cortical Bone		Cancellous Bone
Collagen and mineral	Materials	Collagen and mineral
5-30%	Porosity	30-90%
1.8-2.0 g/cm^3	Density (ρ)	1.8-2.0 g/cm^3
1.4-2.0 g/cm^3	Apparent density (ρ_a)	0.18-1.4 g/cm^3
10-20 GPa	Young's Modulus (E)	$\propto \rho_a^2$
150-200 MPa	Fracture stress (σ_f)	$\propto \rho_a^2$
0.5-3.0%	Fracture deformation (ε_f)	5-10%

Figure 1.2: Mechanical properties

1.1.2 Bone structure

During skeletal growth [2] and bone remodeling, osteoblasts form seams of unmineralized bone organic matrix, called osteoid, on the surface of mineralized bone matrix. Normally, osteoid mineralizes soon after it appears. Therefore, normal bone contains on!)r small amounts of unmineralized matrix. Osteoid lacks the stiffness of mineralized bonematrix. For this reason, failure to mineralize bone matrix during growth or during normal turnover of bone matrix in mature individuals produces weaker bone. Individuals with impaired mineralization of bone matrix may develop skeletal deformi ties or fractures. In children, the clinical conditionassociated with impaired mineralization, rickets,predisposes the patient to skeletal deformity. In adults, the clinical condition associated with impaired mineralization, osteomalacia, predisposes the patient to fractures. Mineralized bone exists in two forms:

- Woven (immature, fiber,or primary)
- Bone and lamellar (mature, secondary)bone

Woven bone forms the embryonic skeleton and the new bone formed in the metaphyseal parts of growth plates. Mature bone replaces this woven bone as the skeleton develops and during skeletal growth. Small amounts of woven bone may persist after skeletal maturity as part of tendon and ligament insertions, the suture margins of cranial bones, and the ear ossicles. With these exceptions,woven bone rarely appears in the normal human skeleton after 4 or 5 years of age, although it is the first bone formed in many healing fractures at any age and it also appears during the rapid turnover and formation of bone associated with metabolic, neoplastic, and infectious or inflammatory diseases. Woven and mature bone differ in mechanical properties and the rate of bone formation. Cells rapidly form the irregular, almost random, collagen fibril matrix of woven bone. The appearance of the irregular arrangement of collagen fibrils gives woven hone its name. It contains approximately four times as many osteocytes per unit volume of lamellar bone, and they vary in size, orientation, and distribution. The mineralization of the woven bone matrix also follows an irregular pattern with mineral deposits varying in size and their relatioship to collagen fibrils. In contrast, cells form lamellar bone more slowly and the cell density is less. The collagen fibrils of lamellar bone vary less in diameter and lie in tightly aligned parallel sheets forming distinct lamellae 4 to 12 microns thick with an almost uniform distribution of mineral through out the matrix. Because

of the lack of collagen fibril orientation,the high cell and water content, and the irregular mineralisation, the mechanical properties of woven one differ from those of lamellar bone. It is more flexible, more easily deformed, and weaker than mature lamellar bone. For this reason, the immature skeleton and healing fractures have less stiffness and strength than the mature skeleton or a fracture remodeled with la mellar bone.

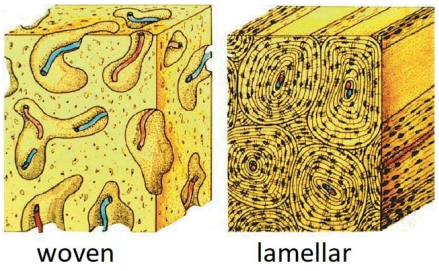

Figure 1.3: Woven and lamellar bone

1.1.3 Components

The formation and maintenance of bone depends on the coordinated actions of different types of bone cells. The morphology, function, and characteristics of bone cells separate them into four groups:

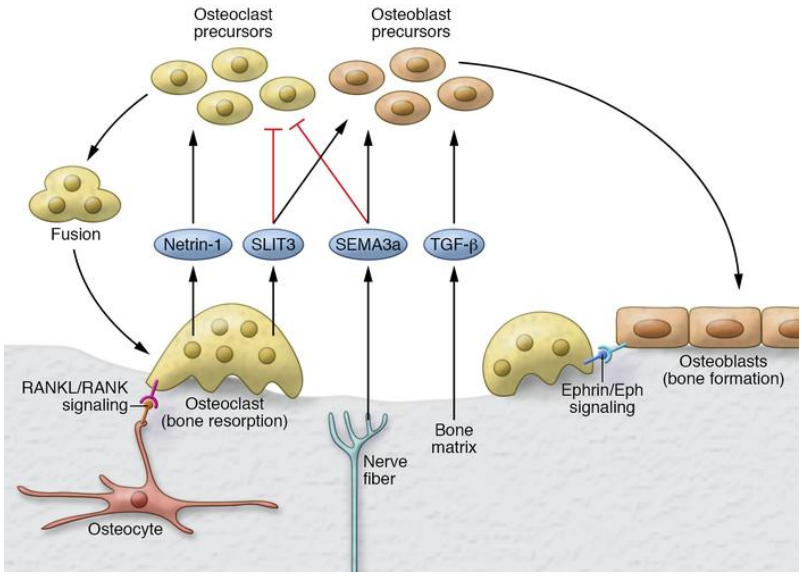

Figure 1.4: Osteoblasts and osteoclasts

- UNDIFFERENTIATED OR OSTEOPROGENITOR CELLS:
  small cells with single nuclei, few organelles, and irregular forms, remain in an undifferentiated state until stimulated to proliferate or differentiate into osteoblasts. [3] They usually reside in the canals of bone, the endosteum, and the periosteum, although cells that can differentiate into osteoblasts also exist in tissues other than bone.

- OSTEOBLASTS:
  Osteoblasts [4], cuboidal cells with a single, usually eccentric, nucleus, con-

tain large volumes of synthetic organelles: endoplasmic reticulum and Golgi membranes. They lie on bone surfaces where, when stimulated, they form new bone organic matrix and participate in controlling matrix mineralization. When active, they assume a round, oval, or polyhedral form and a seam of new osteoid separates them from mineralized matrix. Their cytoplasmic processes extend through the osteoid to contact osteocytes within mineralimed matrix. Once they are actively engaged in synthesizing new matrix, they can follow one of two courses. They can decrease their synthetic activity, remain on the bone surface, and assume the flatter form of a bone surface lining cell or they can surround themselves with matrix and become osteocytes.

- OSTEOCYTES:
  Osteocytes [4] contribute more than 90 percent of the cells of the mature skeleton. Combined with the periosteal and endosteal cells, they cover the bone matrix surfaces. Their long cytoplasmic processes extend from their oval or lens shaped bodies to contact other osteocytes [2] within the bone matrix or the cell processes of osteoblasts,forming a network of cells that extends from the bone surfaces throughout the bone matrix (Figures 1-7 and 1-8). The cell membranes of the osteocytes and their cell processes cover more than 90 percent of the total surface area of mature bone matrix. This arrangement gives them access to almost all the mineralized matrix surface area and may be critical in the cell mediated exchange of mineral that takes place between bone fluid and the blood. ln particular, they may help maintain the composition of bone fluid and the body's mineral balance. [5]

- OSTEOCLASTS:
  Osteoclasts, large irregular cells with multiple nuclei, fill much of their cytoplasm with mitochondria to these cells in resurb lxme [2]. They usually lie directly against the bone matrix on endmteal, perimteal. and Haversian system bone surfaces like osteocytes, and pnesumably osteoblasts. they can move fmm one site of bone resorption to another. Osteoclasts appear to form by fusion of multiple bone marmw-derived mononuclear cells. When they have finished their bone resorbing activity, they may divide to reform multiple mnnonuclear cells [4]. One of the most distinctive features of osteoclasts is the complex folding of their cytoplasmic membrane where it lies against the bone matrix at sites oi bone resorption. This ruffled or brushed border appears to play a critical role in bone resorption, possibly by increasing the surface area of the cell relative to the heme and creating a sharply localized envirunment that rapidly degrades belie matrix. [6] The fluid between the brush border and the bone matrix probably has a high oncentration at hydrogen ions and pruteulytie enzymes: the acidic envimnment muld demineralize bone matrix, and the enzymes could degrade the organic bone matrix. In cancellous bone, osteoclasts resorbing the bone surface create a characteristic depression called a Howship's lacuna. In cortical bone, several osteoclasts lead the osteonal cutting cones that remodel dense cortical bone.

- BONE MATRIX:
  Bone matrix [1]consists of the organic macromolecules, the inorganic mineral, and the matrix fluid. The inorganic matrix component contributes approximately 70% of wet bone weight, although it may contribute up to 80%. The organic macromolecules contribute about 20% of the bone wet weight and water contributes 8 to 10%. The organic matrix gives bone its form and provides its tensile strength; the mineral component gives bone strength in compression. Removal of the bone mineral or digestion of the organic matrix show the contributions of the inorganic and organic matrix components to the mechanical properties of bone. Removal of either component leaves bone with its original form and shape, but demineralized bone, like a tendon or ligament, has great flexibility. A demineralized long bone, such as the fibula, can be twisted or bent without fracture. In contrast, removal of the organic matrix makes bone brittle. Only a slight deformation will crack the inorganic matrix and a sharp blow will shatter it. The organic matrix of bone resembles that of dense fibrous tissues like tendon. ligament, annulus fibrosis, meniscus, and joint capsule.
  Type I collagen contributes over 90% of the organic matrix.The other percent includes small it may have a role in maintaining the structural integrity of the bone tissue. To preserve normal bone mass and mechanical properties, osteoblastic bone formation must balance osteoclastic bone resorption. [3] A variety of stimuli can alter this balance. For example, repetitive loading of the skeleton can increase bone formation relative to bone resorption and thereby increase bone mass and strength. lmmobilization decreases bone formation relative to bone resorption, thereby decreasing bone mass andstrength. Bone mass normally changes with age. It increases to a maximum value about 10 years after completion of skeletal growth, remains stable for a variable period, and then begins to decrease, progressively weakening the skeleton. The reasons for the age-related loss of bone mass and the mechanisms that normally coordinate and control bone cell function remain poorly understood, but investigations of bone tumover show that both systemic and local factors help control osteoclast and osteoblast function.

1.1.4 Osteogenesis

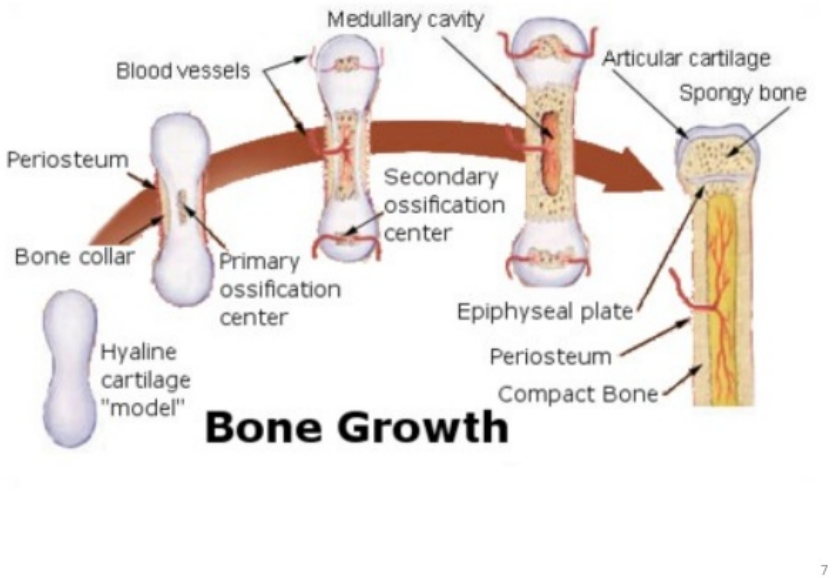

Figure 1.5: Osteogenesis

The osteogenesis [7] or ossification identifies the bone formation process that includes both the formation of organic matrix and the following mineralization of this last one. This process is separated by the calcification, which consists in the deposition of crystals of hydroxyapatite at the level of soft tissues. In some particular cases like the one in which the ratio calcium/phosphorous is very low in the bone extracellular liquid, the ossification process cannot be executed by the calcification and the resulting deposition of organic material brings to the development of osteoid or pre-bone tissue. This characteristic is typical of either rickets or osteomalacia. The mineralization process is the result of the balance between cellular activity and organic matrix components. Although in physiological conditions the extracellular liquids are rich of octacalcium and apatite, the mineralization is not a predominant phenomenon due to the presence both of inhibitors of crystal formation at molecular level like pyrophosphate and of serum protein that tie the ionised calcium. The zone, which will be mineralized, has to be clear from these inhibitors through proteolytic enzymes and phosphatases. The hydroxyapatite precipitation is divided in two different phases called nucleation and multiplicative proliferation respectively. Vesicles deriving from bone cells fluctuate in the zone of the matrix where the calcification process belongs. Then the mineralization process starts. The first mineral formed is amorphous and impure, due to the presence both of Na, K,Mg and CO3 ions and calcium phosphate that influence the crystal dimension. The first precipitate consists in an amorphous calcium-phosphate component called nucleus, which is rapidly transformed in octacalcium phosphate and then hydrolysed o hydroxyapatite. [1] The nucleus formation is originated by an active transport process of ionised calcium in the vesicles. This phenomenon permits the increase of calcium/phosphate production at superior levels of the physiological one, with

the consequent hydroxyapatite formation. The new crystals are concentrated on the internal part of the vesicular membrane, which is full of lipids and proteolipids. Then they continue to grow catalysing the formation of new crystals also in zones where the ratio of calcium/phosphate is not major than the physiological one. For these reasons it is very important to maintain the control of the crystal nucleation process through the action of some non-collagen bone proteins, which can tie themselves to these precursors in a stereospecific way, so it is possible to limit the crystal formation to a specific face controlling both the growth direction and the final form. The homogeneous precipitation of hydroxyapatite occurs in the lumen of the matrix vesicles, where the mineralization process is encouraged by the phosphatases presence, which removes the crystallization inhibitors and also constitutes a protect environment for the development of hydroxyapatite precursors that are characterized by a short half-life.
After the initialization of the mineralization process [7], another heterogeneous process dominated by the collagen takes place. There are two different hypothesis about this process. The first one asserts that some non-collagen protein, which show a higher affinity to the calcium than the collagen molecules, tie themselves to sedimentary crystals obstructing the access of other ions to the crystal growing surfaces. Another theory believes that the collagen is the orientation substrate of the nucleators. It also permits an appropriate topology for the mineral deposition. After that there is a phase characterized by a rapid process expansion in which the major axis of the hydroxyapatite crystal is parallel to the major one of collagen fibre. This process ends when the concentration of the inhibitors reaches the critical level corresponding to the inhibition of the mineralization. In this way, an osteoid layer between the cell and the mineral deposition front is guaranteed.

1.1.5 Vertebral column

Figure 1.6: Vertebral column

The vertebral column [8] consists of 33 vertebrae of which 24 presacral vertebrae (7 cervical, 12 thoracic and 5 lumbar) followed by the sacrum (5 molten sacral vertebrae) and coccyx (4 coccyx vertebrae frequently fused). The 24 presacral vertebrae

allow movement and therefore make the spine flexible. Stability is provided by ligaments, muscles and the shape of the bones. The adult vertebral column presents four anteroposterior curvatures: thoracic and sacral, both concave anteriorly, and cervical and lumbar, both concave posteriorly. The thoracic and sacral curvatures, termed primary, appear during the embryonic period proper, whereas the cervical and lumbar curvatures, termed secondary, appear later (although before birth) and are accentuated in infancy by support of the head and by the adoption of an upright posture.

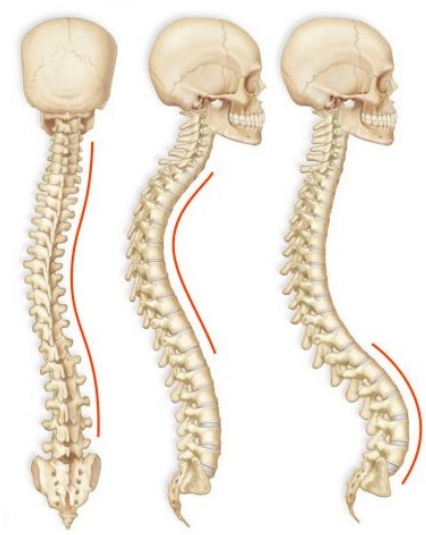

Figure 1.7: Vertebral column curves

Lordosis is defined by an excessive inward curve of the spine. Although it primary affects the lumbar spine, it does occur in the neck too. Patients with excessive lumbar lordosis may appear swayback, the buttocks more prominent, and in general their posture appears exaggerated. [8] Lordosis affects people of all ages and when it affects the low back, it can cause back pain making movement difficult and painful. Spondylolisthesis, osteoporosis, and even obesity may lead to abnormal lordosis. Kyphosis is defined by an excessive outward curve of the spine and may cause a deformity such as a humpback or hunchback. Abnormal kyphosis is more commonly found in the thoracic or thoracolumbar (chest area/low back), but can affect the neck too. Patients with excessive kyphosis may appear with a pitched-forward appearance. There are two types of abnormal kyphosis; that caused by poor posture and structural kyphosis. Scoliosis is the abnormal curving of the spine to the left or right side. Scoliosis most often affects the thoracic spine and children, although it is found in adults too.

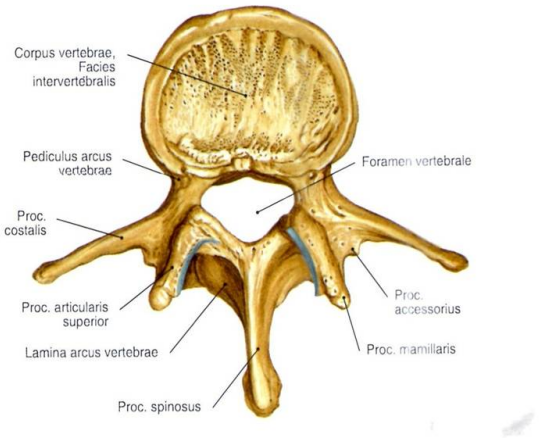

Figure 1.8: Vertebral body structure

A typical vertebra consists of (1) a body and (2) a vertebral arch, which has several processes (articular, transverse, and spinous) for articular and muscular attachments [8]. Between the body and the arch is the vertebral foramen: the sum of the vertebral foramina constitutes the vertebral canal, which houses the spinal cord. In addition to the transverse and spinous processes, which serve as short levers, the 12 thoracic vertebrae are connected by joints with paired, long levers, namely the ribs. The bodies of the vertebrae are separated from each other by intervertebral discs. The body is mainly spongy bone and red marrow, but the margins of the upper and lower surfaces consist of a ring of compact bone, the vertebral end-plates. The body is marked on its sides by vascular foramina. The vertebral arch consists of right and left pedicles (which connect it to the body) and right and left laminae. The transverse processes emerge laterally at the junction of the pedicles and laminae, and the spinous process proceeds posteriorly from the union of the laminae. The superior and inferior articular processes project vertically from the vertebral arches on each side and bear articular facets. When vertebra are in their anatomical position, notches between adjacent pedicles form intervertebral foramina, each of which typically transmitsneural structures including a spinal ganglion and a ventral root of a spinal nerve.

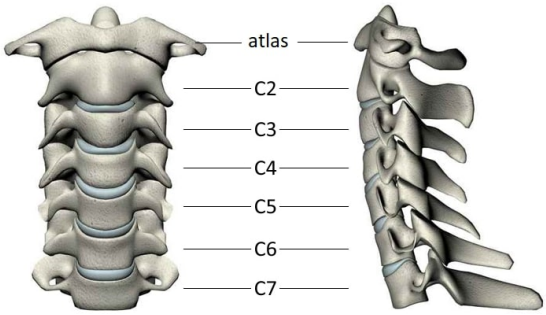

Figure 1.9: Cervical vertebrae

There are seven cervical vertebrae C1-C7 used for flexibility and movement. The cervical spine has a lordotic shape, or a backwards C shape. The first two cervical vertebrae are very specialized to allow us to turn our head from side to side. The

first cervical vertebra (C1) is called the atlas and is aptly named after the Greek god Altas, who carried the world on his shoulders. This bone is formed like a ring that sits upon the second cervical vertebra (C2). The second cervical vertebra (C2) is called the axis as it is the line upon which the head and C1 rotate upon. The C1 vertebra connects the skull to the cervical spine. These two vertebrae have different anatomy than the rest of the spine and present 90 grad of rotation [9]. The C1 vertebra is formed like a ring that sits on top of C2. The C2 vertebra has a bony knob that fits into the front portion of the ring of the C1 vertebra. C3-C7 connect cervical vertebrae to thoracic vertebrae and have found very thin discs between this vertebrae.The inferior cervical vertebrae, from C2 to 6, are typical and have short spinous processes [8] with small and oval bodies. There are lips that project superiorly to the superolateral edges of the vertebral bodies. They closely correspond to the recesses in the lateral edge of the lower aspect of the vertebral body above. Each transverse process, pierced by a foramen transversary, terminates laterally in the anterior and posterior tubercles, which are connected by an "intertubercular lamella" or a bar. The bars are grooved by the primary ventral branches of the spinal nerves, which pass posteriorly to the transversal foramen. The anterior tubercles of the C6 vertebra are large and are called carotid tubercles, because common carotids can be compressed against them. The C7 vertebra has a long, non-bifid prickly process and is known as the prominence of the vertebra. The anterior tubercles (costal processes) of the C7 vertebra can develop separately as cervical ribs.

Figure 1.10: Thoracic vertebrae

There are twelve thoracic vertebrae, named T1-T12, specialized for stability. The thoracic spine aim is keeping the body upright, protects vital chest organs and articulates with each rib to form the rib cage. Each rib is firmly connected to each level of the thoracic spine. The thoracic spine has a kyphotic shape and forme a C shape and thats discs are relatively thin.

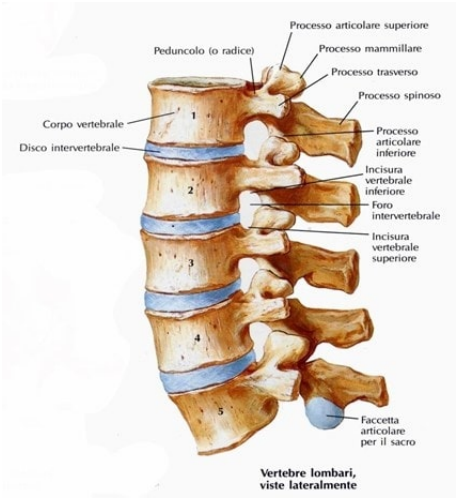

Figure 1.11: Lumbar vertebrae

There are usually five lumbar vertebrae, named L1-L5, designed for weight bearing loads and movement. In some people, they may have developed four or six lumbar vertebrae [8] . In some cases one of the bones of the sacrum, the base of the spine, forms as a vertebra instead of the sacrum. This is called a transitional (or sixth) vertebra and is simply a bony anomaly. The lumbar spine is shaped like the cervical spine; it is lordotic like a backwards "C". The two lordotic curves in the neck and low back are balanced by the thoracic kyphotic "C" curve so the spine's center of gravity is overall balanced in an "S" shape. The vertebrae in the lumbar spine are the largest of the entire spine, designed to hold increasing forces of weight. The lumbar spinal canal is also the largest, allowing for more space for the nerves [10].

Figure 1.12: Sacrum and coccyx

The sacrum is made of five fused vertebrae that form a single bone. The sacrum is shaped like an inverted triangle with the base at the top. It acts as a wedge between the two iliac pelvic bones. [8] On both sides of the pelvis, the sacrum articulates with the ilium through the sacroiliac joints. The coccyx is formed by the fusion of four to five rudimentary vertebrae, commonly referred to as the tailbone.

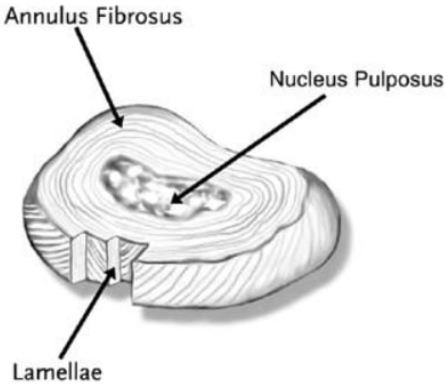

Figure 1.13: Intervertebral disc

The intervertebral discs lie between the vertebral bodies, linking them together. They are the main joints of the spinal column and occupy one-third of its height. Their major role is mechanical, as they constantly transmit loads arising from body weight and muscle activity through the spinal column. They provide flexibility to this, allowing bending, flexion, and torsion [11]. They are approximately 7 to 10 mm thick and 4 cm in diameter in the lumbar region of the spine. 6,7 The intervertebral discs are complex structures that consist of a thick outer ring of fibrous cartilage termed the annulus fibrosus, which surrounds a more gelatinous core known as the nucleus pulposus; the nucleus pulposus is sandwiched inferiorly and superiorly by cartilage endplates.
The central nucleus pulposus contains collagen fibers, [11] which are organized randomly,8 and elastin fibers (sometimes up to 150 mm in length), which are arranged radially; 9 these fibers are embedded in a highly hydrated aggrecan-containing gel. Interspersed at a low density (approximately 5000/mm3,10 are chondrocyte-like cells, sometimes sitting in a capsule within the matrix. Outside the nucleus is the annulus fibrosus, with the boundary between the two regions being very distinct in the young individual (¡10 years). the Annulus is made up of a series of 15 to 25 concentric rings with the collagen fibers lying parallel within each lamella. The fibers are oriented at approximately 60 grad to the vertical axis, alternating to the left and right of it in adjacent lamellae. Elastin fibers lie between the lamellae, possibly helping the disc to return to its A line drawing of the spinal segment consisting of two vertebral bodies and a normal intervertebral disc sandwiched between them. A cut out portion of a normal disc. Note the location of the Nucleus Pulposus, the vertebral end plate and the architecture of Annulus Fibrosis. The intervertebral disc is 4 cm wide and 7–10 mm thick. The central Nucleus Pulposus containing collagen fibers and elastin fibers. The solidified portion of the Nucleus Pulposus is surrounded by gel-like Nucleus Pulposus. original arrangement following bending, whether it is flexion or extension. They may also bind the lamellae together as elastin fibers pass radially from one lamella to the next.9 The cells of the annulus, particularly in the outer region, tend to be fibroblast-like, elongated, thin, and aligned parallel to the collagen fibers. Toward the inner annulus the cells can be more oval. Cells of the disc, both in the annulus and nucleus, can have several long, thin cytoplasmic projections, which may be more than 30 mm long.12,13 Such features are not seen in cells of articular cartilage. Their function in disc is unknown but it has been suggested that they may act as sensors and communicators of mechanical strain within the tissue.

1.2 Biomechanics of vertebral column

Biomechanics is the study of external forces and their effects when applied to humans and Biomechanics of vertebral column consist in the study of the movements of the vertebral body and of the elements of vertebral column appears to be particularly complex [12]. functional unit of vertebral column is composed by different elements and presents by a first class lever composed by spinous processes and vertebral body whose fulcrum is given by the contact of the facet joints. Interaction between two vertebral body is represented by two different stiffness. first of them present vertebral disc and the second one report ligaments.

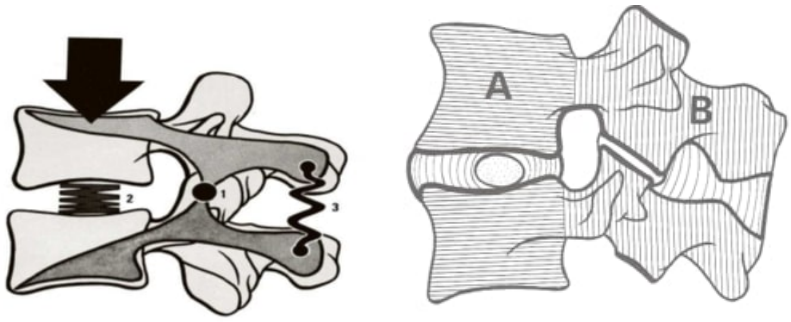

(a) *Functional vertebral unit* (b) *A=support ,B=dynamic function*

Figure 1.14: Vertebral column's different part functions

Each vertebral corp among adjacent vertebral body has 6 degree of freedom that are translation and rotation along three axis [13]. between two vertebral bodies exist a rotation point that allows a correct execution of all movements and kipping correct posture [9].

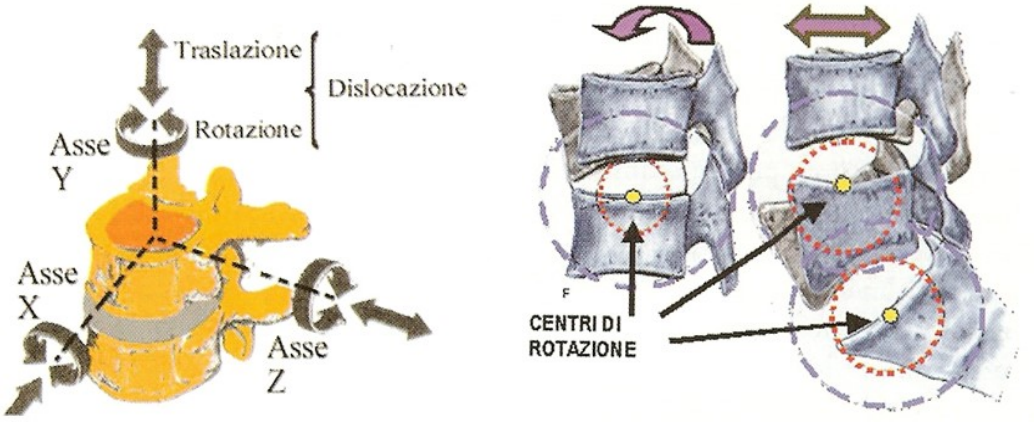

(a) *Vertebral movements* (b) *Rotation center*

Figure 1.15: Vertebral column movment

The principal biomechanical features of vertebral body are:

1. Stability and flexibility
   stability and flexibility [14]express resistance to external forces by vertebra to

avoid damaging the marrow. there were different reaction to horizontal forces and vertical forces. The vertebra reacts to the vertical forces generating a displacement almost proportional to the increase of the normal force to the vertebral plate thanks to the presence of two points of maximum resistance while for horizontal forces we tend to easily reach the breaking point because they act on the areas with less resistance [15]. this happens because the vertebra is made up of a cortical shell structure of dense bone that surrounds spongy tissue and generates on the sagital plane of the fan-shaped fibers.

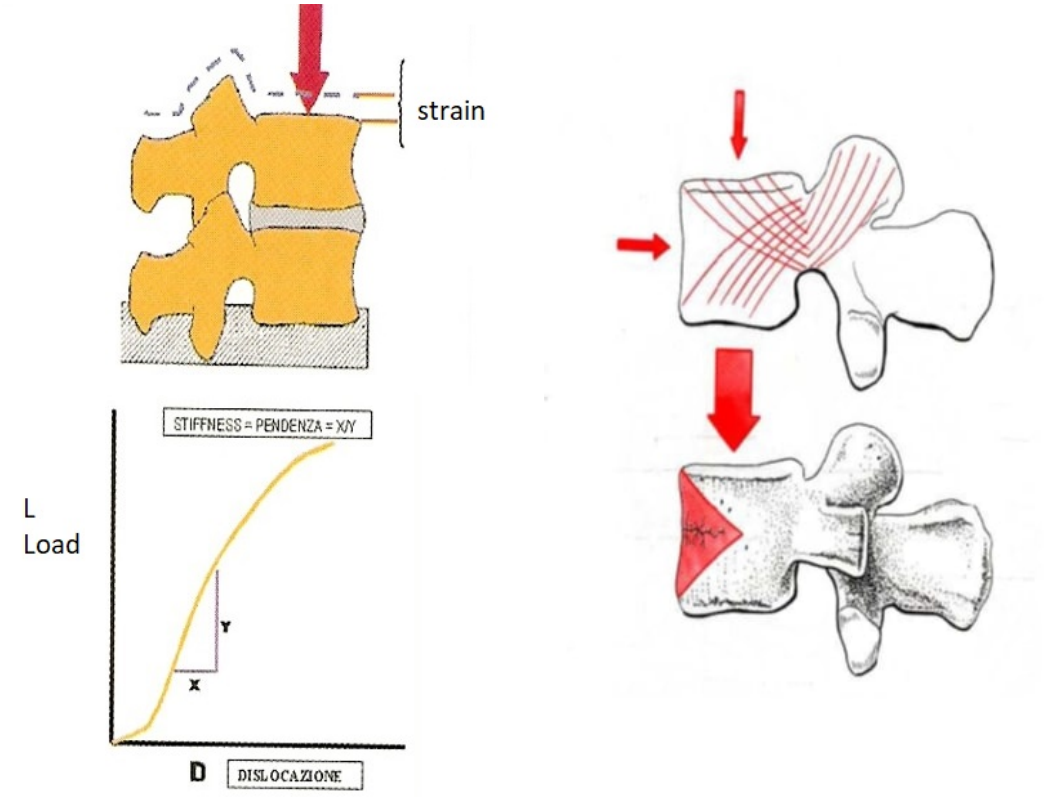

(a) *produced dislocation and applied force relationship*

(b) *Force distribution lines as a function of the applied force*

Figure 1.16: Vertebral column reaction to forces

2. Flexion, extension, lateral rotation and axial rotation

   - Flexion: There is some ambiguity when describing the positions and movements of the cervical and lumbar spine[16]. In the cervical region, rachis flexion is a movement that reduces the physiological anterior curve. The movement continues up to the point to be straightened or flattened in this region of the rachis, but does not normally progress to the point that the column has a convex backward curve. In the thoracic region, the flexion of the spine is a movement that increases the physiological posterior curve. In normal flexion, the column describes a posterior convex curve rounded profile of the entire thoracic region.
   - Extension: The extension of the column is a movement of the head and of the trunk in the posterior direction, while the spine moves, describing

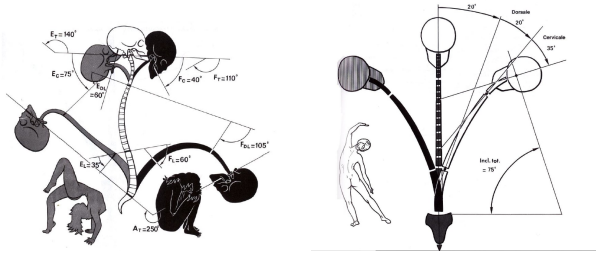

(a) *Flexion and extension*

(b) *Lateral rotation*

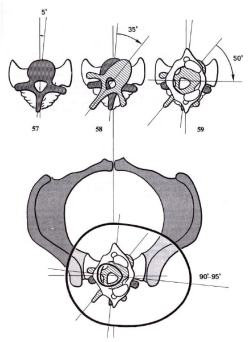

(c) *Axial rotation*

Figure 1.17: Vertebral column movment

a curved curve[16]. In the cervical region, the extension is an increase in physiological curvature and is initiated by the posterior inclination of the head, which is approaching the occiput at the seventh cervical vertebra. In the thoracic region, the extension is a movement that reduces the physiological posterior curvature by straightening the upper part of the back. The movement can progress up to the straight position. In the lumbar region, the extension is a movement that increases the physiological anterior curve and is produced by flexing the trunk backwards or by tilting the pelvis forward. The extension range is highly variable, making it difficult to set a standard for measurement criteria.

- Lateral rotation: Flexion and lateral rotation are described separately, although they are produced in a combined manner and are not considered as simple movements[14]. The lateral flexion of the column is a movement in which the head and the trunk bend on one side, while the column describes a convex curve towards the opposite side. A convex curve to the right is equivalent to a left lateral flexion. The lateral flexion varies according to the regions of the column. It is easier in the cervical and lumbar region and is limited in the thoracic region due to the presence of the rib cage.
- Axial rotation: Axial rotation is a movement on the transverse plane and is easier in the thoracic region and less in the lumbar region[14]. Rotation in the cervical region allows approximately a range of 90° movement of the head and is described as rotation of the face to the right or to the left.

3. Facet's interaction
   Interaction between [16]superior and inferior facet joints of two vertebrae come about apophyseal joints and it can be found different movements such as:

   - Sliding movement between two facets
   - Different movements based on the oblique orientation of the facet joints
   - Role in the stability of the spine

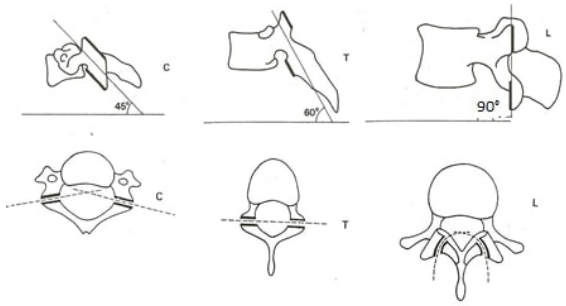

Figure 1.18: Articular faces movements

Facets support only 18% of compression forces but at the same time can support 45% of rotation forces or torsional forces. this indicates that facets have better resistance to torsional forces compared to compression forces.

4. Biomechanics of vertebral discs
   vertebral discs are formed by a central flat part and a fibrous ring that surrounds the central part. The central vertebral flat part has a structure composed of numerous pores. this structure from the physiological point of view allows the vertebra to be crossed by the nutrients contained in the discus when the column is subjected to a high compression while when the body does not under load the substances are sucked disk such as in the supine position.

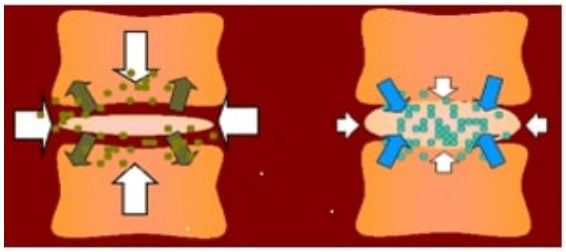

Figure 1.19: Intervertebral discs

Vertebral disk is always kept under load by physiological load and this involves a perpetual pre-compression on disk. As far as the distribution of forces on the disk [11] is concerned, it can be seen that the core supports 75% of the load while the fibrous ring 25%.subjected to a higher pressure than the pre-compression disk is crushed, therefore increasing the internal pressure of the core and the loads will be transmitted to the fibrous ring. in compression

resistance of the vertebral disc is superior than vertebra , however, the disc resists up to 550 kg while the vertebra resists up to 450 kg before breaking.This phenomenon is due to the greater elasticity of the disc compared to the vertebrae.

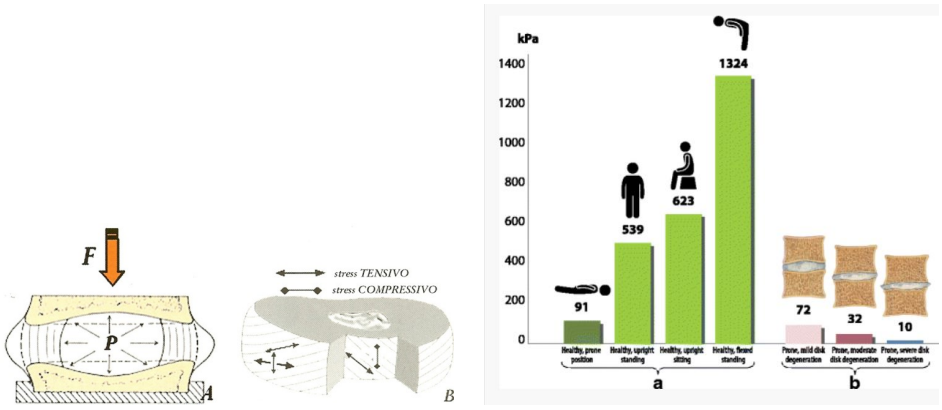

Figure 1.20: Intradiscal pressures. (a) The intradiscal pressures in the physiological postures in healthy individuals. (b) The intradiscal pressures in patients with mild, moderate and severe degeneration.

5. Ligaments
   The ligaments [17] of the spinal column have the function of counterbalancing different movements including rotational and flexional movement. three are different ligaments of the body we can find:

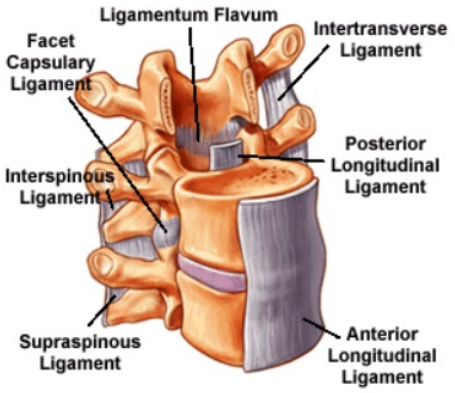

Figure 1.21: Biomecanic of intervertebral discs

- Anterior Longitudinal Ligament
- Posterior Longitudinal Ligament
- Supraspinous Ligament
- Interspinous Ligament
- Ligamentum Flavum
- intransverse ligament

- fact capsulary ligament

Flavum ligament [17] is the most important ligament for it's mechanical features. It connects the laminae, closes the marrow canal. it has a high thickness and high elasticity (composed by 80% of elastin). In flexion position has the aim of protecting back edge foramen conjugation of nerve elements.

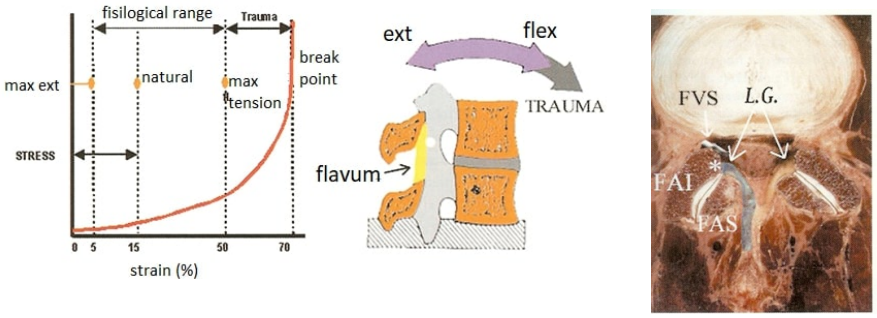

(a) *stress- strain* (b) *flavum ligament*

Figure 1.22: flavum ligamnet

The ligament is deformed with a hyperbolic pattern [17]. in the area between 0 and 50% of the deformation is in the physiological zone, while between 50-70% it suffers trauma due to a higher bending tension than that supported and above 70% it undergoes a break.

6. Anatomical roll of vertebral column curves
   The presence of the curves increases the resistance of the vertebral column to axial compressive stresses. There are 3 mobile curves in the whole spine[8], they are increased by 10 times the resistance of the column to the loads compared to the case in which the column was stright. The curves allow a distribution of loads over the whole curve rather than concentrating it in a single point.

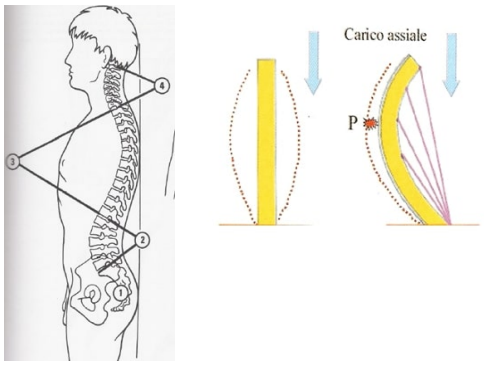

(a) *3 different vertebral curves* (b) *load distribution*

Figure 1.23: vertebral curves

Chapter 2

State of the art

2.1 Bone tumor

Potential adjuvants to surgical treatment for primary spinal tumors include chemotherapy, percutaneous techniques and radiation therapy [18].Management in experienced centers by multidisciplinary teams capable of offering diverse treatment modalities is associated with improved outcomes [18]

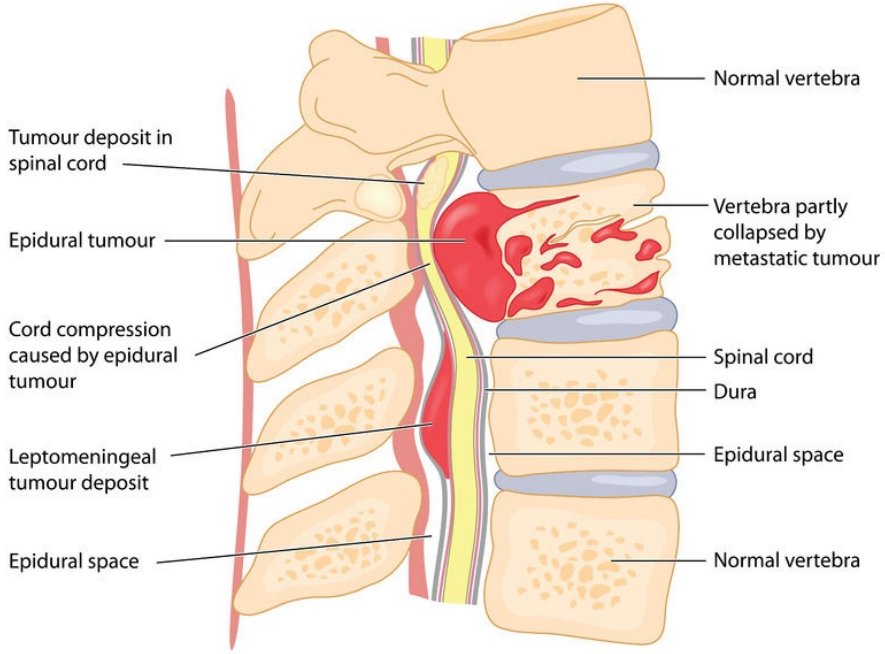

Figure 2.1: Vertebral tumors

2.2 Chemotherapy

The majority of primary spine tumors respond poorly to chemotherapy; however, adjuvant and neoadjuvant chemotherapy protocols exist for select lesions. including osteosarcoma, Ewing's Sarcoma and giant-cell tumor [19]. The use of denosumab neoadjuvant therapy for giankcell tumor has been shown to improve disease control and allow for less morbid surgery [19]. One series described the use of intraoperative chemotherapy using distillcd water and cisplatin chemotherapy in cases where an intralesional T-saw cut of the pedicle was necessary to preserve the nerve roots in a series of patients with aggressive benign tumors and single metastatic lesions [19].However. evidence regarding intraoperative chemotherapy for spinal tumors is very limited. An example of a malignant tumor that may warrant neoadjuvant chemotherapy prior to en bloc resection is Ewing's sarcoma.

2.3 Percutaneous Techniques

Percutaneous techniques such as selective arterial embolization (SAE) and thermal ablation may be appropriate for select lesions. Preoperative SAE is the standard treatment for aneurysmal bone cysts [19], and preliminary data indicate that multiple treatments of standalone SAE may be sufficient for treatment of select cases of aneurysmal bone cysts without extensive neural involvement or high-risk fractures [18]. SAE is also used preoperatively for the treatment of giant-cell tumors and vascular mctastatic tumors. such as rcnal cell carcinoma, thyroid carcinoma, or hepatocellular carcinoma [18]. and may be of use prior to en bloc spmdylectomy for recurrent low-grade osteosarcoma . Percutaneous thermal ablation of osteoid osteoma has been shown to be highly efficacious [19].

2.4 Radiation therapy

The majority of spinal lesions are radioresistant. However, select lesions are radiosensitive , and radiation therapy of an adequate dose can confer a survival advantage for patients with malignant spine tumors . Radiation therapy is a useful therapy in the treatment of chordomas and chondrosarcomas, particularly in lesions in which en bloc resection is not feasible [18]. Multiple modalities have been demonstrated to be effective, including photon-based intensity-modulated radiation therapy, proton beam therapy, carbon ion, and high-dose single-fraction radiosurgery, all of which have been demonstrated to produce similarly high rates of 5-year local control when adequately dosed (typically, over 70 Gy) and combined with surgery for primary spine tumors [19]. Some have advocated for both pre- and postop-erative radiotherapy to reduce the rate of intraoperative secding. The addition of preoperative radiation therapy has been shown to improve local control as compared to surgery and post-operatìve radiation therapy [18]: however, pre-operative radiation therapy is associated with a significant increase in perioperative complications due to impaired wound healing and increased technical challenges intraoperatively due to scarring [18].

2.5 Surgical Approaches

En bloc resection of spinal lesions poses a significant technical challenge and risk of morbidity due to the proximity of vital neural and vascular structures . Spondylectomies are also inherently destabilizing procedures and require reconstruction and instrumentation in order to allow for appropriate patient mobility.However, successful en bloc spondylectomy can confer a significant survival advantage. There are thus three key objectives in en bloc spondylectomy: successful resection of the lesion with acceptable margins to maximize local control and survival. limiting damage to the surrounding structures to limit morbidity and mortality and maximize functional outcomes, and reconstruction to restore stability and function [18]. Three major methods exist for en bloc spondylectomy:

- vertebrectomy
- sagittal rescction
- rescction of the posterior arch

Operative approach is selected based on the location. size, and local extent of the tumor.

2.6 Vertebrectomy

Vertebrectormies are defined as the en-bloc removal of the body and lamina following detachmcnt from the posterior elements via av transpedicular osleotomy and are the preferred approach for centrally located lesions of the vertebral body with at least one pedicle free from disease . This may be achieved via ananterior and/or posterior approach and may be accomplished in one or two stages [20].

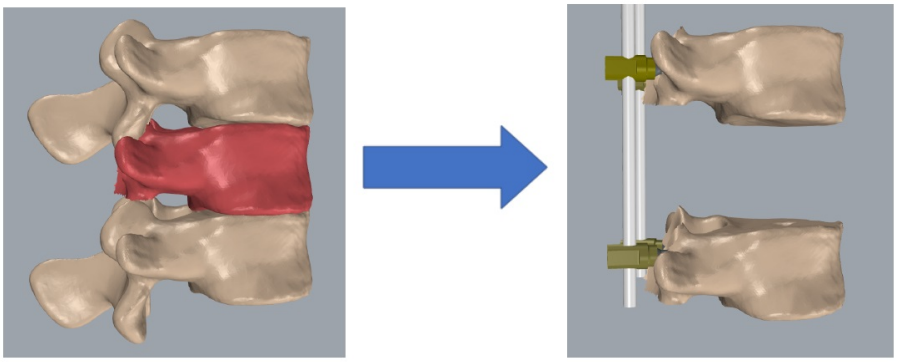

Figure 2.2: vertebrectomy

Is the most commonly utilized approach for resection of vertal body lesions. The posterior approach allows for direct control of epidural venous plexus bleeding and posterior instrumentation[20, 21]. Nerve roots may be sacrificed in the thoracic region to allow for sufficient space for resection of the vertebral body and anterior reconstruction when a posterior approach is taken.However. sacrifice of a nerve root in the thoracolumbar and lumbar spine is avoided when possible. and caution needs to be taken when operating near the artery of Adamkiewicz. lnjury to the artery

of Adamkiewicz leads to anterior spinal cord ischemia and loss of lower extremity function ISI. The single-stage posterior approach is associated with less morbidity for appropriate lesions and may be preferred. particularly for one or two segment en-bloc nesections [22, 21].

However, large lesions and lesions with significant ventral expansion may require a direct anterior approach . Anterior vertebrectomies allow for easier ligation of the segmental vessels and may enable achievement of better margins in tumors with anterior paravertebral expansion or in recurrent disease where resection is complicated by adhesions and seat tissue [20] [21, 23] . The anterior approach may be of particular utility for lesions in close proximity to major vessels; in cases in which the tumor is adherent to or involving major blood vessels, the assistance of a vascular surgeon may be of use. especially if repair of a vessel is warranted. Anterior vertebrectomics arc often combined with a posterior laminectomy and instrumentation prior to anterior en bloc resection and instrumentation in a two-stage approach [20] [23, 22]

Following exposure of the appropriate vertebral body and disc spaces and mobilization of great vessels, the en bloc corpectomy can be performed. Excise the discs distal and proximal to the affected vertebral body [20, 22, 21]. Following complete release of the vertebral body and the tumor, the involved vertebral body and the tumor can then be rolled out en bloc. Histopathological examination of the specimen is necessary in order to determine resection margins. En bloc spondylectomies are inherently highly destabilizing and require reconstruction. Options for anterior reconstruction include titanium mesh cages or carbon cagcs. filled with autografi matcrial. or wide diameter whole shaft femur or tibia allografts. Cages or allografts may be secured and the spine instrumented anteriorly using rods.. Anterior instrumentation may be augmentcd with posterior instrumentation, such as pedicle screw and rod constructs. in a staged approach [20, 23, 21]. Pedicle screws provide superior support as compared to anterolateral plate fixation during flexion. extension. and axial rotation. and stability following en bloc spondylectomy is primarily a function of the number of screws in posterior instrumentation.

2.7 Material used for surgery

Corporectomy surgical intervention is used different instrumentation such as rods,screws and vertebral body substitute. the can be made of many different materials such as titanium, carbon fiber, peek, bone and multiple use of them.

- rods: A rod [24] is a metal cylinder implant used in spinal surgery to stabilize a vertebral segment. A rod is used to connect screws inserted into adjacent vertebral bodies in order to prevent motion and allow fusion. Designed to stabilize and hold the bones together while the fusion heals, these devices have greatly improved the success rate of fusion. This system is designed to preserve natural movement of vertebrae in stabilization even during the physical motion in flexion, extension, lateral bending and rotation [24]. Rods could be made of carbon fiber,titanium and Cobalt chromium and they are selected based on Surgical Approaches ad type of bone tumor.

- screws: Pedicle screws may be used in instrumentation procedures to affix rods and plates to the spine. The screws may also be used to immobilize part of the spine to assist fusion by holding bony structures together. The design of pedicle screw continues to be modified and update[25, 26, 27]. screw with wider cores are generally stronger and less likelu to break. The stress placed upon the screws are greatest at or near the screw- rod interface. At this location that the system most often fails. This occurs through loosening of the screw-rod interface or through screw breakage[25, 26, 27]. Thus, as screw designs have evolved, the core and platform diameters have increased to withstand these higher stresses. The most recent design modification of the system features an integral fixed lower nut that is machined from the same bar stock and thus is stronger and more resistant to breakage. Also, various washers and articulating clamps are now available which allow for a concentric (flush) fit between the screw and rods. This allows loads to be more evenly transmitted between the screws and the linking device. Generally, the threaded portion of most pedicle screws have a larger thread diameter, small core diameter, and a greater pitch for improved purchase[25, 26, 27].

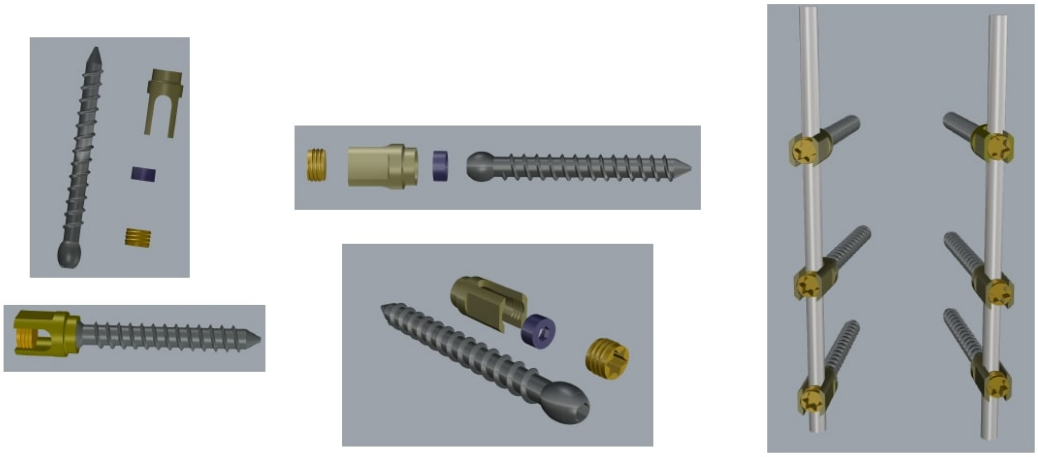

Figure 2.3: screw and rods system

- Vertebral corp substitute: A Vertebral Body Replacement device is designed to replace a damaged or unstable vertebral body due to trauma and/or tumor. When implanted, the device will provide anterior spinal support and restore sagittal alignment. A vertebral body can be replaced by a bone graft, a cement filling with Kirschner wiring, a traditional cage or an expansion implant. The bone graft may be autologic, which involves a disadvantage of the "donor site pain", or homologic, although a potential for reconstruction is not fully evidenced here.

(a) *carbon cages*

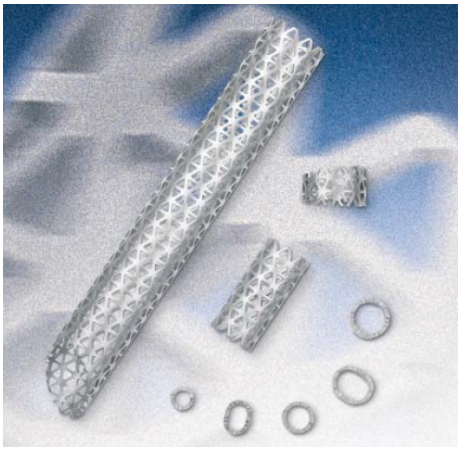

(b) *titanium pyramesh*

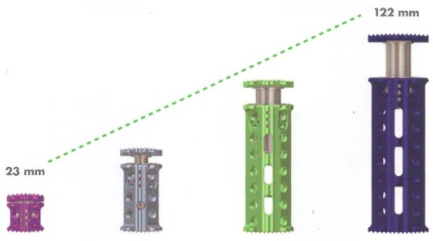

(c) *expansion prosthesis*

(d) *femoral bone*

(e) *titanium custom made*

Figure 2.4: different prosthesis

2.8 Clinical study

Studies based on 80 cases of CVOD(chirurgia vertebrale ortopedica e degenerativa) of Rizzoli orthopedic Institute of Bologna in witch it was carried out vertebrectomy or corporectomy. Strating from this data tried to create a new Database where collect different patient's data since 2012. For each patient collect different value reported in following table.

patient code	surgery unit	patient surname
patient name	date of born	sex
age	surgary date	images
TC pre-surgery	TC post	patology
number of vertebrae	vertebral zone	type of surgery
approches	prosthesis	bone used
instrumentation	length of removed part	

Table 2.1: Databese different data

All patients present primary or secondary cancer and according to this the origin of the tumor can be reported as a primary tumor or metastasis from a secondary tumor. The tumor can affect a vertebra or more vertebrae. our database also reports the type of access performed to do vertebrectomy. according to this database tried to build statistical data to understand which are the most used prostheses, surgical accesses, the most affected vertebrae and patient's sex. Results report that the 90% of patients had a vertebral tumor in lumbar and thoracic section while the most used vertebral corp substitute is made by carbon fiber fallowed by titanium custom made prosthesis.

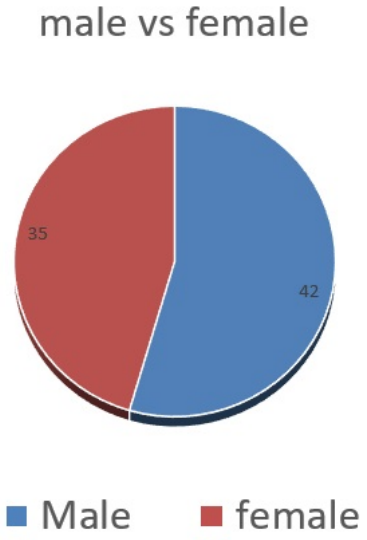

Figure 2.5: male vs female

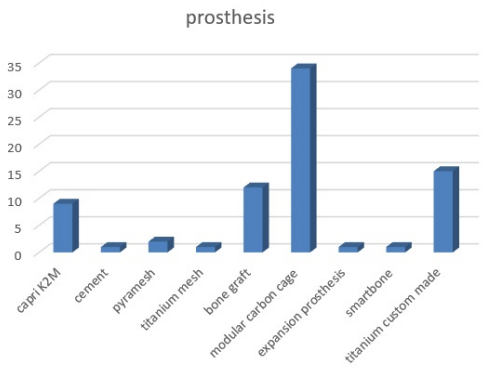

(a) *different kind of prosthesis*

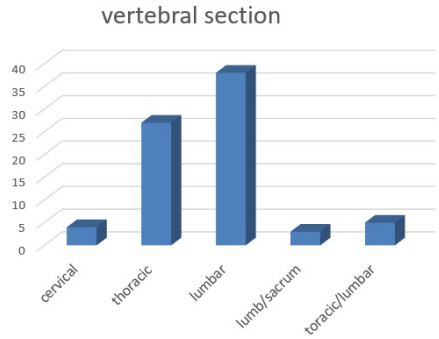

(b) *vertebral section*

Figure 2.6: results of different vertebral body prothesis

Based on the results of the statistics we found that the trachic and lumbar areas are the areas most affected by the tumors we focused more on this vertebral tract. The main solution of the thesis concerns these two sections of the spine. The most used prostheses were the modular carbon prosthesis and the custom made titanium prosthesis. based on these data we went to study the advantages, disadvantages, characteristics and in the end the problems of these prostheses. All of these searches are reported below.

- modular carbon cage [28, 29]:

Figure 2.7: ostaPek VBR Lumbar and Thoracic Vertebral Body Replacement

> *The use of a carbon fiber modular implant may fill any loss of bone substance of the vertebral column, that it allows for immediate weight-bearing, and that if favors bone fusion. Some particular features of the carbon prosthesis favorably adapt to the surgical method of vertebrectomy:*
>
> 1. *The various components of the prosthesis may adapt to any type of bone resection of the vertebral body, even in unexpected situations*
> 2. *Connection to posterior instrumentation in total vertebrectomies avoids the use of an anterior plate, thus reducing the time required for reconstruction of the anterior column*
> 3. *The radiolucency of the prosthesis allows for an easy evaluation of the formation of bone within and around the implant up to definitive anterior fusion*

At the same time based on the fields collected by the doctors of the CVOD at Rizzoli we found that the modular carbon cages [28, 29] present different disadvantages as:

1. have a very high cost.
2. have a high assembly time of the various segments.
3. limit the surgeon to be able to use the screws only in certain areas of the prosthesis.
4. are fragile compared to lateral forces.

- Titanium custom made:

Figure 2.8: Titanium 3D printed

Titanium custom made prosthesis advantages:

1. Have a lower cost than carbon cages [28, 29].
2. Have a low assembly time of the various segments and low time means less chance of infections.
3. Limit the surgeon to be able to use the screws only in certain areas of the prosthesis.
4. Much more biocompatible than the carbon cages [28, 29].

At the same time there are many disadvantages report:

1. Limit the surgeon to be able to use the screws only in certain areas of the prosthesis.
2. The principal problem of titanium prosthesis is that they are not compatible with radiation therapy *Radiation therapy is one of the primary methods of cancer treatment worldwide with computed tomography (CT) being the most commonly used imaging method for treatment planning. In the presence of metal implants such as spinal stabilization implants in spinal or paraspinal treatment or hip replacements in prostate cancer treatments, the extreme photon absorption by the metal object leads to prominent image artifacts. CT metal artifacts affect negatively the treatment planning of radiation therapy either by causing difficulties to delineate the target volume or by reducing the dose calculation accuracy.* This is a very huge problem when the cause of vertebrectomy is cancer because in the post-operative phase all patients will receive radiotrapy treatment and the titanium prosthesis puts such treatments at risk.

Pre-op and post-op images are used to determinate COBB angle. The Cobb angle is the most widely used measurement to quantify the magnitude of spinal deformities, especially in the case of scoliosis, on plain radiographs. Cobb angles are evaluated manually and for this reason there could be a slight error. Even thought, Cobb angles are very helpful to evaluate how vertebral column curves change by a surgical operation. This because not always a vertebral plate without an angle is the best option given that this can not restore the natural vertebral curve. Due vertebral plate without any angle can be a important problem, as can be seen in the charts in the first case we have a 15° and in the second case has 15° of difference between pre-op and post-op Cobb angle measurement.

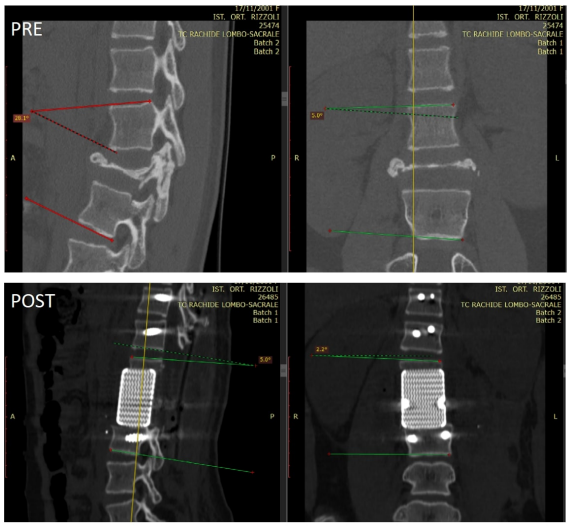

Figure 2.9: CT images cobb angle pre and post surgery with carbon cage [28, 29]

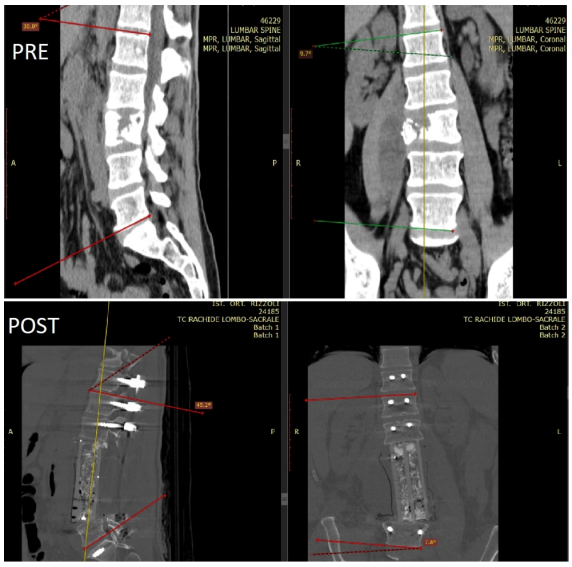

Figure 2.10: CT images cobb angle pre and post surgery with titanium 3D custom made

Chapter 3

Smartbone®

3.1 Smartbone®

3.1.1 Features

Biodegradable scaffolds were relevant in Tissue Engineering, thanks to the possibility to provide an optimal microenvironment where new tissue could be shaped. In particular, the scaffold proposed by I.B.I, which was called SmartBone®, was constituted by bovine bone matrix reinforced by a micrometric thin poly(L-lactic-co-epsilon-caprolactone) film embedding RGD-containing collagen fragments (extracted by purified bovine gelatine). The main structure consists in calcium hydroxyapatite (HA), which chemical form is Ca5(PO4)3, and collagen residuals [30]. The bone xenograft-structure could not be used as bone substitute alone due to its rigid properties. In fact it appeared too fragile for reconstructive surgery application. For this reason the matrix was then reinforced with poly(L-lactide-co-epsilon-caprolactone) and polysaccharides to give more elasticity to the whole structure [30]. Finally, other improved properties were hydrophilicity, cell adhesion and osteogenicity. Furthermore this product needed a sterilisation process to be sold. The chosen techniques was the Ethylene Oxide one (EtO), which was realised by BioSter SpA, Bergamo). Finally SmartBone® was commercialised as medical device of Class III, CE marked. The most relevant characteristic of SmartBone® was the contained variability among samples regarding the heterogeneity. A lot of different bone substitutes showed a significant inter-variability among lots and samples of the same lots due to the natural origin of the sample. The heterogeneity among samples also influenced the microstructure, porosity and density, which in turn caused variability in physical and mechanical properties. In spite of the origin of SmartBone® the samples variability was reduced thanks to the following treatment with polymers and polysaccharides [31].

3.1.2 SmartBone analyses

The main structure of Smartbone is a mineral matrix obtained by bovine trabecular bone of animals bred in New Zealand. They are declared free to bovine spongiform encephalopathy (BSE). The mineral matrix consists of idroxyapatite (HA) reinforced with PLCL, that is a copolymer of Poli(epsilon-caprolactons) and Poli(L-lactic acid), which are biocompatible and bio-absorbable, and collagen containing

RGD sequences. Each of the previous component is focused on the improving of a specific aspect of the construct. In particular the bovine matrix gives the 3D structure and a specific porosity but in any case, it appears excessively rigid to be applied as bone substitute for reconstructive surgery. The fragile structure can be attributed both to the nature of the material and to treatments realised to decellularize it. The decellularization process consists of consecutive steps based on solvents and pressure gradients, realised at room temperature. In this way the 3D structure loses mechanical properties due to the lack of protein structures. Moreover the sterilisation makes the construct excessively porous. Therefore a polymeric layer reinforces the structure deleting the fragile component and improving mechanical properties of the whole structure. Biopolymers are also important to reduce the medium porosity of the scaffold. The final value reached is around 250 micron with a surface-medium volume Ratio around 4.46 mm-1. It also guarantees a significant interconnection among pores. A final key aspect of the polymers is the protection role from the reabsorption of the graft during the first inflammatory phase. As regards the thickness of the layer, Pertici et al. realised a specific degradation study modelling the whole system with partial differential equation of conservation mass. This method was also known as moment method and it wanted to simulate the in vivo degradation of a thin polymeric layer under hydrolytic mechanism [30]. Although the treatment is quiet uniform, several parts of the trabecular surface remain not covered. This is relevant for mesenchymal stem cells coming from hematic flux that can receive specific signals from the bone structure, useful to begin the differentiation. Finally the role of RGD sequence is to increase the cell adhesion and the proliferation of autologous cells, contemporary to the degradation of polymers. In fact the second animal derived component used in the manufacturing of SmartBone® is gelatine: gelatine is commonly used in a huge number of CE-class III products already on the market and wide and deep information are available not only in scientific and technical literature but also on university books [32]. Briefly, gelatine is a mixture of proteins extracted from connective tissue, mostly made.by collagen fragments, most of which is collagen type I. In its pharmaceutical and medical grades, it is obtained according to international standardized process, validated by an international consortium, starting from very low risk tissues (skin and hides for the case of bovines) [32]. In the regeneration of bone a key physiologic phenomenon is the induction of remodelling, which is naturally occurring in union-defect but not in non-union or in bone losses (damages, removals, etc. . .) [32]. The aim of a good bone substitute should be to initiate bone remodelling in the direction of obtaining new bone formation via osteoconduction and finally induction. Briefly, collagen is believed to contribute to fulfil an essential function in the process of bone regeneration. As demonstrated by Duong et al., adhesion of migrating cells can be enhanced by surface modifications with integrin-specific molecules [33] . This approach enabled the development of medical devices for tissue regeneration: those based on gelatine, which is a mixture of collagen fragments. Gelatine is an extremely wellknown compound from both the food and the pharmaceutical industry, which was hence easily “borrowed” to the medical devices industry. Typically of animal origin, it is used mainly as bovine or porcine derived, with the evident risks that however are widely balanced by the known great clinical performances. Bone tissue was, of course, not exempted from a wide variety of studies that underlined and confirmed the interest over gelatine as a potential collagen source [34].

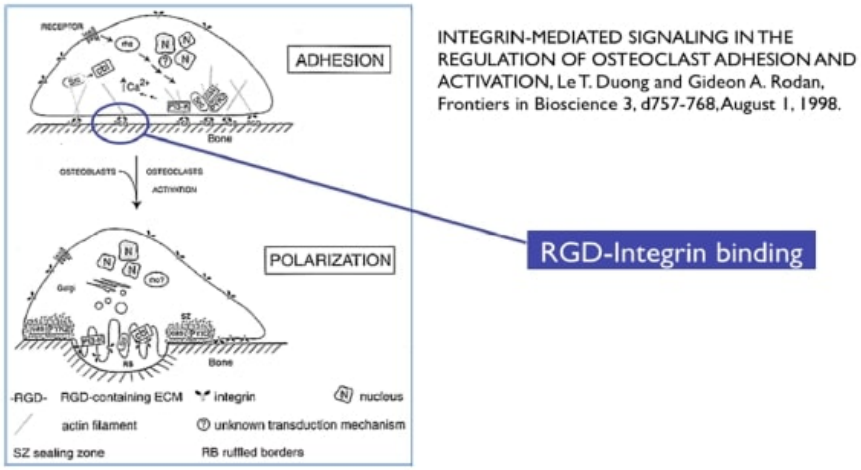

Figure 3.1: : RGD-integrin binding cascade [Duong, 1998].

As regards cellular nutrients, they were inserted in small quantities but with a key role in cellular adhesion improving the tissue remodelling and the device integration. Furthermore it is also important for hydrophilicity of the material itself due to an increase of the wettability. In this way the blood adsorption is favoured and a series of chemical steps happen to promote the osteogenic process [**?**, 35]. SmartBone® polymeric coating degrades in four months, improving the bone growth and tissue integration. This aspect is not strictly related to the thickness of the coating at the beginning of the process . The device is completely reabsorbed after 1-2 years from the implant date, depending on the characteristics of the device itself and its application. As regards the sterilization, SmartBone® is treated with Ethylen Oxide (EtO), followed by a degassing phase which last 24 hours and permits the full gas removal.

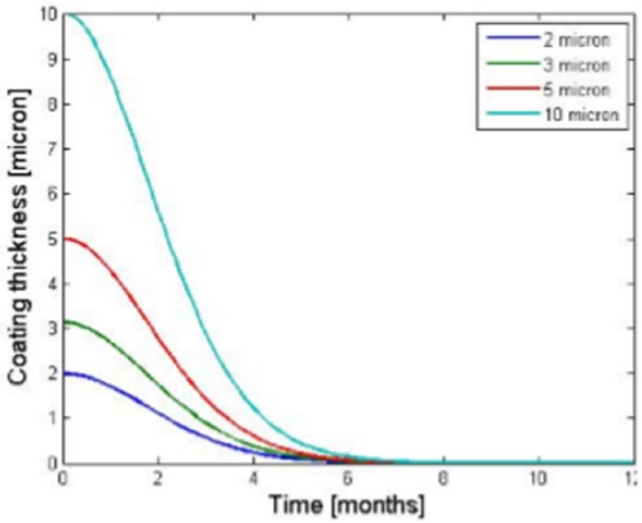

Figure 3.2: Degradation kinetics of the polimeric coating. It appeared indipendent from the initial coating thickness (2μm, 3μm, 5μm e 10μm).

3.1.3 Chemical analyses

Different analyses on Smartbone® samples were realized before this thesis project. These studies were finalised to the obtainment of qualitative analyses using the environmental scanning electron microscopy (ESEM) and quantitative one using axial Micro computed tomography (Micro-CT). After these wide analyses the porosity was found to be excessive in non-treated bovine matrix, while it appeared optimized in the final product treated with polymers.Another key aspect of ESEM analyses was to demonstrate the similarity between SmartBone® structure and the bone one. This aspect was innovative with respect to the competitors' products. As regards the chemical composition, it was analysed using the Energy dispersive Spectrometry (EDS) and Fourier Transform Infrared Spectroscopy (FTIR). The presence of a mineral substrate consisting in Calcium and phosphate was proved by these analyses, as well as the polymeric coating consisting in Carbon and Oxygen.

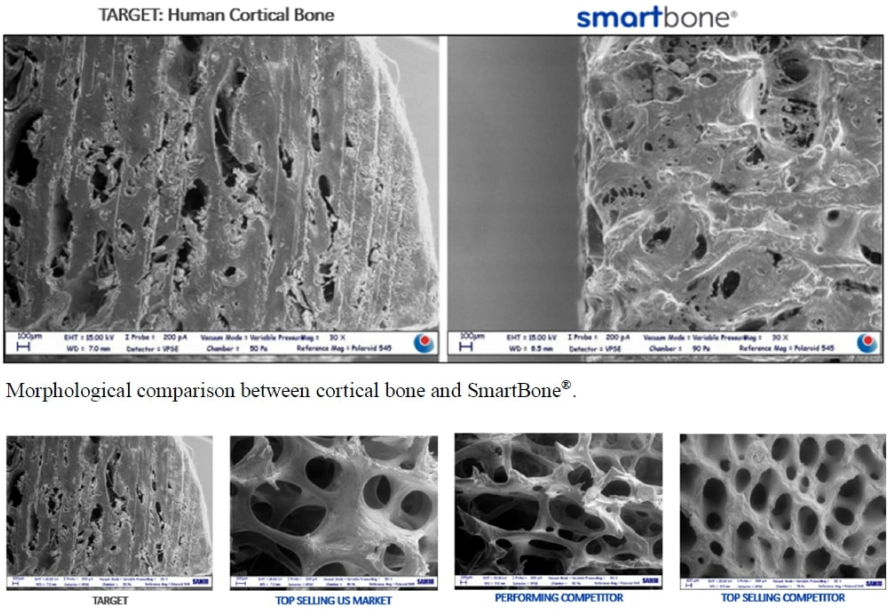

Figure 3.3: Morphological comparison between human cortical bone from iliac crest and the main competitor USA market

3.1.4 Biocompatibility and cytotoxicity analyses

Different studies were realised on the scaffold to obtain a wide range of information about the biocompatibility and cellular adhesion/proliferation. In vitro analyses were made on different cellular lines, including SAOS-2 and MG-63, corresponding to Sarcoma osteogenic and a line derived from an osteosarcoma itself. Finally in vivo tests were realised on specific animal race, called New Zealand white rabbit [30]. According to ISO10993 different tests were realised, including cytotoxicity tests, sensitisation, intra-cutaneous reaction and systemic acute toxicity. All these tests confirmed that SmartBone® is completely biocompatible [36].

3.1.5 Mechanical analyses

As regards mechanical tests, uniaxial test was performed using a MTS 858 MiniBionix (Eden Praire, MN, USA) testing machine equipped with a 10 kN calibrated load cell, compressing the specimen between two parallel plates with a displacement velocity of 1 mm/min: displacement of the upper plate and force were acquired at with a frequency of 10 Hz [56]. Data obtained by these tests showed that the maximum fracture stress was around 13 MPa and a Young's Modulus around 0.2 GPa. This values could be compared to the ones related to the iliac crest. Finally no significant variability was found between dry samples and damp ones. Also in this case it is possible to realise a comparison with the most relevant competitor. In particular SmartBone® was characterized by highest value of compression stress and Young's Modulus. The properties-gap with the best competitor and the one with the biggest level of selling was significant different. In fact their results showed properties included between 10 % and 50 % of the SmartBone® ones [30].

The tests were performed on a MTS 858 Bionix servohydraulic testing machine (S/N 1014952, MTS, Minneapolis, MN) shown in Figure 18. The MTS testing machine was equipped by an axial-torsional hydraulic actuator, with 25 kN axial capacity and 250 Nm torsional capacity, a ± 100 mm range LVDT displacement transducer and a ± 140° range ADT angular transducer mounted on the actuator. The load applied to the test sample was measured by a MTS axial/torsional load cell (model 662.20D-05, S/N 1007099, ± 25 kN maximum axial load,± 250 Nm maximum torsional load). The machine was driven by Test Star 790.01 digital controller. After the measurement of all samples two stainless steel grips were used to catch each of them into the test machine. Each grip was characterized by a cavity with a diameter of 14 millimetres in which the sample was inserted. Each cylindrical sample was fixed into the grips using bone cement to avoid slips between grips and sample itself.

Figure 3.4: MTS 858 Bionix servohydraulic machine used to perform all compression, bending and torsional tests

- Compression test

  The sample 1 of Lot. 274 was sacrificed to find a theoretical breaking load from which preconditioning values would be set. The sample used for this test was chosen after qualitative analyses of the external surface from which it appeared as the most porous one. Before the tests started the operator measured the length of samples out of the grips. This was relevant to elaborate the data obtained at the end of each test. The upper arm of the test machine was lowered with a displacement velocity of 0.05 mm/sec and a frequency of 10 Hz. Displacement velocity was expressly set on a high value to verify a brittle fracture. The obtained value was voluntarily underestimated with respect to the potential of the material, however it could be considered acceptable to find the maximum value and minimum one of preconditioning cycles. During the first test no preconditioning cycles was realized, while all the remained samples were preconditioned with six preconditioning cycles with a maximum value of load equal to 500 N and a minimum one equal to 50 N. The maximum value was set in a range of thirty to fifty per cent of the maximum theoretical value of rupture load. After the first test, the displacement velocity was reset to a lower value of 0.5 mm/min to optimize the yield of Smartbone®. During the whole test it was possible to check the behaviour of the material under load condition by means of a PC connected to MTS 858 Bionix. Checks were focused on the linear behaviour of the material in elastic region, monitoring that no structural failure occurred both in preconditioning phase and in elastic region. At the end of each test, the grips were cleaned from cement and SmartBone® residual fixing the grip in a vise and using a hammer and a screwdriver to detach materials from the grips itself. This passage required using a moderate force to avoid damaging the internal surface of the grips that could be cause of malposition in the following tests.

- Bending test Each rod was arranged over the cylinders of the lower part of the bend test setup, then the actuator of the machine was lowered by the operator until contact between cylinders and sample. The force value applied by the machine was constantly monitored on the Test Star digital controller to prove the contact between the sample and the second grip. After the positioning of the sample the machine test was set on Force-control to control the force applied during the test.The same considerations done for cylinders were valid for rods, so here again Smartbone® samples need preconditioning to analyse their behaviour under bending loads. Therefore the sample 2 of the Lot. 276 was sacrificed to find the theoretical value of fracture stress. Here again it was tested without preconditioning. On the contrary all the remaining rods were preconditioned. The procedure used for these tests were similar to those used for cylindrical samples, except for the extreme values of preconditioning cycles, which was chosen between 5 N and 50 N due to the different behaviour of the sample under bending stress.

- Torsional test Two different types of samples were tested. The first group consisted of 8 cylindrical bovine matrix bone (lot N) without any polymeric component. The second set of samples was a group of 10 SmartBone® samples (lot TT). Each sample of the two groups was fixed into the grips using the same technique of cylinders used for compression test. Two non-treated

samples were sacrificed to obtain a theoretical value of breaking torque. Here again it was assumed an underestimated value of breaking torque but acceptable to set the extreme values of preconditioning cycles. After the sample was fixed into the test machine, the instrument was set on control-Torque to check the torsional value reached during the test. Before the tests started the operator measured the length of samples out of the grips. This was relevant to elaborate the data obtained at the end of each test. The machine was set with a rotational speed of 0.1 deg/s, adapting the set-up of a previous study . The velocity was reduced due to the differences between SmartBone® samples and the ones reported by the literature. During the first two tests no preconditioning phase was realized. All the remaining samples were preconditioned with six preconditioning cycles between a minimum torque value of -600 Nmm and a maximum one of 600 Nmm. Due to the characteristics of this test, it was important that the two arms of the machine was aligned before the test started to avoid that the MTS reached to torsional excursion limit. At the end of the test the grips were prepared for the following one with the same procedure used for samples broken under compression load.

Torsion	Max Torque [Nmm]	Max Stress [MPa]	Max Strain %	Torsional Elastic Modulus [MPa]	Kg/cm²
Medium Value	1'505.4	25.5	5.8	490.6	259.8
Standard Dev.	294.9	4.4	0.9	103.7	44.9
Bending	**Max Force [N]**	**Max Stress [MPa]**	**Max Strain %**	**Flexural Modulus [MPa]**	**Kg/cm²**
Medium Value	100.3	23.8	7.6	340.6	242.4
Standard Dev.	17.4	4.2	0.9	63.1	42.4
Compression	**Max Force [N]**	**Max Stress [MPa]**	**Max Strain %**	**Elasiticity Modulus [MPa]**	**Kg/cm²**
Medium Value	1'914.2	25.8	2.2	1'245.7	262.9
Standard Dev.	590.6	7.8	0.4	225.9	80.1

Figure 3.5: test's results

3.1.6 Comparison with different competitors

Comparative analyzes of SmartBone® with other bone substitutes of comparable function are given here. The SEM analysis of the morphology shows how SmartBone® has a high similarity with the microstructure of the human bone thanks to the height and interconnection of the open porosity along the entire thickness of the scaffold, while the alternative bone substitutes deviate considerably from the architecture of being human iliac crest, with structures characterized by very large pores and high variability. SmartBone®: elevates mechanical performance in particular compressive strength and modulus of elasticity comparable to those of human bone; this results in an appropriate resistance to the application of loads and therefore a fatigue in surgical maneuvers and toughness to fixation screws.

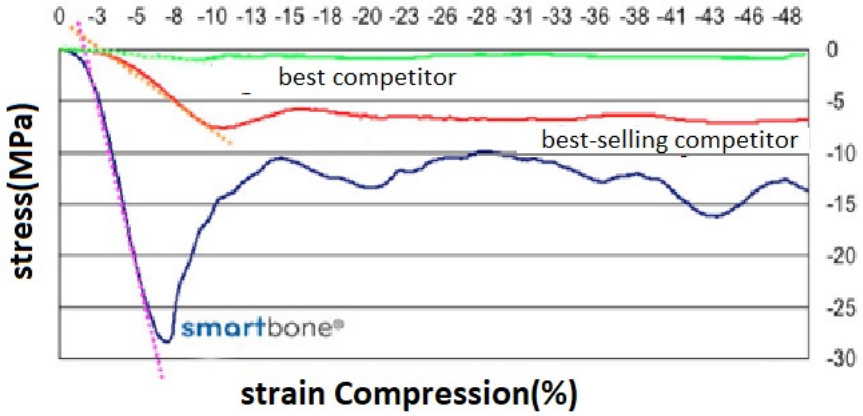

Figure 3.6: Andamento sforzo-deformazione: confronto tra il comportamento rigido-elastico di SmartBone e le caratteristiche meccaniche dei concorrenti.

On the other hand, the best-performing competitor and the best-selling bone substitute show characteristics two and ten times lower than those of human bone, as well as higher fragility. A further feature of SmartBone® is the high homogeneity between samples. Many bone substitutes present on the market show a very high interchange variability even within the same production batch, caused by the natural origin of the starting material; this is reflected in a non-homogeneous microstructure, porosity and density, which translates into a great variability of physical and mechanical properties. Although the starting material of SmartBone® is also natural, the production process followed allows to reduce this variability, so as to obtain more regular and homogeneous bone substitutes [35]

3.1.7 Smartbone commercial models

The smatbone models have different form and dimension such as rods, cube, cylinder, cone and powder,all of them are made by bovine adult woven bone and figure show different dimension of commercial smartbone.

Figure 3.7: smartbone commercial models

ITEM	SIZE	Q.TY
SMB011005	7 X 7 X 7 mm	1
SMB011010	10 X 10 X 10 mm	1
SMB011020	10 x 10 x 20 mm	1
SMB011030	10 x 20 x 20 mm	1
SMB011110	14 x 12 x 6 mm	1
SMB011130	14 x 12 x 8 mm	1
SMB011160	14 x 12 x 12 mm	1
SMB011180	14 x 12 x 20 mm	1
SMB011190	14 x 12 x 24 mm	1
SMB011210	15 x 30 x 20 mm	1
SMB011220	15 x 30 x 30 mm	1
SMB011230	15 x 30 x 40 mm	1
SMB011250	15 x 30 x 60 mm	1
SMB011310	16 x 14 x 6 mm	1
SMB011330	16 x 14 x 8 mm	1

Figure 3.8: smartbone parallelepiped commercial models

Chapter 4

Thesis proposal

4.1 Thesis proposal

The purpose of this thesis project is to study the Bone Substitute proposed by I.B.I. in all its peculiarities and understand its possible application in spinal surgery. To reach the aim all previous data obtained on Smartbone®® were considered and re-evaluated related to the new condition of use. thesis proposal try to solve main part of problems described and reported in chapter two. This capture tries to explain different improvements and futures that introduced with use of Smartbone® prosthesis.

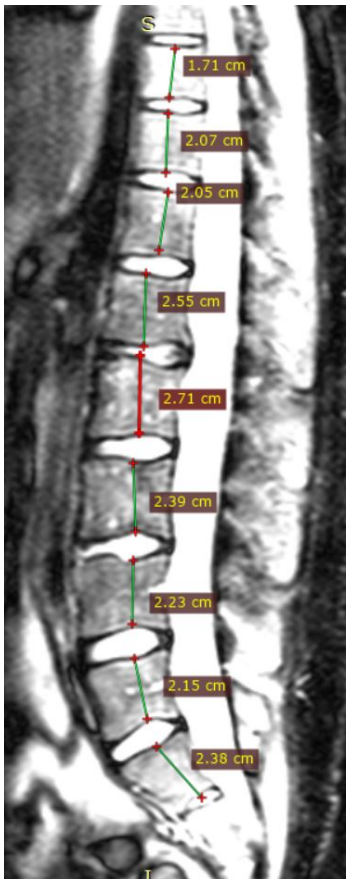

Figure 4.1: vertebral column

Database reports length of different height of different vertebra of vertebral column as shown in figure for cervical,thoracic and lumbar segment. for each vertebral part we gave two different vertebral body because vertebral bodies measurement increases from cervical to lumbar vertebra.

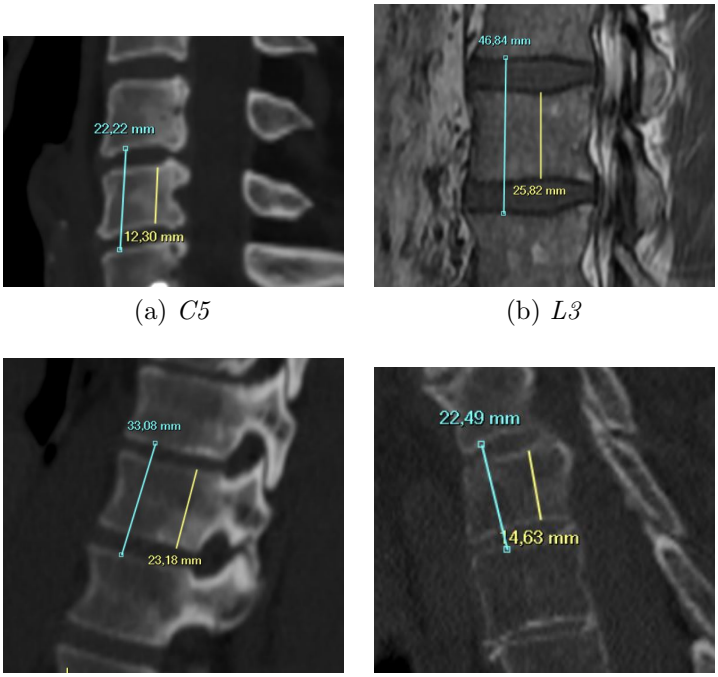

(a) *C5* (b) *L3*

(c) *T10* (d) *T3*

Figure 4.2: vertebral body measurement

According to section 3.2.6 witch reports different size of Smartbone® segments, the biggest size is 15x30x60 and for this reason we were forced to find a solution to make taller our models. According to the literature and different commercial models we have chosen to create a same model as modular carbon cages and an experimental model of Smartbone® prosthesis used in 2016 that make possible to fill in vertebral removed part. The carbon modular cages and the experimental of Smartbone® are kept together with a titanium screw witch lock different movements of prosthesis such as flexion and rotation of each cage. Furthermore, the screw has the function of avoiding that the various modules have a rotation between them. Rotating movement between different modules disturbs the process of osseointegration and osteogenesis witch leads to the failure of the total model going forward over time. looking for a model that would allow to removed this screw, so to had to create the same feature even with the joint. However, continued with the study of the joint in order to find the best interlocking model to avoid the rotation of the various modules and to facilitate the osseointegration of the prosthesis. At the same time joint should not disturb pedicle screws insertion, make easier screw position is important to decrease surgery timing and make better prosthesis stabilization.

(a) *No rotation*

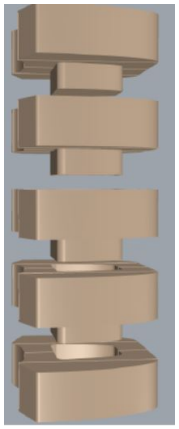

(b) *model's idea*

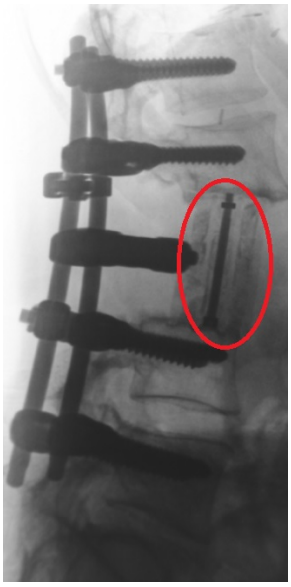

(c) *screw witch lock different modulus*

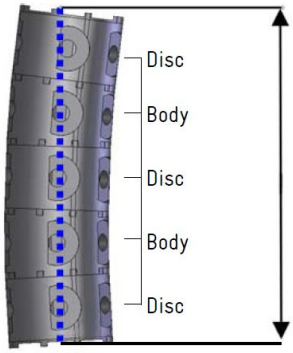

(d) *carbon cages*

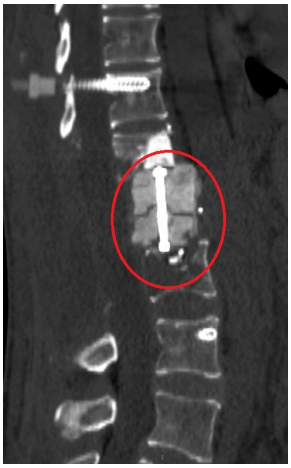

(e) *screw witch lock different modulus of Smartbone®*

(f) *Smartbone® prosthesis*

Figure 4.3: Joint model

4.1.1 Prosthesis model

Started from different CT images to create a model very similar to the natural vertebral body and to give a shape much closer to the physiological shape of the vertebra. subsequently to study the shape of the vertebra starting from the CT images and have measured the vertebral plate in different directions. performed this process throughout the spine for cervical, lumbar and thoracic vertebrae. we obtained different measures as we can see in the figure.

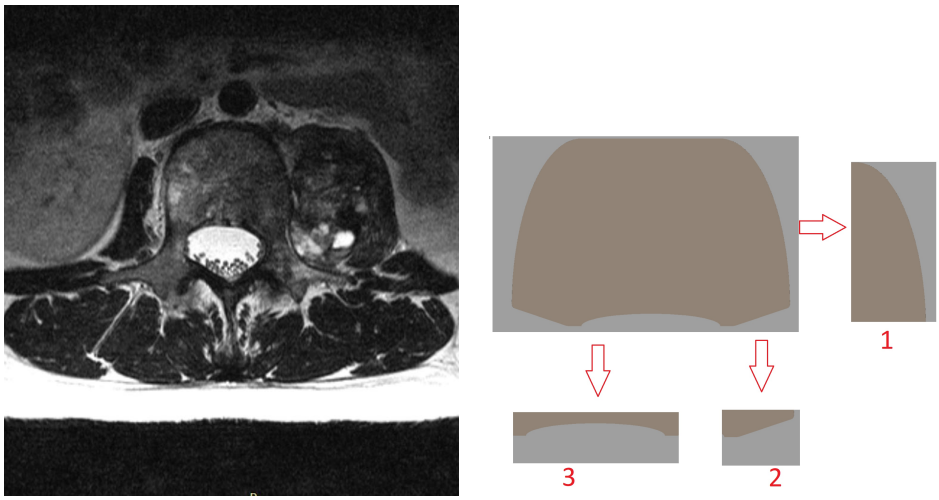

(a) *Vertebral body* (b) *prosthesis different parts*

Figure 4.4: prosthesis model

Starting from the the shape of the vertebrae we tried to find the shape of the prosthesis that was closer to the natural shape of the vertebral body.As it is shown in the image 1 of figure[] there is a slight curvature that has the purpose of not presenting corners and give the model softer curves that avoid damage to the surrounding tissues and facilitate the insertion of the prosthesis.

when the laminectomy is performed a cut is made on both peduncles and the cutting surface created is a guide to the doctors in order to insert the pedicle screws and for this reason have decided to create a inclined surface with an angle of about 20 degrees that allows surgeons to have a surface on which to insert the screw perpendicularly, to prevent the screw coming out from the front of the prosthesis and at the same time does not allow surgeons to do not damage the joint image 2 of figure.

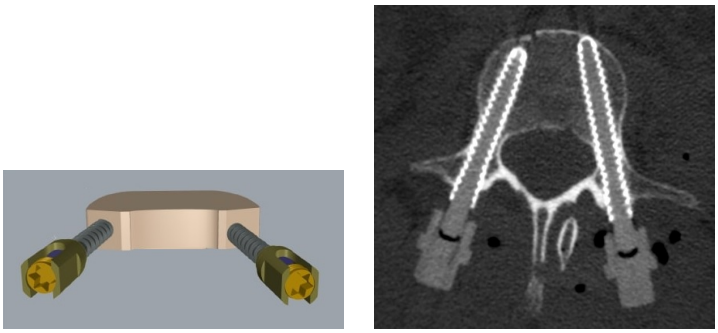

(a) *screws + Smartbone® model*

(b) *CT with pedicle screws*

Figure 4.5: screw insertion

image 3 of figure shows a curvature that was designed to give the prosthesis the same appearance of the back of a vertebra and to avoid damage to the marrow. Have seen later that a smooth surface would still be a good result and we decided not to cut that part to have a greater contact surface even if minimal compared to before. This at the same time allowed us to decrease the time of the process and have a less number of milling passages.

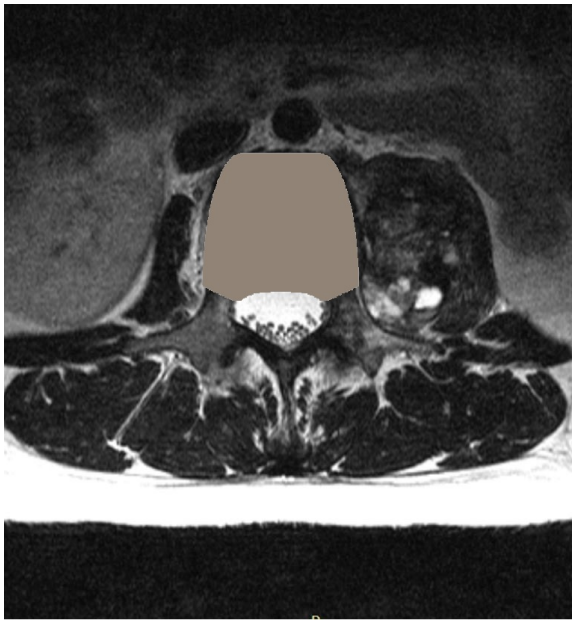

Figure 4.6: Smartbone® model

Start to make the body of the prosthesis so that it was adaptable to different use cases and to different patients. to create a fixed initial and final module that are the parts that will come into contact with the vertebra and a central part that has the function of lengthening the model and its number changes according to how long it is desired to lengthen the model.

- Initial part: It has a superior smooth superice that comes into contact with the vertebral plate of the superior healthy vertebra and is the part where the osseointegration between the healthy vertebra and the prosthesis occurs. There is a joint witch goes to interact with the central piece or the final piece to create the complete prosthesis

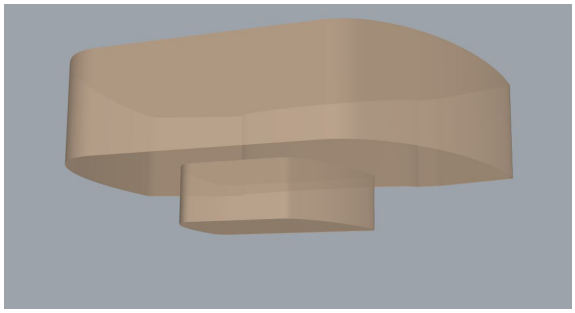

Figure 4.7: initial part

- Final part: Just as the initial model has a lower smooth superice that comes into contact with the vertebral plate of the lower healthy vertebra and is the part where we have osseointegration. This part part absorbs all loads of the prosthesis and transmits them to the lower vertebrae. In this case we have a hole that houses the joint of another module that can be either central or initial.

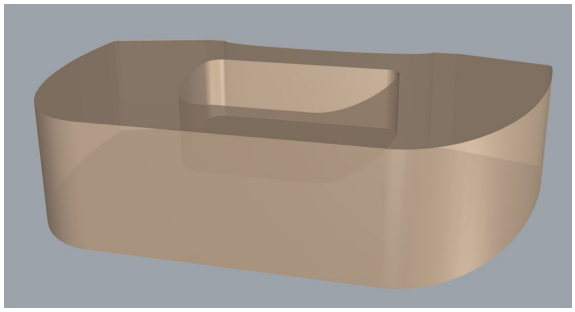

Figure 4.8: final part

- Central part: The central part is the most present module in our prosthesis and is the part that has the task of lengthening the model up to the desired height. It has a contact through a joint with the lower segment and houses the joint of the upper module .

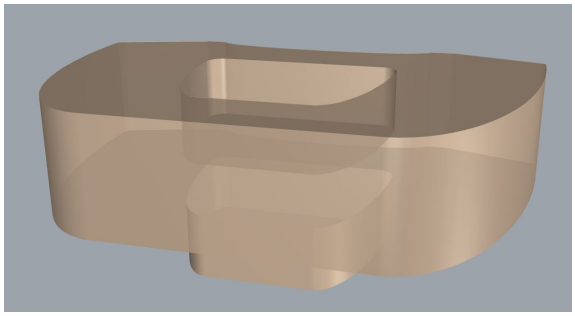

Figure 4.9: central part

4.1.2 model sizing

The vertebral column is not the same dimension in all its length, the size grows starting from the cervical vertebrae up to the lumbar vertebrae and also varies according to age, gender and the patient dimensions. For this reason we have created different sizes of vertebral prostheses in order to cover all three vertebral departments. to search for the correct size based on measurements and images To measure the dimensions of the vertebrae from the CT images and the information taken from the literature. Starting from this information begin to create three different models of three different sizes in order to cover the entire length of the column and at the same time patients with different sizes and gender

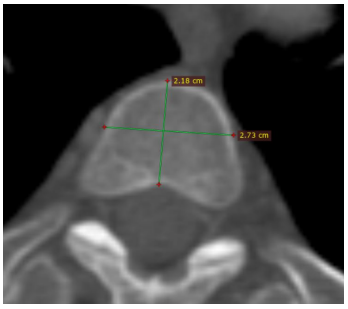

(a) *Cervical vertebral plate measurement*

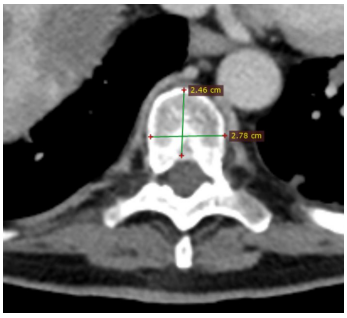

(b) *Thoracic vertebral plate measurement*

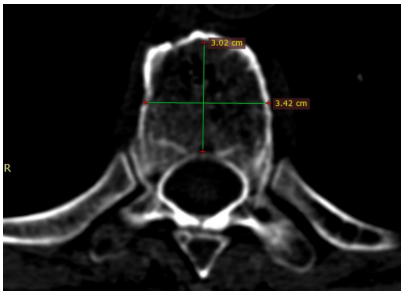

(c) *Thoracic vertebral plate measurement*

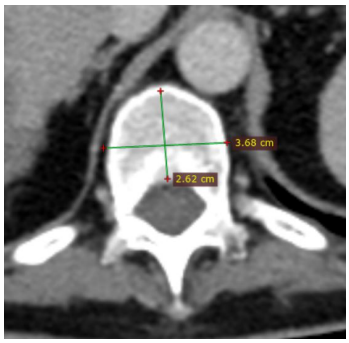

(d) *Thoracic vertebral plate measurement*

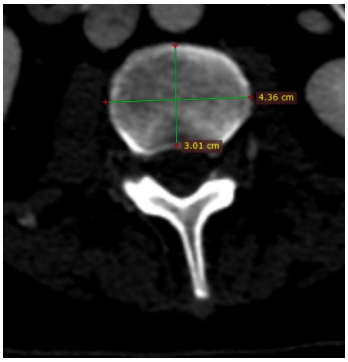

(e) *lumbar vertebral plate measurement*

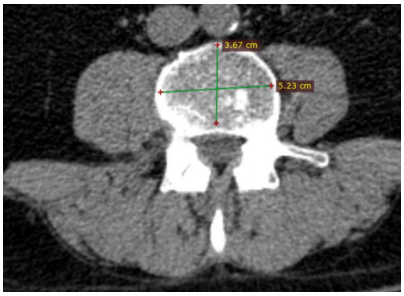

(f) *lumbar vertebral plate measurement*

Figure 4.10: different vertebral plates sizes

Different measure obtained by image and from literature are presented in figure. There are four different size of vertebra and different for cervical, thoracic first part, thoracic second part and lumbar part of vertebral column. Starting from these measures we went to check if they were feasible with the biggest form of Smartbone®. As mentioned in chapter 2 during the milling process to keep fixed Smartbone® we use two rings and for this reason we will lose a side part of the parallelepiped of Smartbone®s as support. However, we went to draw the trajectories of the cutter through the program of the milling machine and as we can see in the figure the trajectory escapes from the raw piece that is the rectangle that presents the Smartbone®. It was not feasible for the milling process for which we had to resize by correcting some dimensions as we can see in the figure.

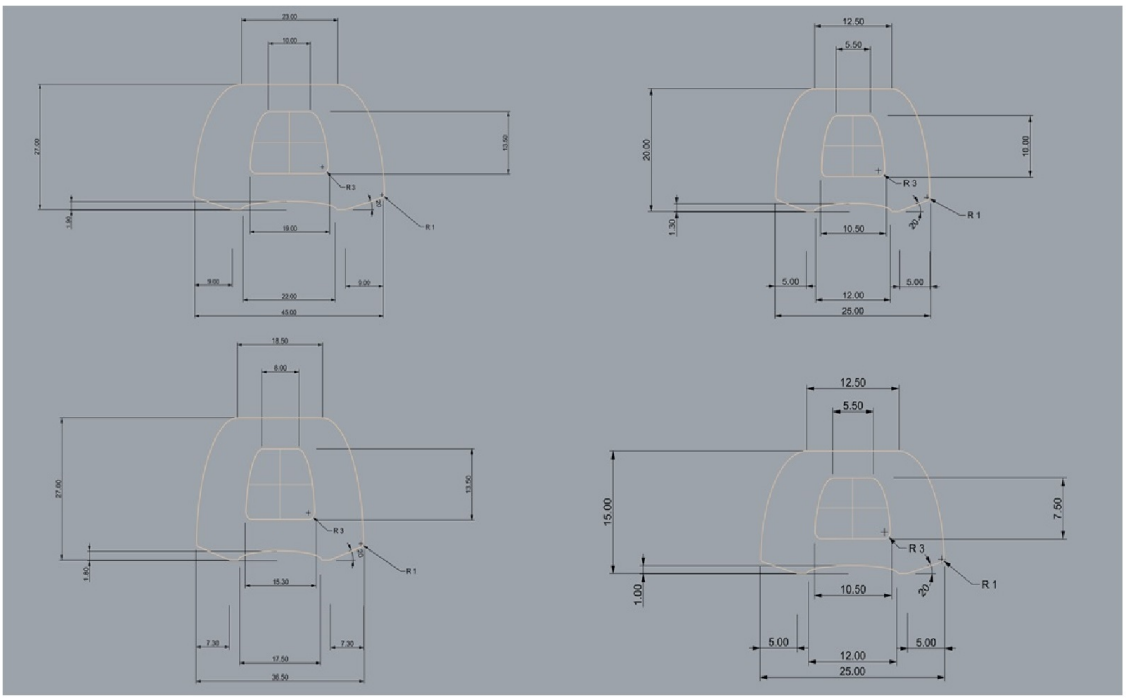

Figure 4.11: sizes takes from CT images

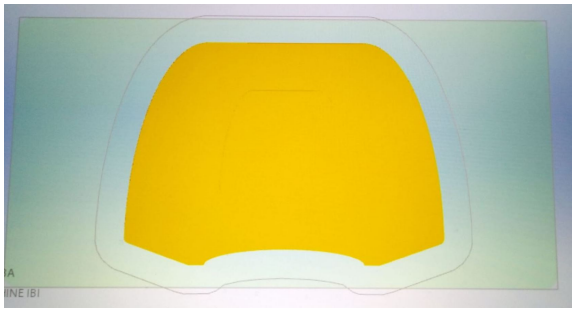

Figure 4.12: Smartbone® parallelepiped with our model

In order to have a feasible model to make changes and modify some measures. continued with the elimination of the posterior curve because with a smaller model are sure that the marrow will have no contact with the prosthesis.

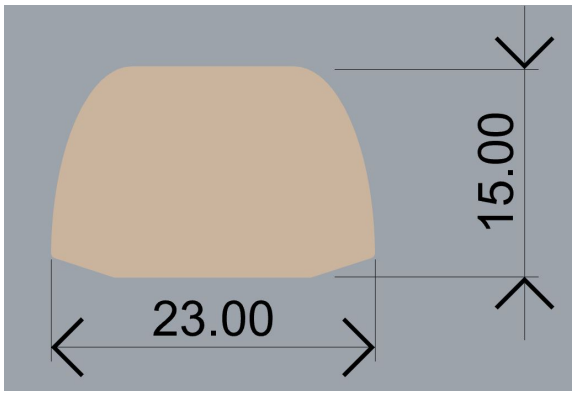

(a) *small prothesis*

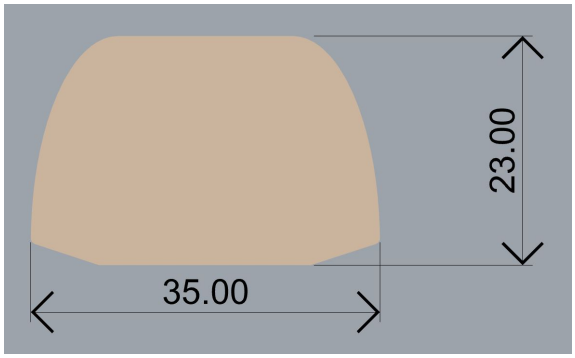

(b) *medium prosthesis*

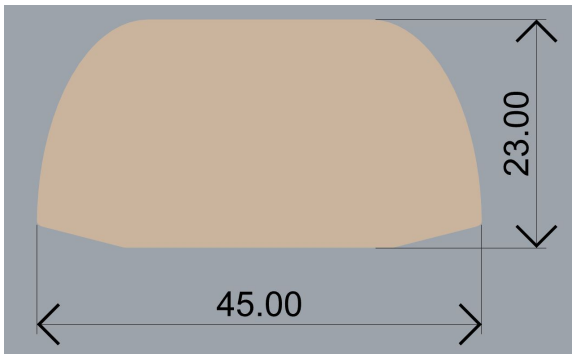

(c) *large prosthesis*

Figure 4.13: different Smartbone® models with three correct sizes

4.1.3 Joint

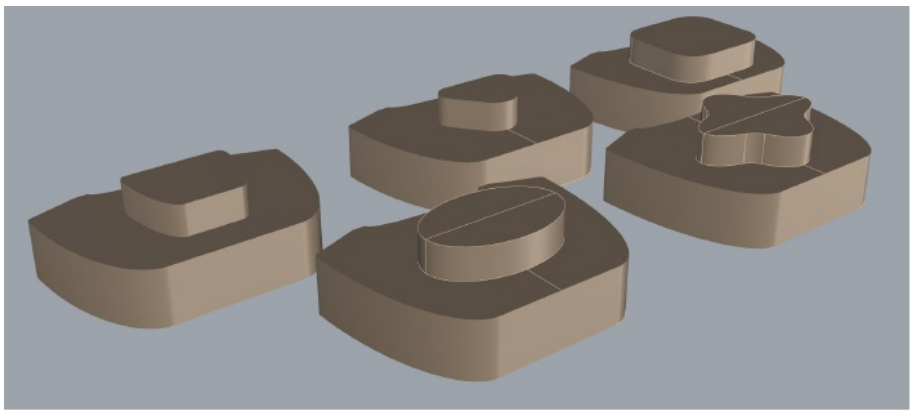

Figure 4.14: different joints

Different joint models won't be able to lock modulus and helps screw insertion. Started from 5 different joints such as cross, square, triangle and ellipse models. The ellipse and cross joints disturb the pedicle screw insertion and this could bring to the failure of the prosthesis in the time. A crew's bad position could bring to break one of joints and for this cause prosthesis could lose it's effectiveness in time upon to break. At the same time we are compared the rectangural model with the tringular model; have gone to analyze the problem list of both models. The rectangular one has the advantage to give us a surface with enough great contact between a joint and the another one but at the same could disturb the insertion of the screw and this could bring to the break of the prosthesis. The triangular model allows us to insert the pedicle screws without any disturbance but the problem of having a minor contact surface remains. According to this reason choosen to combine both models creating a trapezoidal model that allows to have a greater contact surface witch allows a better osseointegration and at the same time doesn't upset pedicle screws insertion.

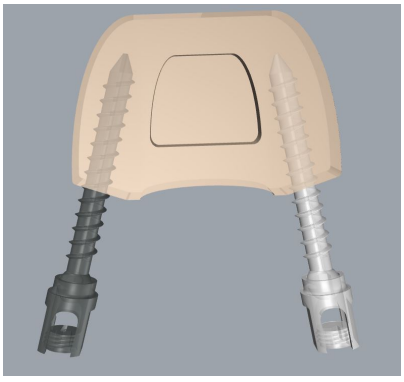

(a) *joint and screws relationship*

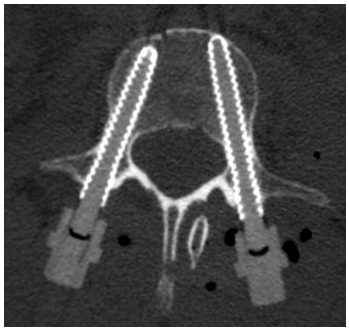

(b) *pedicle screws CT image*

Figure 4.15: joint and screws

Having a maximum height of 15 mm, we have dedicated 10 mm to the body of the prosthesis and 5 mm remaining in the joint as can be seen in the figure. A height of 10 mm has been chosen as it can give an advantage to simplify the calculation of the length (1 module added lengthens by 1 cm) and at the same time this can decrease the time of operation in the surgery room.

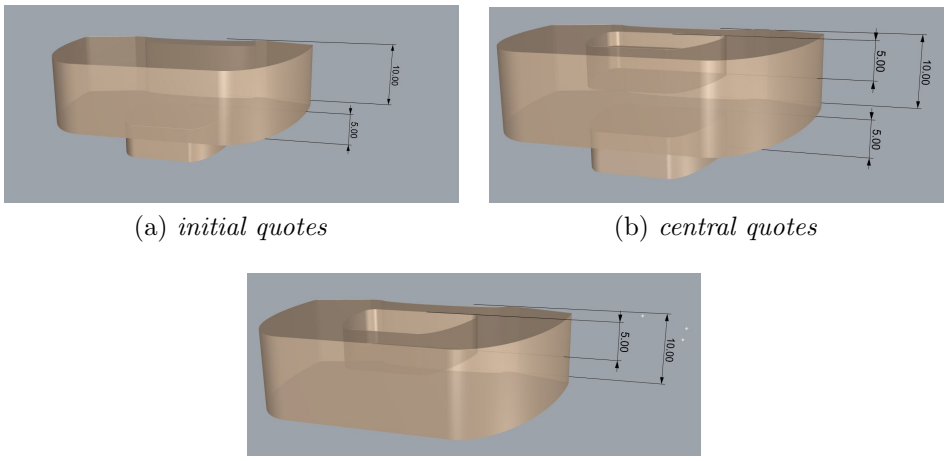

(a) *initial quotes* (b) *central quotes*

(c) *final quotes*

Figure 4.16: Smartbone® model height

Tumor surgery is difficult to planing and possibility of modeling prosthesis with a cutter directly in the surgery room could offer a huge advantage to surgeons, this feature is one of the most important feature the could be offer by Smartbone® and obviously this feature could make a prosthesis made of Smartbone® more malleable than all of other prosthesis. This is another important way to change prosthesis length and made it shorter and this surgeons can use it to shape the modulus of smarthbone.

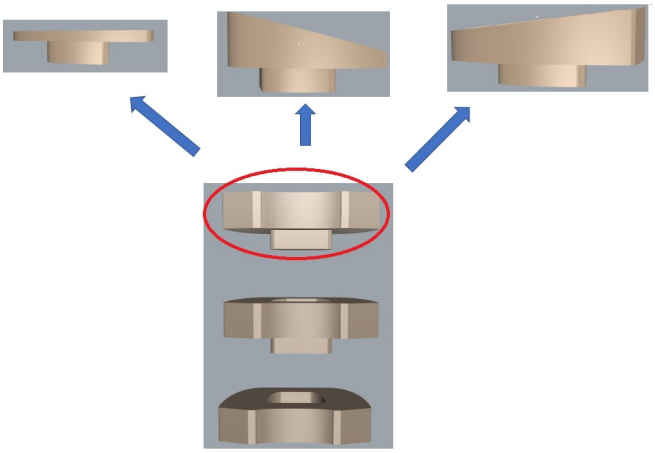

Figure 4.17: show how to milling Smartbone® prosthesis

However, this can be a further advantage as it allows us even in some cases to create a sloping surface allowing to reproduce a kyphosis or lordosis.

- Modello cervicale:

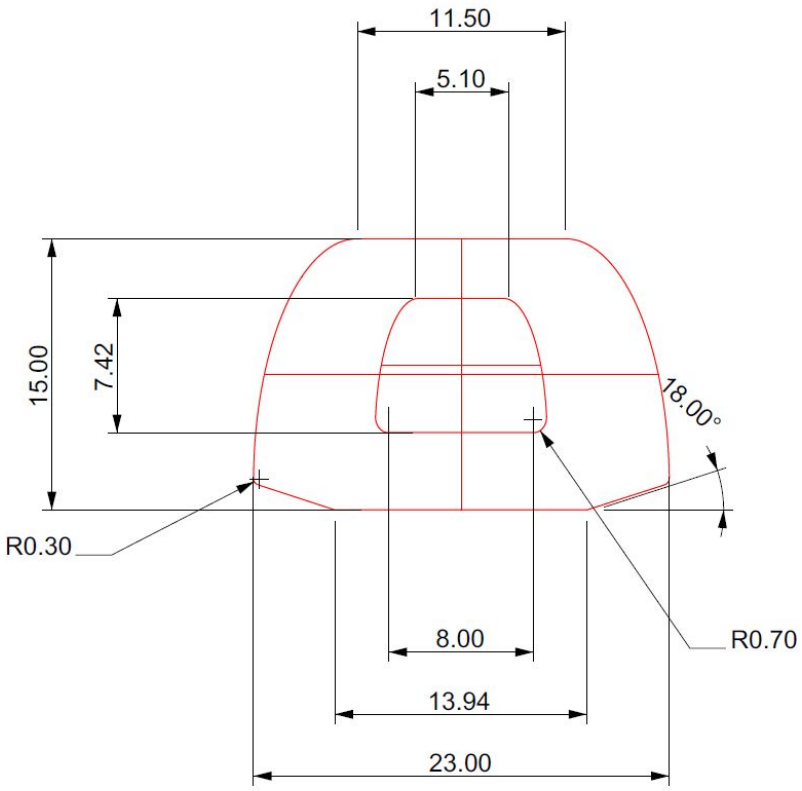

(a)

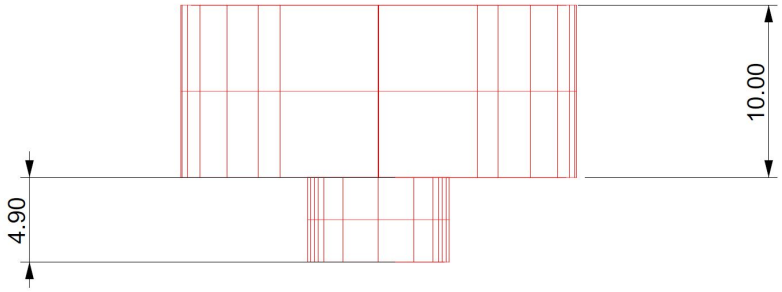

(b)

Figure 4.18: initial small part quotes

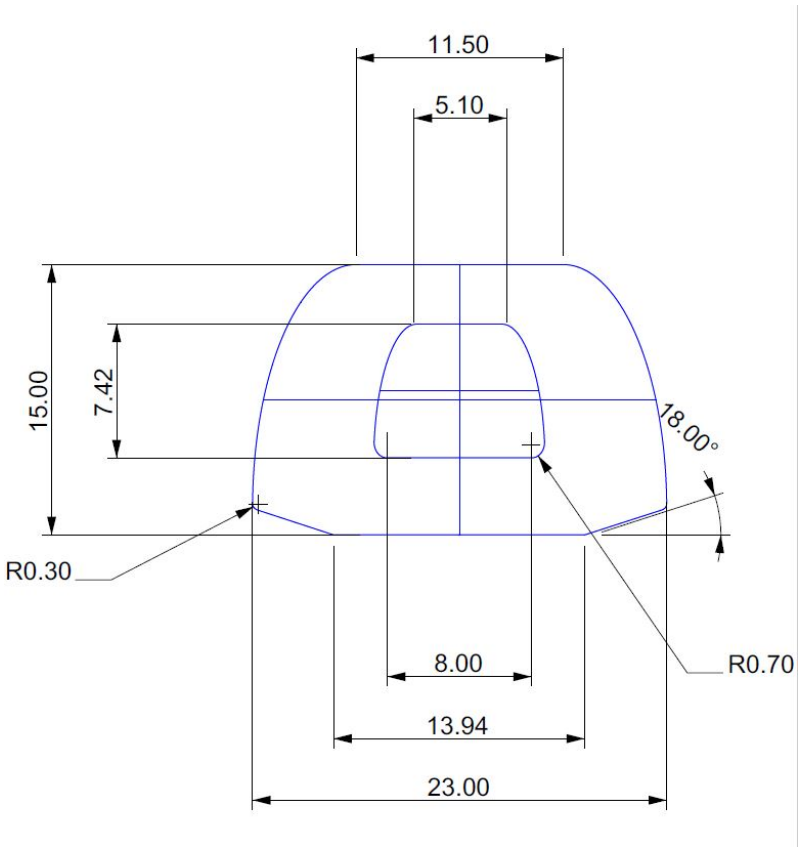

(a)

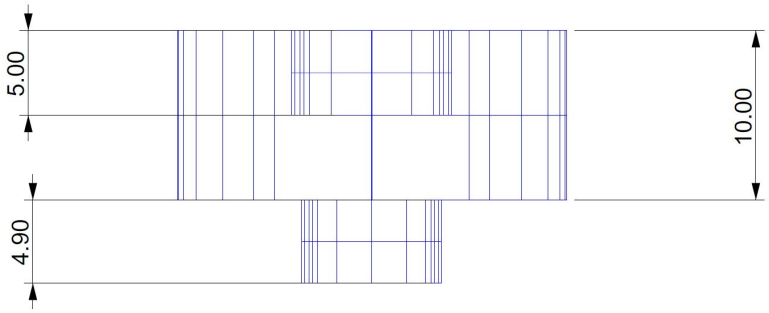

(b)

Figure 4.19: central small part quotes

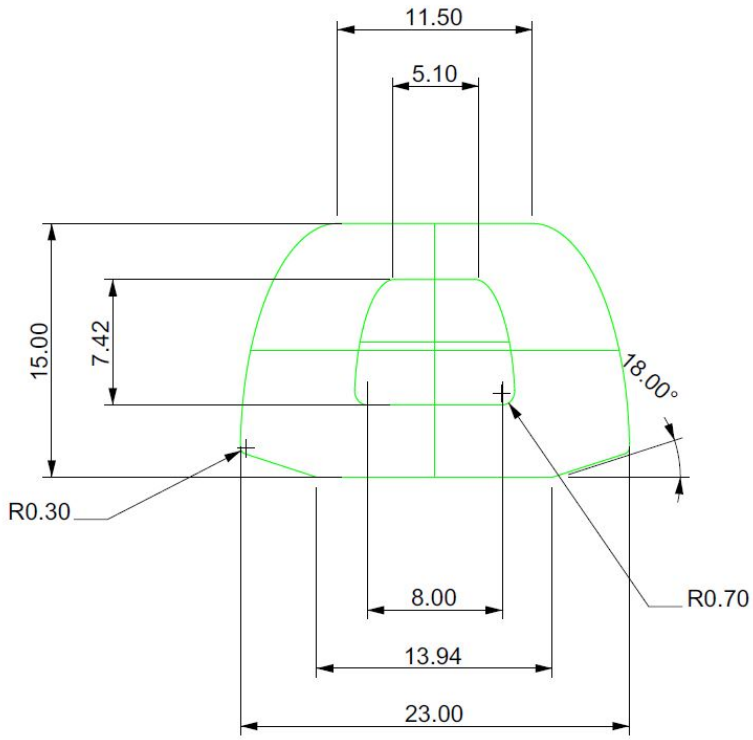

(a)

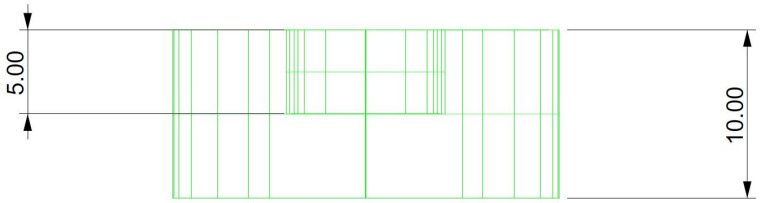

(b)

Figure 4.20: final small part quotes

- Modello toracico:

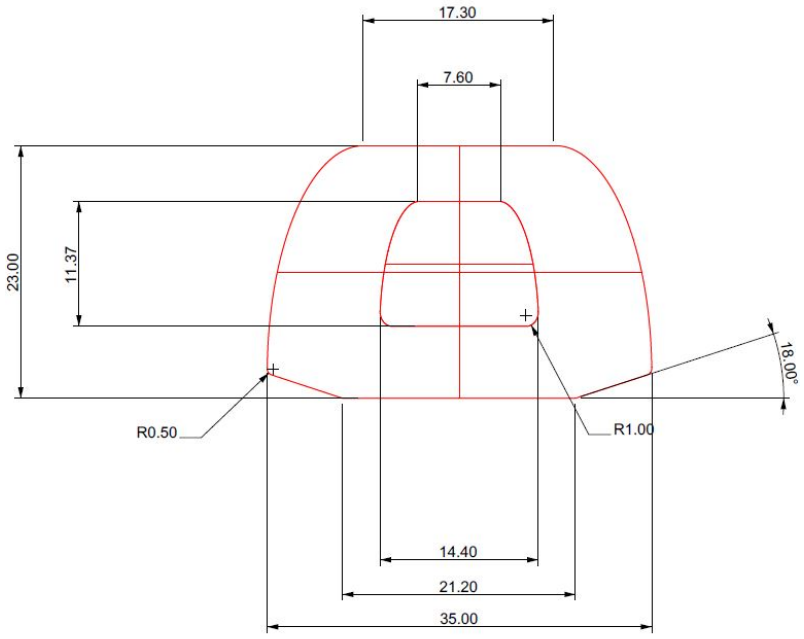

(a)

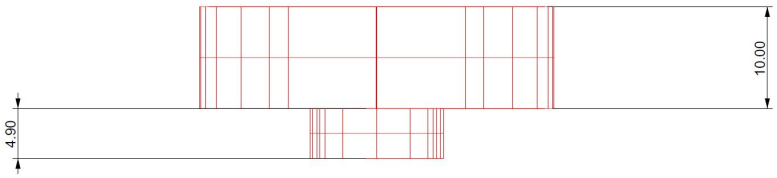

(b)

Figure 4.21: final medium part quotes

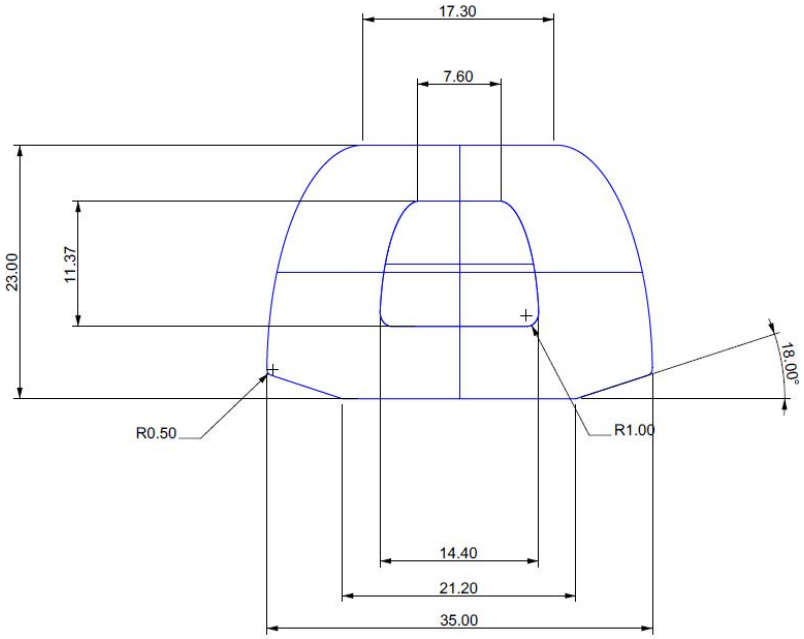

(a)

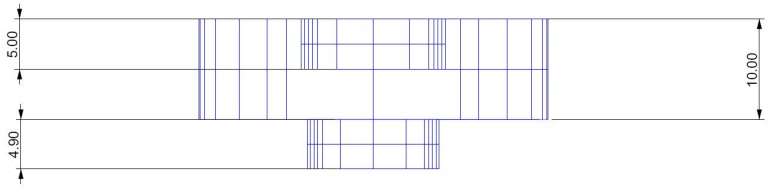

(b)

Figure 4.22: central medium part quotes

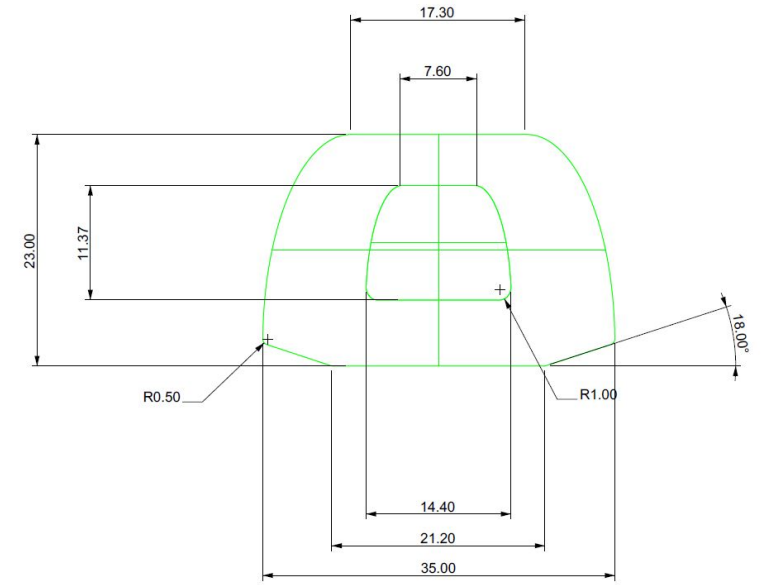

(a)

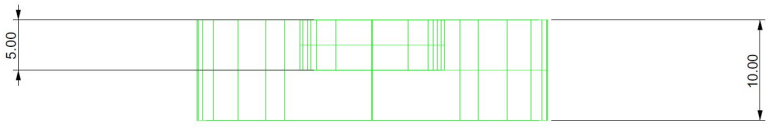

(b)

Figure 4.23: final medium part quotes

- Modello lombare:

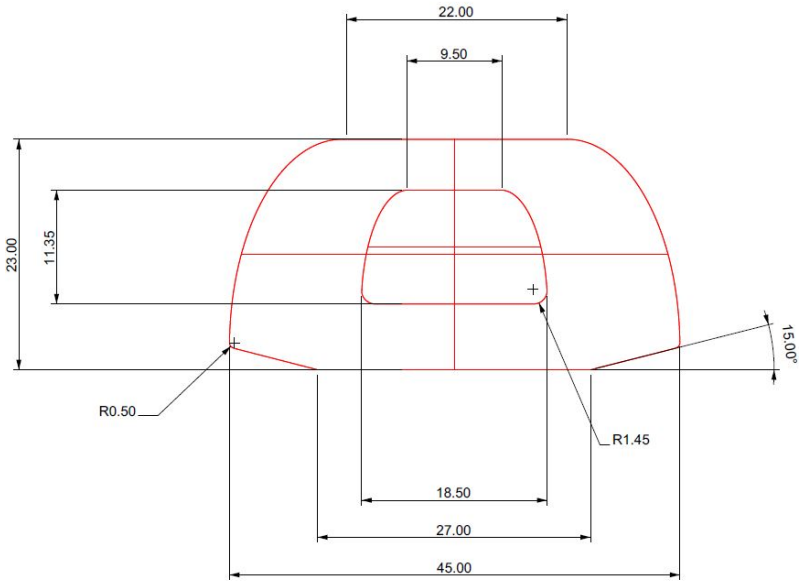

(a)

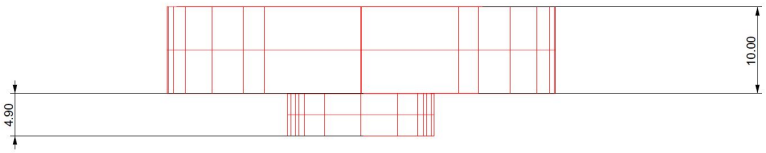

(b)

Figure 4.24: initial large part quotes

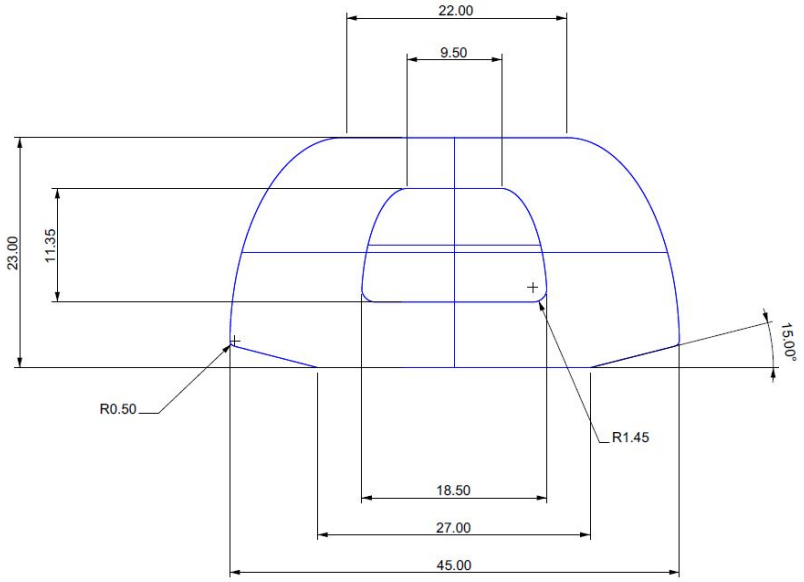

(a)

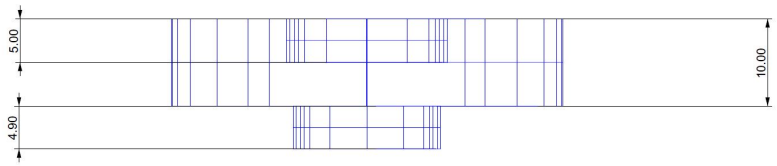

(b)

Figure 4.25: central large part quotes

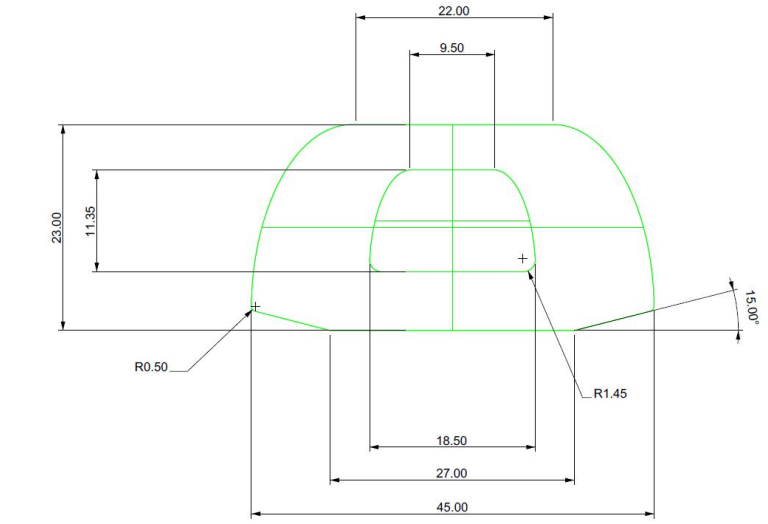

(a)

(b)

Figure 4.26: final large part quotes

4.1.4 Mechanical tests

Mechanical tests have been carried out on the initial and final prosthesis to evaluate how the joint acts under stress. For this reason, on the model we performed some mechanical tests and we have studied the joint in different cases. We assumed that there are 3 different cases as we can see in the figure .

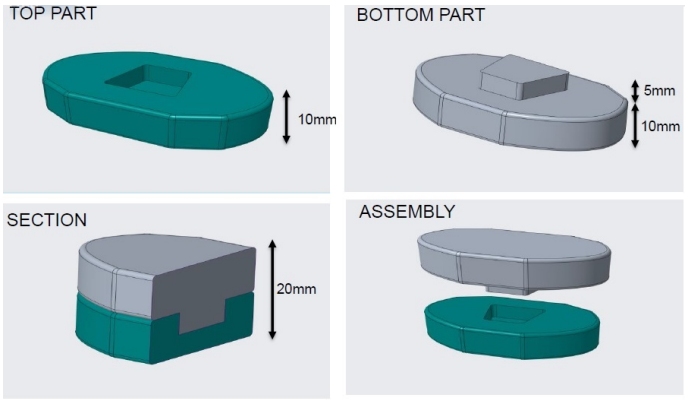

Figure 4.27

- case 1: Case in which there is contact between the upper and the lower part and at the same time a perfect contact between the bodies of the two prostheses. this is the case that we try to have in all the different joints in our model.

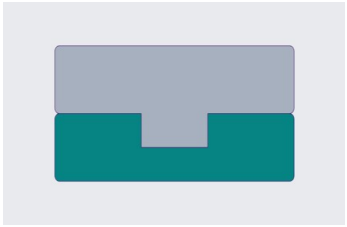

Figure 4.28

- case 2: Case where we have a joint with a lower pitch than the standard one and this means that there is no perfect contact between the joint at the top and the bottom.

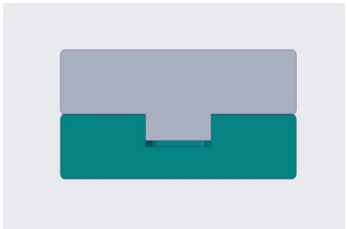

Figure 4.29

- case 3: In which case we have a longer joint than expected and this causes contact between only two joints of the upper and lower part and not between the two vertebral bodies.

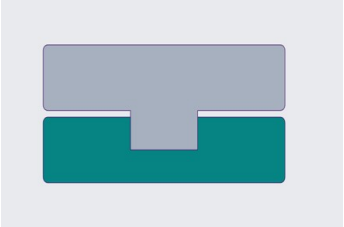

Figure 4.30

Starting from these three cases we went to evaluate the 3 different cases under loads. However, we have chosen in both cases to lock the model to the surface of the lower part and then be able to apply a concentrated force of 1000 N at the central point of the upper surface of the model and then we applied a bending moment that was applied equal to 7.5 Nm.

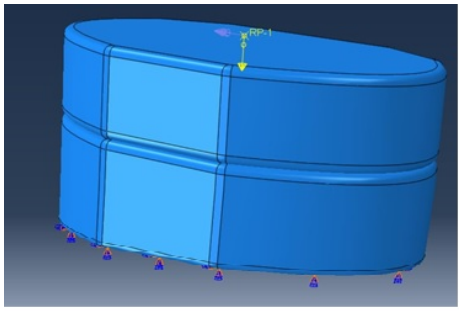

(a)

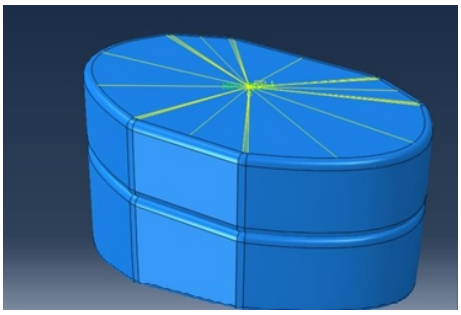

(b)

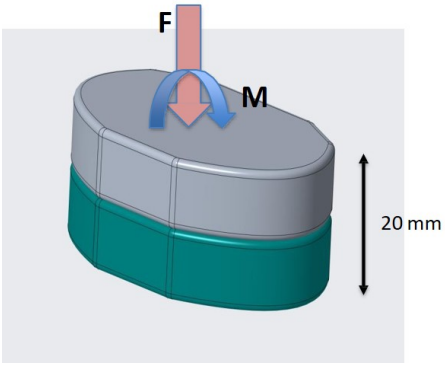

(c)

Figure 4.31: modello centrale

The main purpose of mechanical tests is to simulate how the prosthesis behaves under compression and bending to simulate the most common daily movements such as a forward or backward bend or the distribution of the load over the prosthesis in an upright position.

mechanical test reporrts:

1. Possible deformation
2. Possible cracks at points where stress is most concentrated.
3. Possible movements between modules that could disturb the osseointegration.

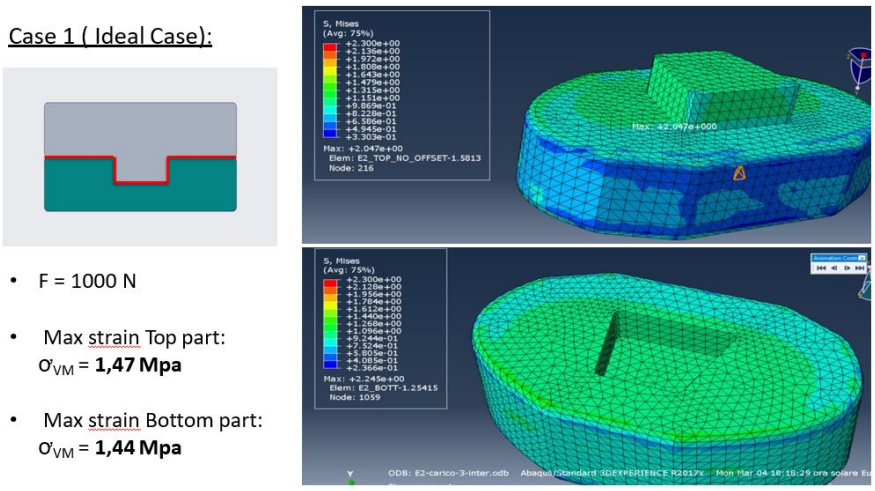

Figure 4.32

As can be seen in figure loads are equally distributed and there is a maximum concentration in correspondence with the edges of the joint because it is the point of maximum carving angle while there is a minimum distribution on the lateral surface of the prosthesis body. For this reason it is possible to observe that the forces are concentrated more in the area of the joint than in the area further away from it, and color scale go from green to blue starting from the joint up to the outher part and this shows that the forces are more concentrate on the joint and they are slightly different. The maximum tension obtained is 2.47 MPa for top part and 2.24 MPa for the bottom part, values that compared with experimental tests reported in the table in chapter 2 are 10 time smaller, so we can be sure that the prosthesis does not arrive to breaking at any point under compression.

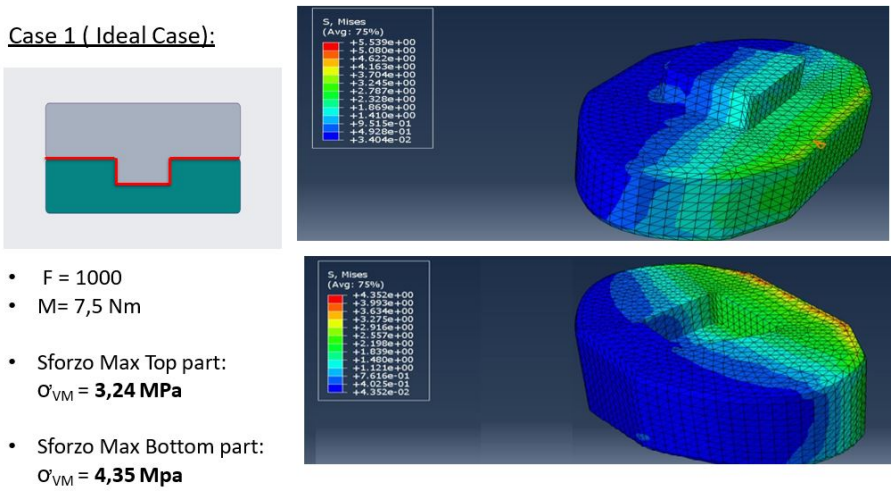

Figure 4.33

In the case of flexion there is a greater concentration of stress on the edge opposite to the surface on which the force that generates bending moment is applied, stress increases gradually from the point in which this force is applied to the opposite side along the entire prosthesis. the maximum tension obtained is 5.5 MPa for the top part and 4.35 MPa for the bottom part, values that compared with the experimental

tests reported in the table chapter two are 5 times lower so we can be sure that the prosthesis does not reach break in no bending point.

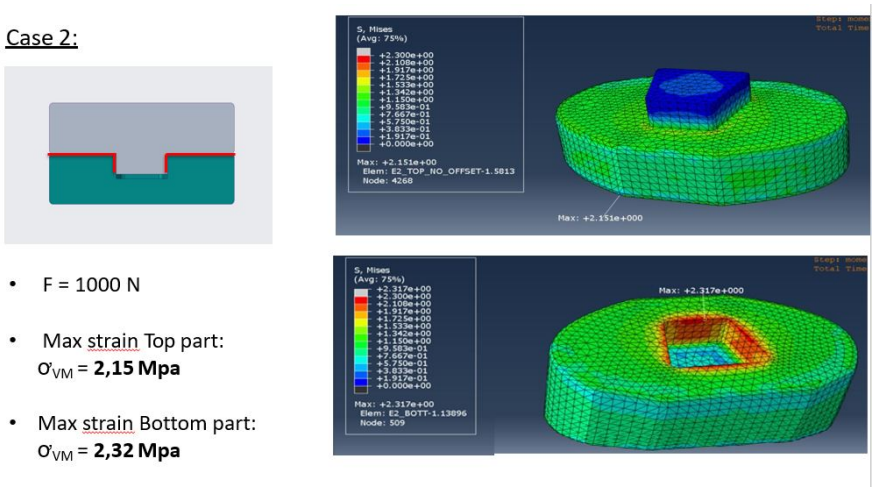

Figure 4.34

In this case, there is a concentration of the maximum stress on the interface between the lateral surface of the joint in the bottom part and in the top part, stress is transmitted completely on the lateral surface of the joint of the the bottom part. the maximum value reached by tension is 2.32 MPa witch compared to the values reported in the table in chapter two are 10 times smaller so we can be sure that the prosthesis does not reach breaking point under compression. At the same time the other surfaces of the prosthesis present homogeneous distribution of loads.

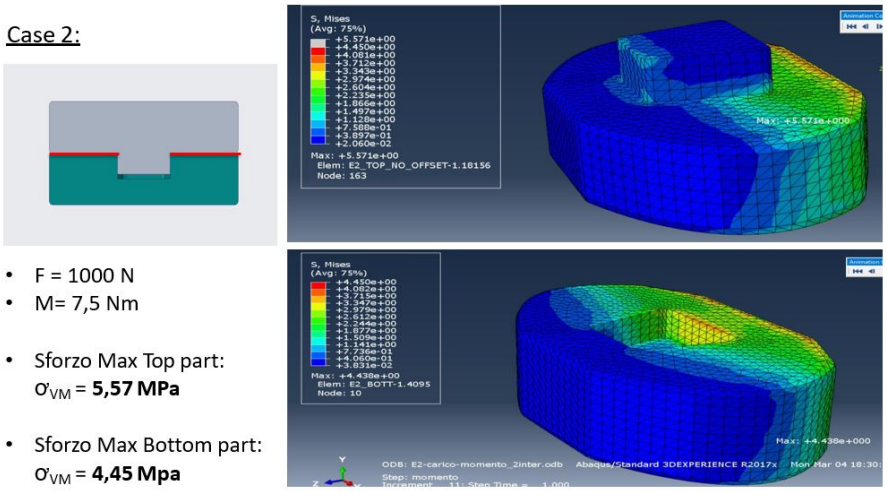

Figure 4.35

In the case of bending, there is a greater concentration of stress on the edge opposite to the surface on which the force generating bending moment is applied. this time, compared to the ideal case, there is a greater concentration of stresses in the top part along the lower edge of the rear surface and along the two edges of the front part of the joint and along the junction between the rear surface of the joint and the lower surface of the vertebral body. Along the bottom part, the greatest stresses are on the surfaces that interface with the surfaces on witch there was the

greatest stress in top part, but with values less than 1 MPa, since it is the part that directly resists stress. this stress allows to say that there is no detachment between the two parts and is concentrated on the edges of the front part of the joint that blocks the reising of the top part than the bottom part. Form the simulation we can see the impossibility of generating micro-movements between the parts, since the are blocked thanks to the contact between the lateral surfaces of the joints, this will allows a faster osteointegration. the maximum tension is 5.57 MPa fot the to p part and 4.45 MPa fot the pottom, values that compared with experimental tests reported in table in chapter two are 4/5 times lower, so we can be sure that the prosthesis does not arrive breaking point.

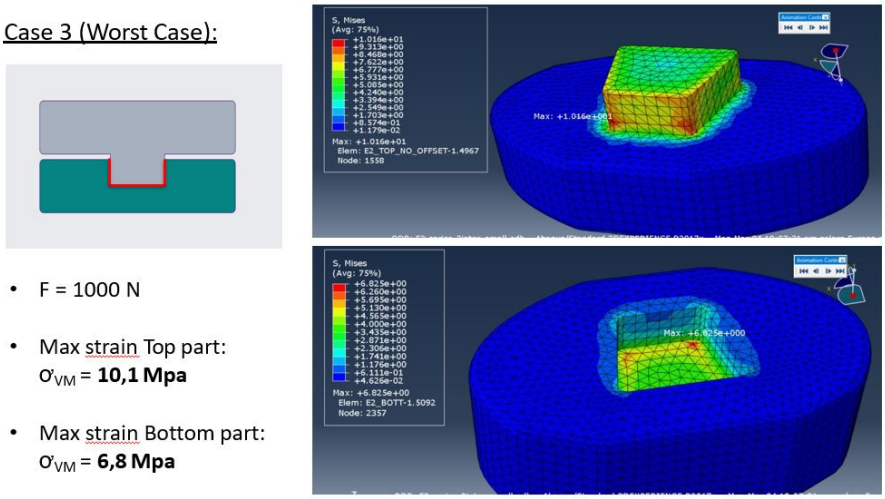

Figure 4.36

In this case, having any contact between the surfaces of the vertebral bodies, stress concentrates onluyy on the surface of the joint in a greater way on the edges. the maximum value reached by tension is 10.1 MPA, witch compared to the values shown in tabe in chapter two is the half the maximum value of breaking point,therefor we can have a higher demand than two previous cases.

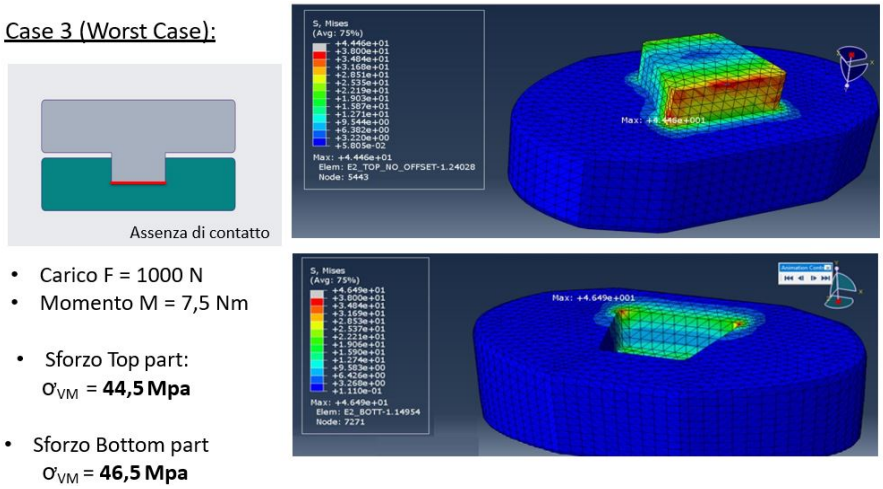

Figure 4.37

For the bending we can see that stress concentrates on the posterior surface of

the joint creating a dislocation between the bottom and top part. The maximum tension is 44.5 MPa for the top part and 46.5 MPa for the bottom part, values that compared with the experimental test reported in the table chapter two are 2 times higher and this would lead the failure of prosthesis.

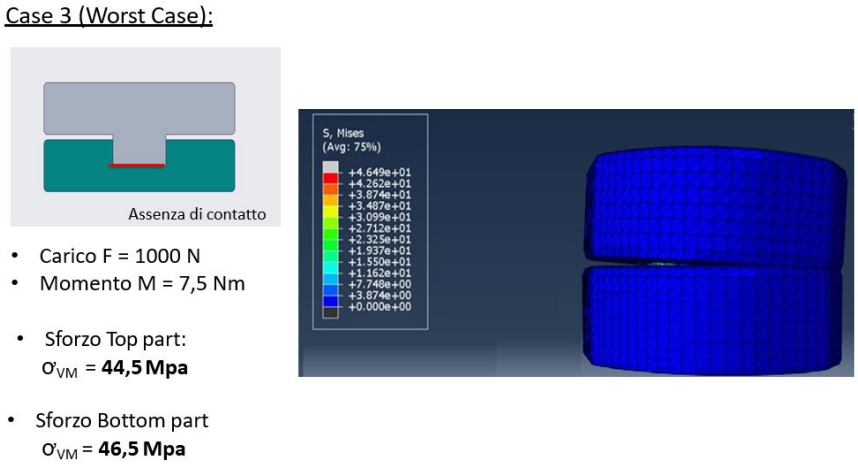

Figure 4.38

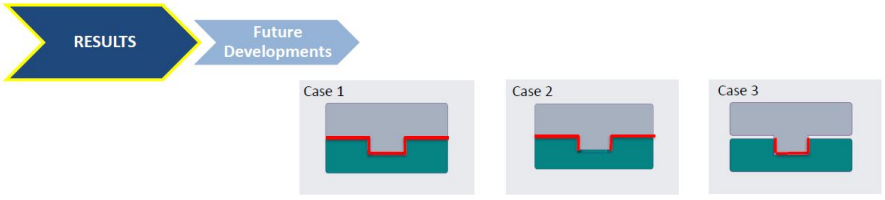

	TOP PART			BOTTOM PART		
# CASE	CASE 1	CASE 2	CASE 3	CASE 1	CASE 2	CASE 3
Compression TEST **(Mpa)**	1,47	2,15	10,1	1,44	2,32	6,8
Compression + Bending TEST **(Mpa)**	3,24	5,57	44,5	4,35	4,45	46,5

Figure 4.39

Among the simulated models the ideal case is the best but it is possible to drow but not to reproduce becouse due to the accuracy of the milling process one cuold have case1, case 2 or case 3. As the case 1 case2 has values that do not deviate too much from each other and do not lead to the failure of prosthesis as in the case 3. It was decided to decrease the height of the joint by 0.1mm in orter to be sure not to reach the failure of the prosthesis and make sure to remain in case 2 with little probability in the ideal case. After defining the optimal measures to have good mechanical coupling as well as a model with a functional geometry, we moved on to the production phase.

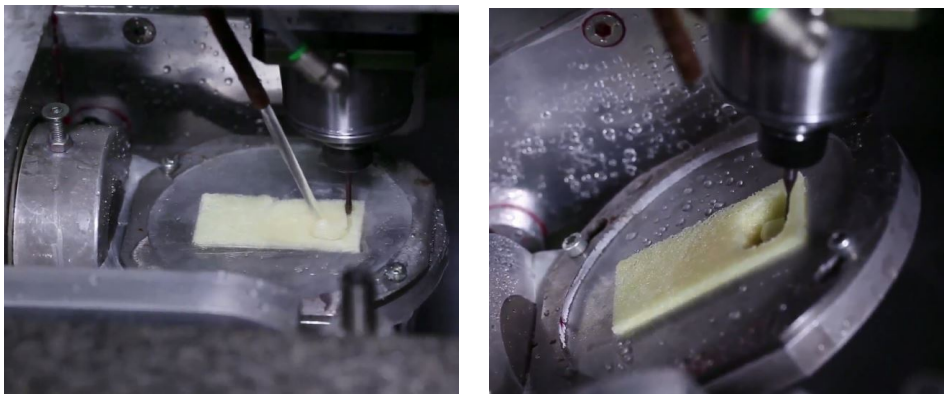

(a) (b)

Figure 4.40: modello finale

Finally, 3 prosthesis models were produced in which we took into account the measurements of the Smartbone® and milling processes. van be seen than original model, the back cuves wa removed, which took into account the area of positioning of the marrow in that it was irrelevant when resizing the various models. Furthermore, there is a tolerance of 0.05 mm for the vertical faces of the joint and 0.1 mm for the horizontal faces than respect to initial model as to be sure that a joint enters inside a cavity without scratching and damage the next modulus.

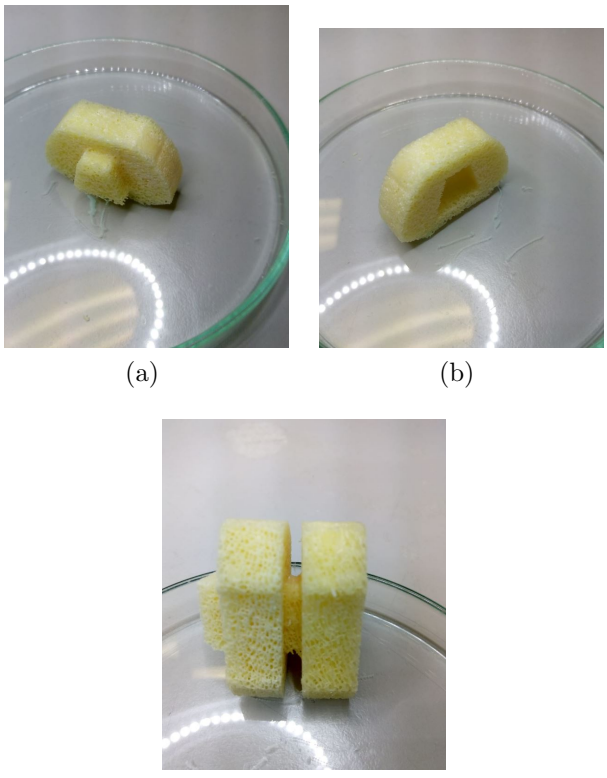

(a) (b)

(c)

Figure 4.41: modello finale

4.1.5 Alternative model

The size of the vertebral body varies with the age for which we have seen that in the case of very young patients we have the cervical vertebrae that are smaller than the vertebrae previously produced, so that the constructed models were not appropriate to them. As we can see in the figure the measure of the vertebrae is less than 15mm that is the minimum measure of our prostheses.

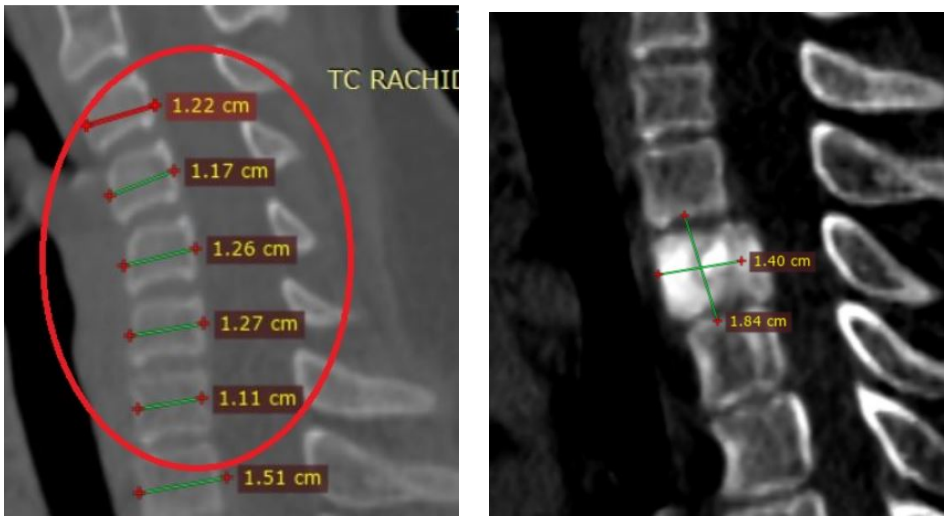

(a) *cervical and thoracic CT* (b) *cervical and thoracic CT*

Figure 4.42: vertebral column

For these few cases we have decided to create a prosthesis that has the same shape as the previous prostheses except that the modularity is lost and the changes in the size of the prosthesis are milled directly in the surgery room. At the same time no longer having the limits imposed previously measured by the parallelepiped of Smartbone® and having to make a prosthesis with a size of 15 mm we decided to mill it in long and thus obtain a height of 25mm but not modulated.

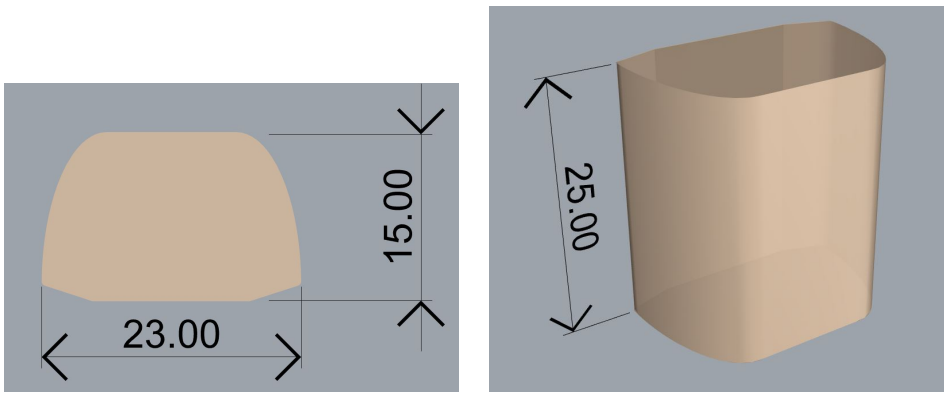

(a) *size* (b) *height*

Figure 4.43: alternative model

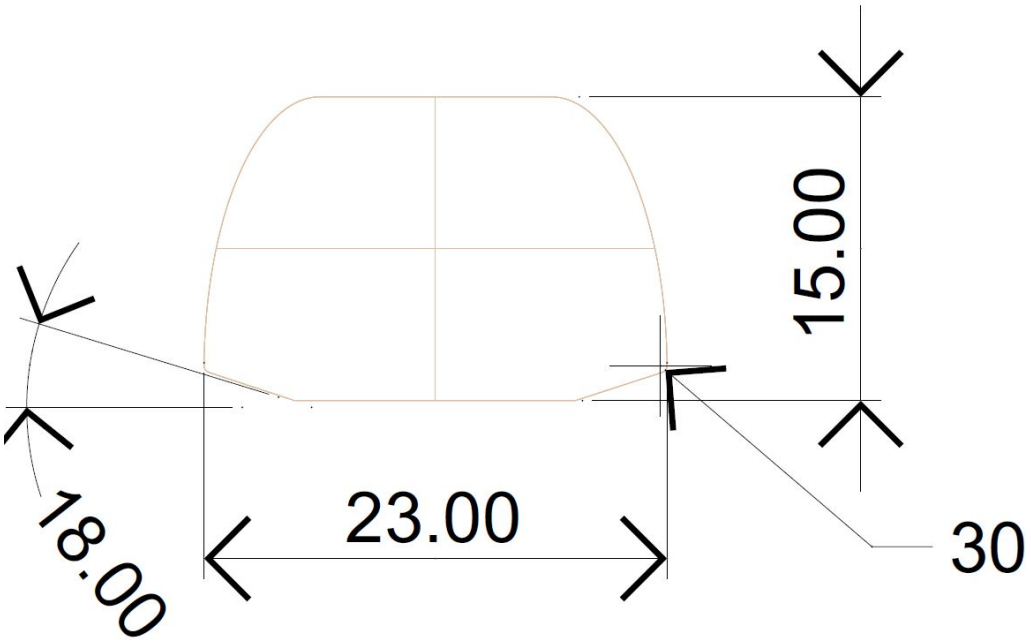

(a)

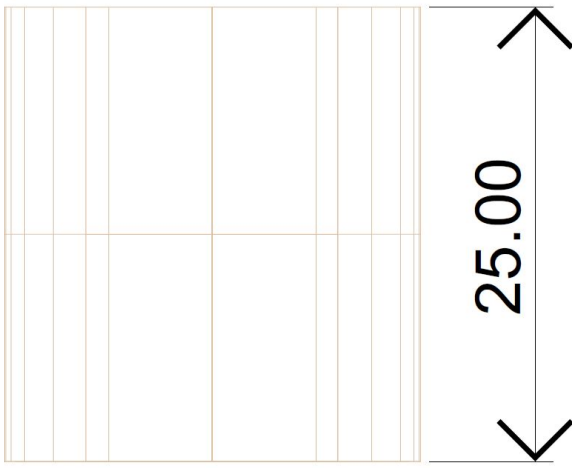

(b)

Figure 4.44: alternative model quotes

4.2 surgical operation

4.2.1 Lumbar operation case with modular Smartbone® prosthesis

The modular prosthesis produced was implanted on a patient affected by primitive neoplasm- Ewing's sarcoma in the lumbar and sacral part of the column with a high degree of malignancy that affected 3 lumbar vertebrae. the vertebrectomy was performed in two phases with an anterior approach combined with the posterior one. With the anterior approach the vertebrae were isolated from the tissues present around the vertebral column, subsequently the patient was turned in order to continue with the posterior approach during which the tissues around the column were separated and a laminectomy was performed for to be able to remove the posterior laminae until reaching the marrow. The marrow has been bandaged and the nerve roots have been isolated to avoid damaging them

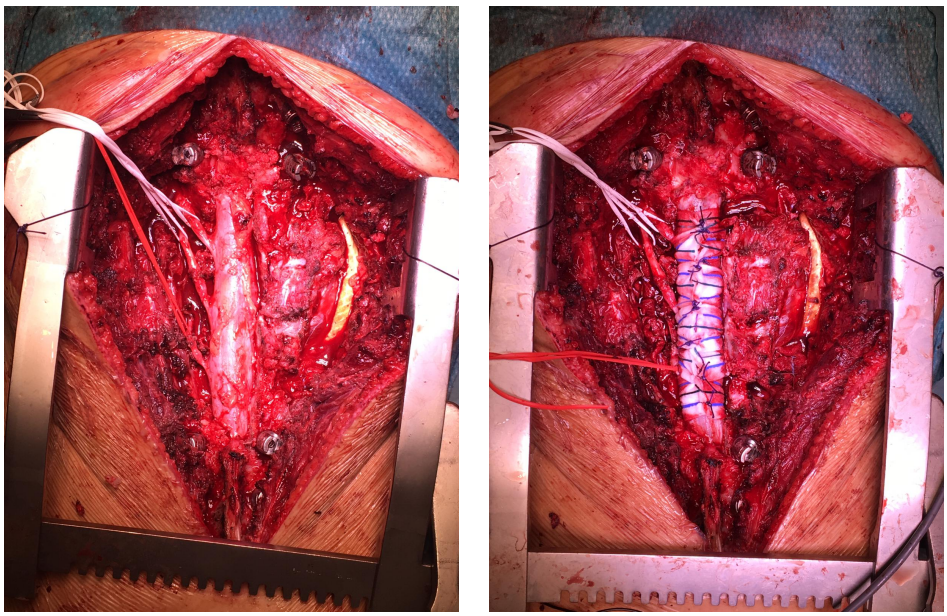

(a) *midollo* (b) *midollo fasciato*

Figure 4.45: posterior approach, laminectomy, banded spinal cord

The column was fixed by means of the pair of screws that were inserted into the healthy vertebrae T10, T11, T12, L5 and S1 and connected through the titanium fixing rods, in order to have a larger operating space only one of the bars is inserted which guarantees us to block the system partially while at the end the second bar is inserted to totally block the prosthesis. The column was cut with a wire saw as we can see in figure and the three vertebral bodies L1-L3 and the upper part of the L4 were removed.

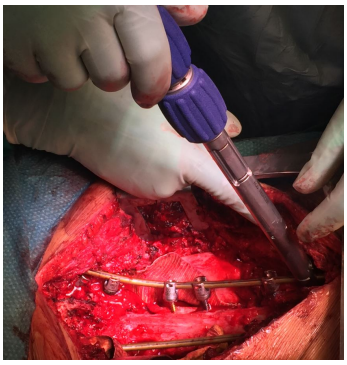

(a) *rods and screws*

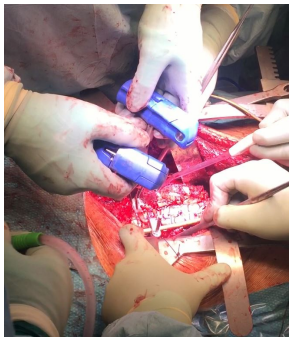

(b) *wire saw*

(c) *tumor removed*

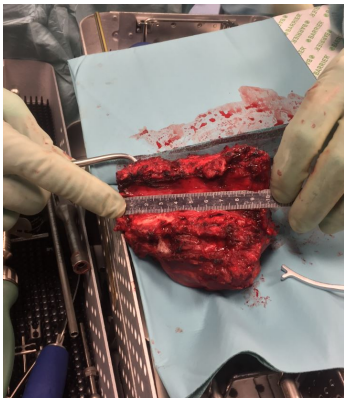

(d) *tumor measurement*

Figure 4.46

After removing the body affected by the tumor the distance between the two healthy vertebrae was measured in order to proceed with the assembly of the Smartbone® prosthesis. 10 modules were used as we can see in the figure [].

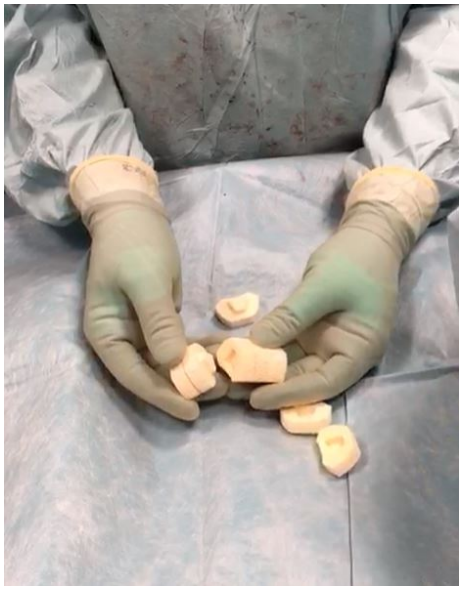

(a) *Smartbone® prostheis*

(b) *Smartbone® prosthesis*

Figure 4.47: Smartbone® prosthesis segments

The lower plate of the Smartbone® has been filed in order to generate a curve similar to the physiological curve, creating a lordosis and inserting the model into the space freed from the tumor vertebrae and fixed by lightly compressing the posterior rods slightly.

(a) *milling*

(b) *ightly compressing the posterior bars slightly*

Figure 4.48

Two holes are made to insert two screws that will connect the bone prosthesis to the posterior rods. Then the second bar blocked by the screws is inserted.

(a) *Smartbone® 's screw howl creation*

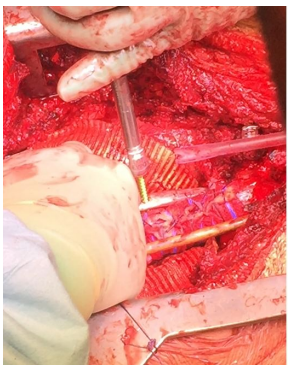

(b) *Smartbone® 's screw insertion*

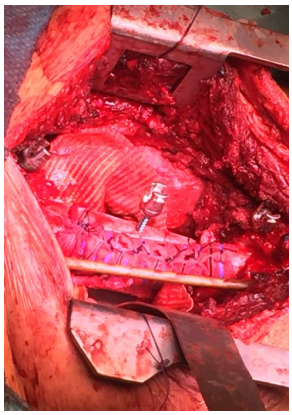

(c) *Smartbone® 's screw insertion*

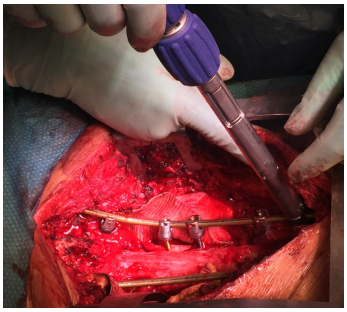

(d) *second rod insertion*

Figure 4.49: Joint model

To give further protection to the spinal cord, the tibial bone is used which is cut in half and tied between the two bars as we can see in the figure , now the surgery is finished and the wound can be sutured.

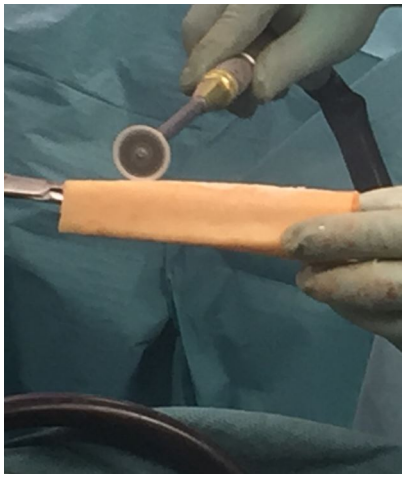

(a) *tibial bone*

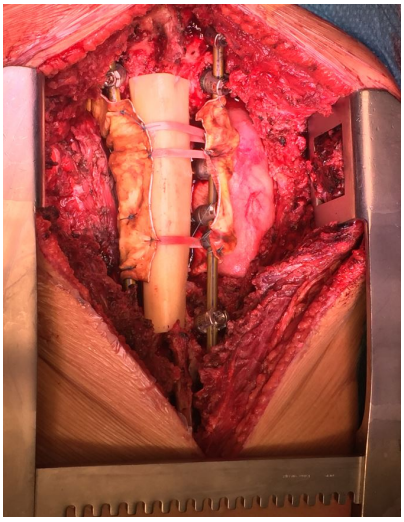

(b) *tibial bone fixed between rods*

Figure 4.50: all componets fixed

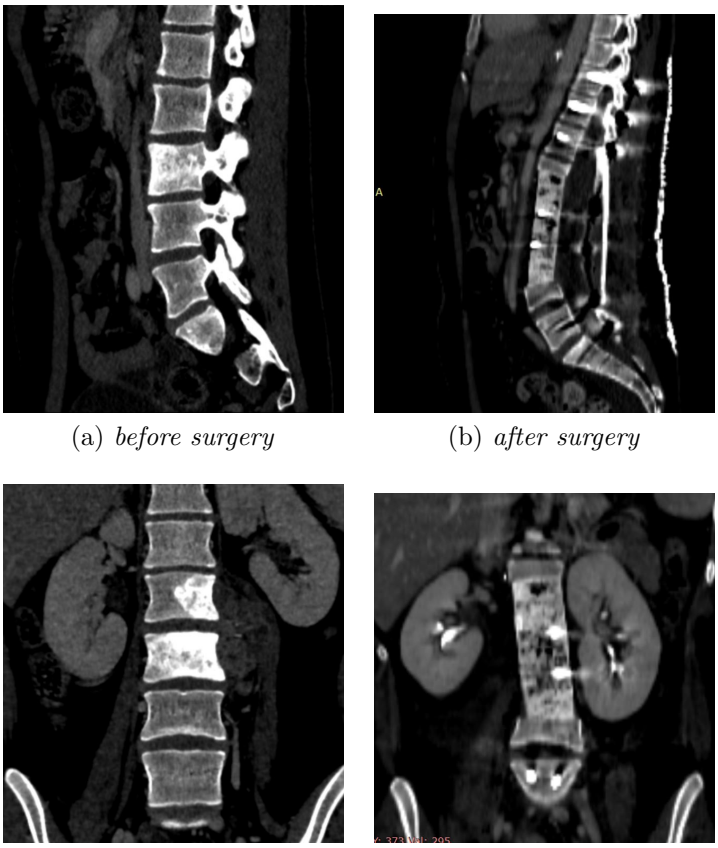

(a) *before surgery* (b) *after surgery*

(c) *before surgery* (d) *after surgery*

Figure 4.51: CT images before and after surgery

4.2.2 Thoracic vertebral body operation with alternative prosthesis model of Smartbone®

The alternative model of prosthesis produced was implanted on a patient affected by Osteoblastoma in the thoracic part of the column with a high degree of malignancy that affected 1 thoracic vertebral body. The vertebrectomy was performed in a single phase with an anterior approach through the cut of the sternum and the opening of the patient's rib cage to reach the vertebral body in order to isolate it and extract it completely.In this case, unlike before, the laminectomy was not performed and therefore no screws and bars were used to fix the vertebral column

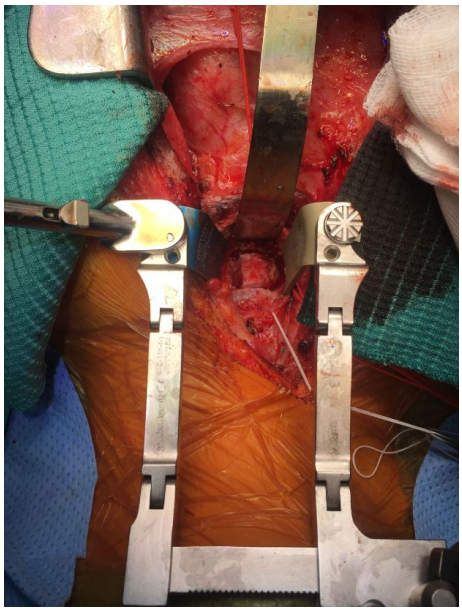

(a) *anterior approach*

(b) *rtumoral vertebral body measurement*

Figure 4.52

After extraction the tumoral vertebral body is measured in order to model the prosthesis, creating a suitable shape for the patient. At this point the prosthesis is inserted and blocked through a titanium plate which is fixed with titanium screws to the upper and lower healthy vertebra.

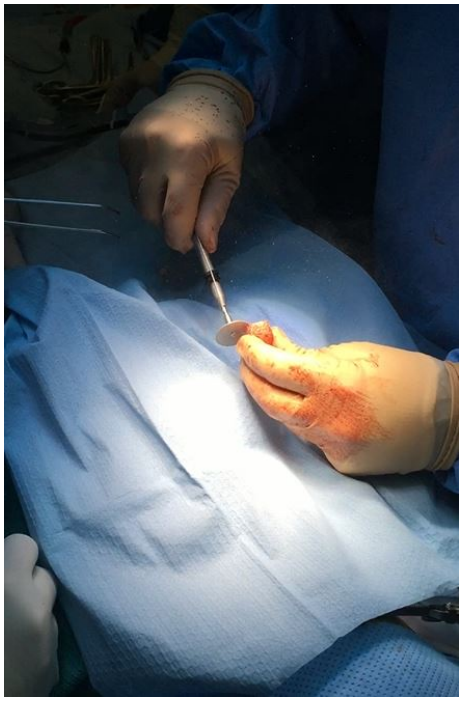

(a) *Smartbone® modeling*

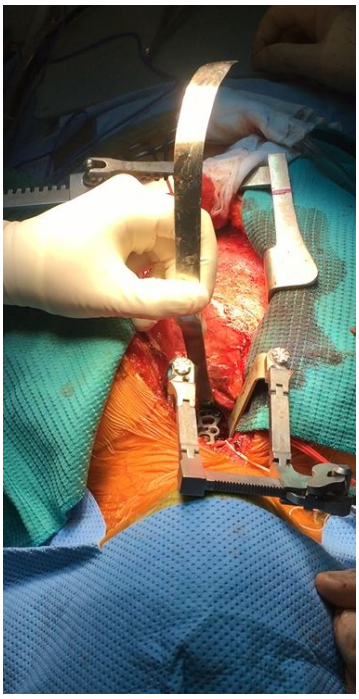

(b) *titanium plate fixed*

Figure 4.53

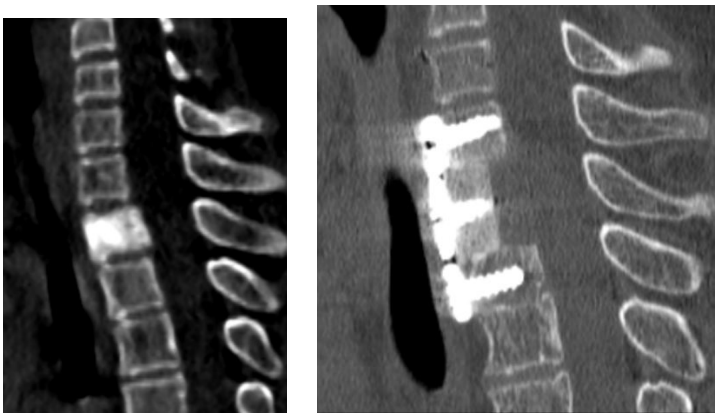

(a) *before surgery* (b) *after surgery*

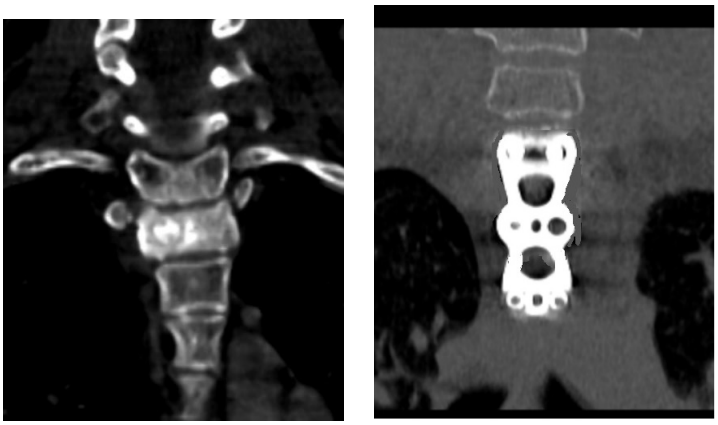

(c) *before surgery* (d) *after surgery*

Figure 4.54: Ct image before and after surgery

Chapter 5

Conclusions

5.1 Conclusions

The final design of the Smartbone® prosthesis has been studied in order to have a shape very close to the natural structure of the vertebral body specifioc which will replace the original shape:

- Simple to implant for the surgeon.
- Favors osseointegration
- To avoid mechanical micromovements between the prosthesis and the healthy vertebra and the various modules.

Finally, 3 different models of standard prostheses were designed, starting from different tc images, so as to cover all three vertebral tracts (cervical, thoracic and lumbar) and an alternative smaller model that can be modeled directly in the operating theatre, which could be used in specific cases where the vertebra affected by the tumour is smaller in size, such as in children.

The joint is the most vulnerable part of the structure because it is an angular shape and smaller than the body of the prosthesis. For this reason the shape of the joint has a fundamental role in the structure of the prosthesis model per cui

The mechanical tests performed are compression and bending; compression is important because about 80% of the loads of the upper vertebra are transmitted to the prosthesis and it is a load constantly from the patient's body weight. The bwnding test simulates the patient's movements such as forward and backward bending of the patient. In both cases it can be seen that the prosthesis perfectly simulates the vertebral body and there is no evidence of failure.

Smartbone® is a deformable material and for this reason it is possible to study new structures and new ways of using it, such as sending the shape chosen by us and changing the shape of the joint or totally distorting the project and creating new models with different structures.

In the future, the results of the fallow up examinations of patients treated with our prosthesis will be important because we will be able to see how osteointegration between the prosthesis and the vertebra will be. moreover, from this tests it is possible to evaluate how the reabsorption of the Smartbone® will be in reaction to vertebral loads and in physiological environment. one of the most important

developments will be to carry out a very thorough mechanical study especially with regards to time-consuming tests and to assess how continuous prosthesis is achieved.

At the same time it is also possible to study the reabsorption of the Smartbone® through mechanical tests, creating on the computer an environment very similar to the physiological one and studying the reactions of the prosthesis and its changes in an environment similar to the physiological one.

Chapter 6

Appendix

Database:

	A	B	C	D	E	F	G	H	I	J	K	L	M	N	O	P	Q	R	S	T
1	CARTI	UNITÀ	COGN	NOME	DATA NAS	se	DC	DATA INT	TC PRE		TC POST	PATOLOGIA	sede	livello	intervento	approccio	protesi	innesto	strumentari	tratto str
2	273473	CVOD	######	######	02/12/1941	F	75	08/02/2010	27/01/2010	confronto	25/02/2010	neoplasia primitiva	RACH. LOMBARE	L2-L3	VERTEBRECTOMIA INTRA	doppio accesso (1-	INNESTO ARMATO CO	INNESTO ARMATO CON M	CARBOFIX	63
3	293991	CVOD	######	######	22/01/1962	M	56	31/01/2012	23/01/2012	confronto	06/02/2012	discopatia degenera	RACH. TORACO/LOMBARE	T11-T12-L1	VERTEBRECTOMIA IN BLO	accesso posteriore	MODULARE DI CARBO	OSSO AUTOPLASTICO E OT	STRH 3D TITANI	60,32
4	304337	CVOD	######	######	22/02/1988	M	25	22/02/2013	17/01/2013	confronto	28/02/2013	neoplasia primitiva	RACH. LOMBARE	L3	VERTEBRECTOMIA IN BLO	doppio accesso (1-	MODULARE DI CARBO	costa	MESA K2M TITA	43,46
5	305141	CVOD	######	######	08/12/1971	F	55	08/03/2013	05/03/2013	confronto	13/03/2013	neoplasia primitiva	RACH. LOMBARE	L2	VERTEBRECTOMIA IN BLO	accesso posteriore	MODULARE DI CARBO	OMOPLASTICO eCOSTE AU	FILO FIBERWIRE	63,1
6	304800	CVOD	######	######	08/10/1967	M	45	22/03/2013	19/03/2013	confronto	30/03/2013	neoplasia primitiva	RACH. LOMBARE	L2-L3-L4	VERTEBRECTOMIA IN BLO	doppio accesso (1-	MODULARE DI CARBO	omoplastic(i)	BARRE K2 5,5 CI	52,78
7	308224	CVOD	######	######	14/07/1948	M	65	04/06/2013	31/05/2013	confronto	06/06/2013	neoplasia primitiva	RACH. TORACICO	T11-T12	VERTEBRECTOMIA IN BLO	doppio accesso (1-	INNESTO OSSEO	OSSO OMOPLASTICO DI B	MESA K2M TITA	70,8
8	310407	CVOD	######	######	09/05/1977	F	36	20/08/2013	16/08/2013	confronto	23/08/2013	neoplasia primitiva	RACH. TORACICO	T7-7-8-T9	VERTEBRECTOMIA IN BLO	accesso posteriore	MODULARE DI CARBO	MODULARE DI CARBONIO	MESA K2M TITA	41,44
9	310752	CVOD	######	######	20/12/1990	M	23	06/09/2013	30/08/2013	confronto	10/09/2013	neoplasia primitiva	RACH. TORACO/LOMBARE	T12-L1	VERTEBRECTOMIA IN BLO	doppio accesso (1-	MODULARE DI CARBO	MODULARE IN CARBONIO	MESA K2M TITA	96,34
10	315574	CVOD	######	######	03/03/1942	F	74	21/02/2014	17/02/2014	confronto	27/02/2014	neoplasia primitiva	RACH. TORACICO	T10	VERTEBRECTOMIA INTRA	accesso posteriore	CEMENTO	CEMENTO	CARBOFIX	25,96
11	318043	CVOD	######	######	29/07/1994	M	20	13/05/2014	07/01/2014	confronto	19/05/2014	neoplasia primitiva	RACH. TORACICO	T9-T10-T11	VERTEBRECTOMIA IN BLO	doppio accesso (1-	INNESTO OSSEO	INNESTO OSSEO COSTA	MESA K2M TITA	82,93
12	318879	CVOD	######	######	22/02/1952	F	62	10/06/2014	06/05/2014	confronto	18/06/2014	neoplasia primitiva	RACH. TORACICO	T3-T4-T5-T6	VERTEBRECTOMIA IN BLO	accesso posteriore	INNESTO OSSEO	INNESTO OSSEO TIBIA (ri	MESA K2M TITA	66,88
13	268802	CVOD	######	######	20/07/1973	M	41	01/07/2014	27/06/2014	confronto	09/07/2014	neoplasia primitiva	RACH. TORACICO	T10-T11-T12-L1	VERTEBRECTOMIA IN BLO	accesso posteriore	CILINDRO IN TITANIO	CILINDRO IN TITANIO PYR	MESA K2M TITA	18,45
14	311910	CVOD	######	######	23/10/1986	F	28	04/07/2014	08/05/2014	confronto	10/07/2014	neoplasia primitiva	RACH. LOMBARE	L3	VERTEBRECTOMIA IN BLO	doppio accesso (1-	MODULARE DI CARBO	MODULARE IN CARBONIO	MESA K2M TITA	41,81
15	316840	CVOD	######	######	11/04/1974	M	40	05/08/2014	01/08/2014	confronto	08/08/2014	neoplasia primitiva	RACH. LOMBARE	L3	VERTEBRECTOMIA IN BLO	doppio accesso (1-	INNESTO OSSEO	INNESTO OMOPLASTICO F	MESA K2M TITA	58,8
16	310970	CVOD	######	######	03/03/1940	F	74	17/09/2013	18/07/2013	confronto	18/07/2013	neoplasia primitiva	RACH. TORACO/LOMBARE	T10-T11-T12-L1-L2-L	VERTEBRECTOMIA IN BLO	doppio accesso (1-ANT; 2-POST)			MESA K2M TITA	98,91
17	324167	CVOD	######	######	03/07/1977	M	37	19/12/2014	21/08/2013	confronto	23/12/2014	neoplasia primitiva	RACH. TORACICO	T8	EMIVERTEBRECTOMIA	doppio accesso (1-	CILINDRO IN TITANIO	CILINDRO IN TITANIO PYR	MESA K2M TITA	78,83
18	319897	CVOD	######	######	11/12/1971	M	43	27/01/2015	22/01/2015	confronto	06/02/2015	neoplasia primitiva	RACH. LOMBARE	L2-L3	VERTEBRECTOMIA IN BLO	doppio accesso (1-	CAPRI K2M	CAPRI K2M	MESA K2M TITA	74,68
19	323378	CVOD	######	######	03/12/1969	F	45	24/03/2015	20/03/2015	confronto	01/04/2015	neoplasia primitiva	RACH. LOMBO/SACRALE	(L3-L4-) L5	VERTEBRECTOMIA IN BLO	doppio accesso (1-	PROTESI AD ESPANSIC	PROTESI AD ESPANSIONE (	MESA K2M TITA	77,82
20	327753	CVOD	######	######	27/01/1963	M	52	23/04/2015	30/03/2015	confronto	27/04/2015	neoplasia secondaria	RACH. LOMBARE	L2	VERTEBRECTOMIA INTRA	accesso posteriore	CAPRI K2M	CAPRI K2M	MESA K2M TITA	42,49
21	328012	CVOD	######	######	17/10/1991	M	24	05/05/2015	30/04/2015	confronto	11/05/2015	neoplasia primitiva	RACH. LOMBARE	L3-L4	ESCISSIONE (osteotomia	doppio accesso (1-	INNESTO OSSEO	INNESTO OSSEO	MESA K2M TITA	46,88
22	328247	CVOD	######	######	18/06/1953	M	62	15/05/2015	08/05/2015	confronto	25/05/2015	neoplasia primitiva	RACH. LOMBARE	L3	VERTEBRECTOMIA IN BLO	doppio accesso (1-	MODULARE DI CARBO	CARBONIO (3 segmenti, ui	MESA K2M TITA	39,1
23	326499	CVOD	######	######	25/05/1967	M	48	09/06/2015	04/05/2015	confronto	15/06/2015	neoplasia primitiva	RACH. TORACICO	T4	VERTEBRECTOMIA IN BLO	accesso posteriore	MODULARE DI CARBO	MODULARE IN CARBONIO	MESA K2M TITA	57,67
24	329430	CVOD	######	######	15/01/1944	F	71	23/06/2015	02/03/2015	confronto	29/06/2015	neoplasia primitiva	RACH. LOMBARE	L2	VERTEBRECTOMIA IN BLO	doppio accesso (1-	MODULARE DI CARBO	SISTEMA COMPONIBILE IN	MESA K2M TITA	50,56
25	254107	CVOD	######	######	19/05/1974	M	41	01/07/2015	25/06/2015	confronto	06/07/2015	neoplasia secondaria	RACH. TORACICO	T8-T9-T10	VERTEBRECTOMIA IN BLO	doppio accesso (1-	CAPRI K2M	CAPRI K2M	MESA K2M TITA	89,84
26	316709	CVOD	######	######	19/12/1994	M	21	15/09/2015	10/09/2015	confronto	21/09/2015	neoplasia primitiva	RACH. TORACICO	T12-L1-L2	VERTEBRECTOMIA IN BLO	doppio accesso (1-	MODULARE DI CARBO	ABC IN FIBRA DI CARBONI	MESA K2M TITA	59,99
27	332090	CVOD	######	######	14/02/1960	F	56	09/10/2015	08/10/2015	confronto	13/10/2015	neoplasia primitiva	RACH. LOMBARE	L3	VERTEBRECTOMIA IN BLO	doppio accesso (1-	MODULARE DI CARBO	MODULARE IN CARBONIO	MESA K2M TITA	53,31
28	324586	CVOD	######	######	13/02/1950	F	67	27/11/2015	25/11/2015	confronto	02/12/2015	neoplasia primitiva	RACH. TORACICO	T12	VERTEBRECTOMIA IN BLO	doppio accesso (1-	MODULARE DI CARBO	MODULARE IN CARBONIO	CARBOFIX	73,58
29	333727	CVOD	######	######	13/12/1945	F	70	01/12/2015	26/11/2015	confronto	03/12/2015	neoplasia primitiva	RACH. TORACICO	(T11)-T12-L1-(L2)	VERTEBRECTOMIA IN BLO	doppio accesso (1-	MODULARE DI CARBO	MODULARE IN CARBONIO	MESA K2M TITA	10,28
30	335201	CVOD	######	######	22/03/1954	F	62	29/01/2016	26/01/2016	confronto	04/02/2016	neoplasia primitiva	RACH. LOMBARE	L1	VERTEBRECTOMIA IN BLO	doppio accesso (1-	TITANIO POROSO CUS	TITANIO POROSO CUSTOM	MESA K2M TITA	88,56
31	334431	CVOD	######	######	17/11/1983	F	32	02/02/2016	30/10/2015	confronto	09/02/2016	neoplasia primitiva	RACH. LOMBARE	L1-L2-L3	VERTEBRECTOMIA IN BLO	accesso posteriore	TITANIO POROSO CUS	TITANIO	MESA K2M TITA	67,33
32	335587	CVOD	######	######	26/11/1974	F	41	10/02/2016	20/01/2016	confronto	17/02/2016	neoplasia primitiva	RACH. TORACO/LOMBARE	T12-L1-L2	VERTEBRECTOMIA IN BLO	doppio accesso (1-	MODULARE DI CARBO	CARBONIO BBT+COSTA AU	CARBOFIX	27
33	334646	CVOD	######	######	01/07/1968	M	48	01/03/2016		confronto	07/03/2016	stenosi rachide cervi	RACH. CERVICALE	C5-C6	CORPORECTOMIA APERT	accesso anteriore	INNESTO OSSEO	INNESTO PERONE OMOPL	VERTEX MAX	43,48
34	336409	CVOD	######	######	28/03/1969	M	47	07/03/2016	05/03/2016	confronto	10/03/2016	neoplasia primitiva	RACH. LOMBARE	L2-L3	VERTEBRECTOMIA IN BLO	doppio accesso (1-	MODULARE DI CARBO	MODULARE IN CARBONIO	SOLERA MEDTRI	11,07
35	336546	CVOD	######	######	14/03/1961	M	55	11/03/2016	10/03/2016	confronto	17/03/2016	neoplasia secondaria	RACH. LOMBARE	L4	VERTEBRECTOMIA IN BLO	doppio accesso (1-	TITANIO POROSO CUS	TITANIO CUSTOM MADE	EVEREST	50,3
36	337423	CVOD	######	######	31/07/1956	M	60	18/04/2016	15/04/2016	confronto	22/04/2016	neoplasia secondaria	RACH. LOMBARE	T4-T5	VERTEBRECTOMIA INTRA	accesso posteriore	TITANIO POROSO CUS	TITANIO POROSO CUSTOM	SOLERA MEDTRI	60
37	338075	CVOD	######	######	02/08/1985	F	31	04/05/2016	02/05/2016	confronto	06/05/2016	neoplasia primitiva	RACH. TORACICO	T11-T12	VERTEBRECTOMIA IN BLO	accesso posteriore	TITANIO POROSO CUS	TITANIO CUSTOM MADE	MESA K2M TITA	56,27
38	338258	CVOD	######	######	09/10/1955	M	61	13/05/2016	12/05/2016	confronto	19/05/2016	neoplasia secondaria	RACH. TORACICO	T11-T12-L1	VERTEBRECTOMIA IN BLO	accesso posteriore	TITANIO POROSO CUS	TITANIO POROSO CUSTOM	MESA K2M TITA	56,88
39	338928	CVOD	######	######	14/02/1956	M	60	06/06/2016	01/06/2016	confronto	09/06/2016	neoplasia secondaria	RACH. TORACICO	T9-T10-T11	VERTEBRECTOMIA IN BLO	doppio accesso (1-	MODULARE DI CARBO	CARBONIO COMPONIBILE	SOLERA TITANIC	77,69
40	339209	CVOD	######	######	15/10/1975	M	41	15/06/2016	13/06/2016	confronto	20/06/2016	neoplasia secondaria	RACH. TORACICO	T10	BLOCCO	accesso posteriore	TITANIO POROSO CUS	3D (ITC)		38,83

	A	B	C	D	E	F	G	H	I	J	K	L	M	N	O	P	Q	R	S	T
1	CARTI	UNITÀ	COGN	NOME	DATA NAS	se	DC	DATA INT	TC PRE		TC POST	PATOLOGIA	sede	livello	intervento	approccio	protesi	innesto	strumentari	tratto str
40	339209	CVOD	######	######	15/10/1975	M	41	15/06/2016	13/06/2016	confronto	20/06/2016	neoplasia secondaria	RACH. TORACICO	T10	BLOCCO	accesso posteriore	TITANIO POROSO CUS	3D (ITC)		38,83
41	339533	CVOD	######	######	23/07/1958	F	58	29/06/2016	17/03/2016	confronto	29/06/2016	neoplasia secondaria	RACH. LOMBARE	L4	CORPORECTOMIA APERT	accesso anteriore	CAPRI K2M	CAPRI K2M		49,33
42	340013	CVOD	######	######	16/10/1938	F	78	04/08/2016	01/08/2016	confronto	08/08/2016	neoplasia secondaria	RACH. LOMBARE	L4	VERTEBRECTOMIA IN BLO	doppio accesso (1-	CAPRI K2M	CAPRI K2M	EVEREST	50,99
43	334633	CVOD	######	######	17/11/2001	F	15	30/08/2016	07/07/2016	confronto	06/09/2016	neoplasia primitiva	RACH. LOMBARE	L2	VERTEBRECTOMIA IN BLO	doppio accesso (1-	TITANIO POROSO CUS	TITANIO CUSTOM MADE		49
44	341075	CVOD	######	######	02/04/1959	M	57	06/09/2016	02/09/2016	confronto	13/09/2016	neoplasia primitiva	RACH. LOMBARE	T1	VERTEBRECTOMIA IN BLO	doppio accesso (1-	MODULARE DI CARBO	BBT A+B+C (con innesti omoplastici)		42,65
45	341159	CVOD	######	######	30/05/1949	F	67	09/09/2016	18/08/2016	confronto	10/10/2016	neoplasia primitiva	RACH. LOMBARE	L3	VERTEBRECTOMIA IN BLO	doppio accesso (1-	MODULARE DI CARBO	CARBONIO+CUNEO RIPIEN	IMPIANTO IN C	42,82
46	341526	CVOD	######	######	07/09/1943	M	73	20/09/2016	19/09/2016	confronto	26/09/2016	neoplasia primitiva	RACH. LOMBARE	L2	VERTEBRECTOMIA IN BLO	doppio accesso (1-	TITANIO POROSO CUS	TITANIO STAMPA 3D		62,74
47	341971	CVOD	######	######	24/08/1966	M	50	07/10/2016	22/07/2016	confronto	24/10/2016	neoplasia secondaria	RACH. LOMBARE	T6	VERTEBRECTOMIA IN BLO	accesso posteriore	CAPRI K2M	CAPRI K2M		58,46
48	342653	CVOD	######	######	19/08/1959	F	57	28/10/2016	03/10/2016	confronto	02/11/2016	neoplasia primitiva	RACH. CERVICALE	C3-C4	VERTEBRECTOMIA INTRA	doppio accesso (1-	INNESTO OSSEO	INNESTO OSSEO-SEGMENT	ICOTEC	43,4
49	342796	CVOD	######	######	26/04/1979	M	38	02/11/2016	26/10/2016	confronto	07/11/2016	mobilizzazione mezz	RACH. LOMBARE	L2	REVISIONE PROTESI	accesso posteriore	CAPRI K2M	CAPRI K2M		73,69
50	342529	CVOD	######	######	18/12/1977	M	39	30/11/2016	28/11/2016	confronto	05/12/2016	neoplasia secondaria	RACH. LOMBARE	L1	VERTEBRECTOMIA IN BLO	doppio accesso (1-	TITANIO POROSO CUS	TITANIO CUSTOM MADE		45,27
51	344398	CVOD	######	######	23/05/1983	F	34	13/01/2017	11/01/2017	confronto	17/01/2017	neoplasia primitiva	RACH. CERVICALE	C4-C5-C6	VERTEBRECTOMIA IN BLO	doppio accesso (1-	INNESTO OSSEO	INNESTO OMOPLASTICO P	PLACCA FIBRA C	62,42
52	343612	CVOD	######	######	10/05/1960	F	57	20/01/2017	18/01/2017	confronto	25/01/2017	neoplasia primitiva	RACH. LOMBO/SACRALE	L2-L3	VERTEBRECTOMIA IN BLO	doppio accesso (1-	MODULARE DI CARBO	MODULARE IN CARBONIO	CFR/PEEK+ PDS	74,54
53	345883	CVOD	######	######	29/06/1944	F	73	07/03/2017	06/03/2017	confronto	10/03/2017	neoplasia primitiva	RACH. LOMBARE	T12-L1-L2	VERTEBRECTOMIA IN BLO	accesso posteriore	TITANIO POROSO CUS	TITANIO POROSO STAMPA 3D		64,48
54	331036	CVOD	######	######	19/02/1962	F	55	21/03/2017	20/03/2017	confronto	27/03/2017	neoplasia primitiva	RACH. LOMBARE	T12	VERTEBRECTOMIA INTRA	doppio accesso (1-	CAPRI K2M	CAPRI K2M		38,4
55	347650	CVOD	######	######	04/03/1942	F	75	09/05/2017	08/05/2017	confronto	12/05/2017	neoplasia primitiva	RACH. LOMBARE	L4	VERTEBRECTOMIA INTRA	doppio accesso (1-	MODULARE DI CARBO	CARBONIO STACKABLE CA	CARBONCLEAR	43,39
56	347686	CVOD	######	######	24/02/1976	M	41	16/05/2017	15/05/2017	confronto	22/05/2017	neoplasia primitiva	RACH. TORACICO	T9-T10-T11	VERTEBRECTOMIA IN BLO	accesso posteriore	MODULARE DI CARBO	MODULARE IN CARBONIO	CARBOCLEA+PR	42,25
57	348056	CVOD	######	######	31/08/1992	M	25	23/05/2017	19/05/2017	confronto	12/06/2017	neoformazione ossea	RACH. TORACICO	T4-T5	ASPORTAZIONE (osteoton	accesso posteriore	INNESTO OSSEO	INNESTO OMOPLASTICO T	JAZZ LOCK	59
58	348641	CVOD	######	######	11/03/1947	F	70	16/06/2017	12/06/2017	confronto	19/06/2017	neoplasia primitiva	RACH. TORACICO	T5-T6	VERTEBRECTOMIA IN BLO	accesso posteriore	MODULARE DI CARBO	CARBONIO riempita con i	BARRE CARBOFI	71,98
59	350551	CVOD	######	######	09/01/1969	M	49	15/09/2017	09/02/2017	confronto	18/09/2017	neoplasia primitiva	RACH. LOMBARE	L4-L5	VERTEBRECTOMIA IN BLO	doppio accesso (1-	CAPRI K2M	CAPRI K2M		65,18
60	347283	CVOD	######	######	13/03/2001	F	17	10/10/2017	09/10/2017	confronto	13/10/2017	neoplasia primitiva	RACH. TORACICO	T9-T10	VERTEBRECTOMIA IN BLO	accesso posteriore	MODULARE DI CARBO	MODULARE IN CARBONIO	(AMS group)	30,9
61	352091	CVOD	######	######	07/12/1948	M	69	08/11/2017	06/11/2017	confronto		neoplasia primitiva	RACH. TORACO/LOMBARE	T11-T12-L1	VERTEBRECTOMIA IN BLO	doppio accesso (1-	TITANIO POROSO CUS	TITANIO STAMPA 3D CUSTOM MADE		65
62	262209	CVOD	######	######	08/07/1951	F	67	07/02/2018	05/02/2018	confronto	12/02/2018	neoplasia secondaria	RACH. LOMBARE	L2	VERTEBRECTOMIA IN BLO	doppio accesso (1-	MODULARE DI CARBO	MODULARE IN CARBONIO	ICOTEC	42,44
63	354280	CVOD	######	######	08/12/1971	F	46	09/02/2018	19/12/2017	confronto	12/02/2018	neoplasia primitiva	RACH. LOMBARE	L1	VERTEBRECTOMIA IN BLO	accesso posteriore	(1-SMARTBONE	SMARTBONE	CARBOFIX	38,53
64	355026	CVOD	######	######	21/10/1974	F	43	02/03/2018	01/03/2018	confronto	05/03/2018	neoplasia secondaria	RACH. LOMBARE	L3	VERTEBRECTOMIA IN BLO	doppio accesso (1-	MODULARE DI CARBO	BBT + INNESTO OSSEO	EVEREST	44,34
65	354513	CVOD	######	######	07/02/1973	F	45	13/03/2018	08/11/2017	confronto	15/03/2018	neoplasia secondaria	RACH. LOMBO/SACRALE	L5-S1	VERTEBRECTOMIA IN BLO	doppio accesso (1-	TITANIO POROSO CUS	TITANIO CUSTOM MADE 3	EVEREST	60,33
66	355880	CVOD	######	######	28/09/1940	M	78	30/03/2018	29/03/2018	confronto	03/04/2018	neoplasia secondaria	RACH. LOMBARE	L4	VERTEBRECTOMIA IN BLO	doppio accesso (1-	MODULARE DI CARBO	CARBONIO VBR + FRAMME	TITANIO	51,89
67	355891	CVOD	######	######	13/03/1949	M	69	04/04/2018	29/03/2018	confronto	11/04/2018	neoplasia secondaria	RACH. TORACICO	T11	VERTEBRECTOMIA IN BLO	doppio accesso (1-	MODULARE DI CARBO	CARBONIO VBR+FRAMME	EVEREST	57,2
68	355963	CVOD	######	######	04/06/1964	F	54	06/04/2018	03/04/2018	confronto	09/04/2018	neoplasia primitiva	RACH. TORACICO	T9	VERTEBRECTOMIA IN BLO	doppio accesso (1-	MODULARE DI CARBO	CARBONIO VBR	EVEREST	56,35
69	356337	CVOD	######	######	02/10/1979	M	39	20/04/2018	31/01/2018	confronto	23/04/2018	neoplasia primitiva	RACH. LOMBARE	L3	VERTEBRECTOMIA IN BLO	doppio accesso (1-	TITANIO POROSO CUS	TITANIO CUSTOM MADE 3	EVEREST	40,46
70	357767	CVOD	######	######	28/09/1955	F	63	08/06/2018	07/06/2018	confronto	14/06/2018	neoplasia secondaria	RACH. LOMBARE	L2-L3	VERTEBRECTOMIA IN BLO	doppio accesso (1-	TITANIO POROSO CUS	TITANIO CUSTOM MADE 3	EVEREST	55,36
71	356804	CVOD	######	######	16/05/1969	M	49	13/06/2018	05/06/2018	confronto	14/06/2018	neoplasia secondaria	RACH. TORACICO	T5-T6-T7	VERTEBRECTOMIA IN BLO	doppio accesso (1-	MODULARE DI CARBO	CARBONIO VBR+FRAMME	EVEREST	51,69
72	359076	CVOD	######	######	29/04/1996	M	22	25/07/2018	27/07/2016	confronto	02/08/2018	neoplasia primitiva	RACH. TORACICO	T7-T8-T9	VERTEBRECTOMIA IN BLO	accesso posteriore	MODULARE DI CARBO	CARBONIO VBR	K2M EVEREST-C	59,3
73	356737	CVOD	######	######	16/07/1965	F	53	05/09/2018	30/08/2018	confronto	05/09/2018	neoplasia secondaria	RACH. LOMBARE	L5	VERTEBRECTOMIA IN BLO	doppio accesso (1-	MODULARE DI CARBO	MODULARE IN CARBONIO	(VBR)+INNESTO	27,93
74	359387	CVOD	######	######	20/04/1961	M	57	07/09/2018	05/09/2018	confronto	10/09/2018	neoplasia secondaria	RACH. LOMBARE	L4	VERTEBRECTOMIA IN BLO	doppio accesso (1-	MODULARE DI CARBO	CARBONIO VBR	EVEREST	47,2
75	359931	CVOD	######	######	02/12/1957	M	61	11/09/2018	07/09/2018	confronto	14/09/2018	neoplasia primitiva	RACH. LOMBARE	L3	VERTEBRECTOMIA INTRA	doppio accesso (1-	INNESTO OSSEO	INNESTO OMOLOGO DIAF	CARBOFIX+LEGA	58,1
76	354648	CVOD	######	######	14/05/1974	M	44	18/09/2018	17/09/2018	confronto	20/09/2018	neoplasia primitiva	RACH. LOMBARE	L3	VERTEBRECTOMIA IN BLO	doppio accesso (1-	INNESTO OSSEO	INNESTO FEMORE DI BAN	EVEREST	44,19
77	360138	CVOD	######	######	02/04/1962	M	56	03/10/2018	01/10/2018	confronto	08/10/2018	neoplasia primitiva	RACH. LOMBARE	L2	VERTEBRECTOMIA IN BLO	doppio accesso (1-	MODULARE DI CARBO	CARBONIO VBR	Everest	91,48
78	360736	CVOD	######	######	05/05/2007	M	11	16/10/2018	03/10/2018	confronto	19/10/2018	neoplasia primitiva	RACH. CERVICALE	C6-C7-T1	VERTEBRECTOMIA IN BLO	doppio accesso (1-	INNESTO OSSEO	INNESTO FEMORE DI BAN	carbonio+carbi	44,26

Figure 6.1: Database

The above data over the EU regulation 2016/679 GDPR

Rhinoceros: We used rhinoceros version 4 and 6 for all component design

Figure 6.2: rhinoceros

Bibliography

[1] T. Hentunen, N. Cunningham, O. Vuolteenaho, A. Reddi, and H. Väänänen, "Osteoclast recruiting activity in bone matrix," *Bone and Mineral*, vol. 25, no. 3, pp. 183 – 198, 1994.

[2] B. Clarke, "Normal bone anatomy and physiology," *Clinical Journal of the American Society of Nephrology*, vol. 3, no. Supplement 3, pp. S131–S139, 2008.

[3] L. J. Raggatt and N. C. Partridge, "Cellular and molecular mechanisms of bone remodeling." The Journal of biological chemistry, 285(33), 25103-8, 2010.

[4] S. L. Weinstein and A. Joseph, "Buckwalter lippincott williams wilkins." 2005 - 761 pagine.

[5] L. J. Raggatt and P. N. C. and, "and molecular mechanisms of bone remodeling." J Biol Chem285(33):25103-8, 2010.

[6] A. Kiapour. *et al.*, ""biomechanical effects of spinal flexibility and rigidity on lumbar spine loading: A finite element analysis study"." EC Orthopaedics 3.4 : 351-358, 2016.

[7] F. Thiele, C. M. Cohrs, A. Flor, *et al.*, "Cardiopulmonary dysfunction in the osteogenesis imperfecta mouse model aga2 and human patients are caused by bone-independent mechanisms." Hum Mol Genet21(16):3535-45, 2012.

[8] V. Mahadevan, "Anatomy of the vertebral column," *Surgery (Oxford)*, vol. 36, no. 7, pp. 327 – 332, 2018.

[9] T. A. J. O. F. P. M. O. F. T. C. S. D. R. Worth, "M.a.. p.a." M.e.s.p. for The Orthopaedic Study Group.

[10] O. Editors Bert Lasat [[Reviewed and updated by Matthew Richards 29/7/2014]].

[11] P. Raj, "Intervertebral disc: Anatomy-physiology-pathophysiology-treatment," *Pain practice : the official journal of World Institute of Pain*, vol. 8, pp. 18–44, 04 2008.

[12] T. R. Oxland, "Fundamental biomechanics of the spine—what we have learned in the past 25 years and future directions," *Journal of Biomechanics*, vol. 49, no. 6, pp. 817 – 832, 2016. SI: Spine Loading and Deformation.

[13] S. V. Kushchayev, T. Glushko, M. Jarraya, K. H. Schuleri, M. C. Preul, M. L. Brooks, and O. M. Teytelboym, "Abcs of the degenerative spine," *Insights into Imaging*, vol. 9, pp. 253–274, Apr 2018.

[14] www.fisiokinesiterapia.biz/download/anaspine.pdf.

[15] A. Kiapour. *et al.*, ""biomechanical effects of spinal flexibility and rigidity on lumbar spine loading: A finite element analysis study"." EC Orthopaedics 3.4 : 351-358, 2016.

[16] www.fisiokinesiterapia.biz/download/biomrach.pdf.

[17] J. Chazal, A. Tanguy, M. Bourges, G. Gaurel, G. Escande, M. Guillot, and G. Vanneuville, "Biomechanical properties of spinal ligaments and a histological study of the supraspinal ligament in traction," *Journal of Biomechanics*, vol. 18, no. 3, pp. 167 – 176, 1985.

[18] D. Sciubba, *Spinal Tumor Surgery: A Case-Based Approach*. Springer International Publishing, 2018.

[19] V. Denaro, A. Di Martino, and A. Piccioli, *Management of Bone Metastases: A multidisciplinary guide*. Springer International Publishing, 2018.

[20] M. Berchuck, S. R. Garfin, J. Abitbol, and R. G. Wilber, "Vertebrectomy for tumors and infections in the lumbar spine," *Operative Techniques in Orthopaedics*, vol. 1, no. 1, pp. 97 – 105, 1991.

[21] U. Lange, S. Edeling, C. Knop, L. Bastian, M. Oeser, C. Krettek, and M. Blauth, "Anterior vertebral body replacement with a titanium implant of adjustable height: a prospective clinical study." European spine journal : official publication of the European Spine Society, the European Spinal Deformity Society, and the European Section of the Cervical Spine Research Society, 16(2), 161-72, 2006.

[22] U. Lange, S. Edeling, C. Knop, *et al.*, "Anterior vertebral body replacement with a titanium implant of adjustable height: a prospective clinical study." Eur Spine J16(2):161-72, 2006.

[23] U. Lange *et al.*, ""anterior vertebral body replacement with a titanium implant of adjustable height: a prospective clinical study" european spine journal : official publication of the european spine society, the european spinal deformity society." and the European Section of the Cervical Spine Research Society vol. 16,2 : 161-72, 2006.

[24] T. Akazawa, T. Kotani, T. Sakuma, T. Nemoto, and S. Minami, "Rod fracture after long construct fusion for spinal deformity: clinical and radiographic risk factors," *Journal of Orthopaedic Science*, vol. 18, no. 6, pp. 926 – 931, 2013.

[25] M. B. Kabins and J. N. Weinstein "The History of Vertebral Screw and Pedicle Screw Fixation" Iowa Orthopaedic Journal vol. 11 : 127–136, 1991.

[26] M. B. Kabins and W. Jn., "The history of vertebral screw and pedicle screw fixation." Iowa Orthop J11:127–136, 1991.

[27] M. B. Kabins and J. N. Weinstein, "The history of vertebral screw and pedicle screw fixation." The Iowa Orthopaedic Journal, 11, 127–136, 1991.

[28] S. Boriani, S. Bandiera, R. Biagini, F. De Iure, and A. Giunti, "The use of the carbon-fiber reinforced modular implant for the reconstruction of the anterior column of the spine. a clinical and experimental study conducted on 42 cases," *La Chirurgia degli organi di movimento*, vol. 85, pp. 309–35, 10 2000.

[29] H. Herkowitz and I. Spine, *The Lumbar Spine*. LWW medical book collection, Lippincott Williams & Wilkins, 2004.

[30] G. Pertici, F. Carinci, G. Carusi, D. Epistatus, T. Villa, F. Crivelli, F. Rossi, and G. Perale, "Composite polymer-coated mineral scaffolds for bone regeneration: From material characterization to human studies., j. biol. regul. homeost," *Agents*, vol. 29, p. 3, 2015.

[31] L. Jiang, J. Zhang, G. Pertici, F. Rossi, T. Casalini, G. Perale, K. Jurczyk, M. M. Kubicka, M. Ratajczak, M. U. Jurczyk, K. Niespodziana, D. M. Nowak, M. Gajecka, M. U. Jurczyk, I. Allan, H. Newman, and M. Wilson, ""composite polymer-coated mineral grafts for bone regeneration: Material characterisation and model study," ann. oral maxilofac." Surg., vol. 2, no. 1, pp. 1–7, 2014.

[32] M. Santoro, "[book 1; book 2; book 3; book 4; book10; gme," vol. 2017, 2005.

[33] G. A. Duong and R. L. T., "Integrin-mediated signaling in the regulation of osteoclast adhesion and activation," *in Frontiers in Bioscience*, vol. 3, 1998.

[34] Xiaohuma, "[book 3," 2009.

[35] F. Grecchi, G. Perale, and V. Candotto, "a." Busato, M. Pascali, and F. Carinci, "Reconstruction of the zygomatic bone with smartbone®: Case report," J. Biol. Regul. Homeost. Agents, vol. 29, no. 3, pp. 42–47, 2015.

[36] J. Goode, "Use of international standard iso 10993-1, biological evaluation of medical devices - part 1: Evaluation and testing within a risk management process, dep. heal," *Hum*, vol. 68, 2016.